

Durability of Flax Fibre Reinforced Concrete

A Thesis

Submitted to the College of Graduate Studies and Research

In Partial Fulfillment of the Requirements

for the

Degree of Master of Science

in the

Department of Civil Engineering

University of Saskatchewan

Saskatoon

by

Cam Yaremko

©Copyright Cam Yaremko, July 2012. All rights reserved.

Permission to Use

The author has agreed that the library, University of Saskatchewan, may make this thesis freely available for inspection. Moreover, the author has agreed that permission for extensive copying of this thesis for scholarly purposes may be granted by the professors who supervised the thesis work recorded herein or, in their absence, by the head of the Department or the Dean of the College in which the thesis work was done. It is understood that due recognition will be given to the author of this thesis and to the University of Saskatchewan in any use of the material in this thesis. Copying or publication or any other use of the thesis for financial gain without approval by the University of Saskatchewan and the author's written permission is prohibited.

Requests for permission to copy or to make any other use of material in this thesis in whole or part should be addressed to:

Head of Department of Civil Engineering
University of Saskatchewan
Engineering Building
57 Campus Drive
Saskatoon, Saskatchewan
Canada, S7N 5A9

Abstract

Flax fibre-reinforced concrete has been found to perform as well as concrete reinforced with fibres made from glass and plastic in terms of its resistance to plastic shrinkage cracking. However, flax fibres alone have been found to lose their strength and stiffness when subjected to simulated concrete pore solutions. This thesis describes an experimental program to measure the degradation of the mechanical properties of flax fibre-reinforced concrete subjected to wet-dry and freeze-thaw cycling. Three types of flax fibre (untreated, Duralin treated, and silane treated) were used at lengths and volume fractions of 38 mm and 0.3%, respectively, to determine whether different fibre types would generate different mechanical properties.

The compressive strength, flexural strength and flexural toughness were found for all types of concrete, both before and after cycling, to determine if weathering cycles produced degradation of these mechanical properties. Flax fibre-reinforced concrete was found to experience no significant degradation when compared to the unreinforced concrete. Duralin and silane fibre-reinforced concrete were also found to encounter no significant degradation or improvement when compared to untreated flax fibre or unreinforced concrete. This was found after subjecting all four types of concrete to both wet-dry and freeze-thaw cycling.

Non-destructive testing found that the dynamic modulus of elasticity of beams subjected to wet-dry cycling gradually changed as cycling went on. This was attributed to the changing of the microstructure in the cement paste, as moisture was cycled in and out. Degradation of the cement paste itself was not found to be the cause of this gradual change in dynamic modulus of elasticity.

Analysis performed on scanning electron microscope images of the failed fibres, on the crack surface of the beams, showed that there were no correlations between the final conditions of each fibre type and the type of weathering it was subjected to. Energy-dispersive x-ray spectroscopy analysis also found that elements from the cement paste adhered the surface of the fibres, once mixed in the concrete.

Acknowledgements

I wish to express my most sincere gratitude and appreciation to Dr. Leon D. Wegner for his help, guidance and encouragement throughout the course of this investigation. His continued support and interest in this research made this work possible. I am also indebted to the members of my advisory committee, Dr. Moh Boulfiza and Dr. Lisa Feldman, for their kind advice from time to time. I would also like to thank Brennan Pokoyoway for his guidance in carrying out the experimental program.

Financial support provided by the University of Saskatchewan in forms of scholarship and assistance are gratefully acknowledged. Thanks are extended to the Agriculture Development Fund for providing me with additional financial support for this project. Thanks are also extended to Biolin Research Inc., Lafarge Construction Materials, and Inland Concrete Ltd. for providing me with additional support for this project.

I wish to thank my family and friends for their love and support throughout this project. Finally, I wish to thank my parents, Willard and Cheryl, for their sincere support during this study, to whom this thesis is dedicated.

Table of Contents

Permission to Use.....	i
Abstract.....	ii
Acknowledgements.....	iii
Table of Contents.....	iv
List of Tables.....	vii
List of Figures.....	viii
1. Introduction.....	1
1.1. Background.....	1
1.2. Objectives.....	3
1.3. Scope and Methodology.....	4
1.4. Outline of Thesis.....	4
2. Literature Review.....	5
2.1. Fibres.....	5
2.1.1. Vegetable Fibre Structure.....	6
2.1.2. Vegetable Fibre Mechanics.....	7
2.1.3. Effect of Alkaline Substances on Vegetable Fibres.....	8
2.1.4. Vegetable Fibre Treatment.....	9
2.2. Fibre-Reinforced Concrete.....	11
2.2.1. Fibre-Reinforced Concrete Performance.....	12
2.2.2. Bonding between Vegetable Fibre and Cement Paste.....	13
2.2.3. Vegetable Fibre-Reinforced Concrete Performance.....	16
2.2.4. Effect of Weathering on Vegetable Fibre-Reinforced Concrete Performance.....	18
2.2.5. Effect of Fibre Treatments on Bonding of Vegetable Fibre and Cement Paste.....	22

2.2.6. Effect of Fibre Treatments on Weathered Vegetable Fibre-Reinforced Concrete Performance	23
2.3. Flexural Testing.....	24
2.3.1. Open and Closed-Loop Testing.....	25
2.4. Weathering	28
2.4.1. Porosity of a Cement Matrix.....	28
2.4.2. Wetting and Drying Cycles	29
2.4.3. Freezing and Thawing Cycles	32
2.4.4. Dynamic Modulus of Elasticity	33
2.5. Literature Review Summary	34
3. Description of Experimental Study.....	36
3.1. Overview	36
3.2. Materials.....	39
3.2.1. Concrete Ingredients.....	39
3.2.2. Fibre Types	41
3.2.3. Concrete Mix Portions.....	43
3.3. Specimen Preparation.....	44
3.4. Weathering	46
3.5. Test Procedures	47
3.5.1. Compressive Strength.....	48
3.5.2. Dynamic Modulus of Elasticity	48
3.5.3. Flexural Strength and Toughness	49
3.5.4. Scanning Electron Microscope.....	51
3.5.5. Energy-Dispersive X-Ray Spectroscopy	52
4. Experimental Results and Discussion.....	53
4.1. Group One – Wetting and Drying Cycles	53
4.1.1. Fresh Concrete Properties.....	53
4.1.2. Compressive Strength.....	54
4.1.3. Dynamic Modulus of Elasticity	60
4.1.4. Flexural Strength and Toughness	66

4.1.5. Failure Modes of Fibres.....	69
4.2. Group Two – Freezing and Thawing Cycles.....	72
4.2.1. Fresh Concrete Properties.....	72
4.2.2. Compressive Strength.....	73
4.2.3. Dynamic Modulus of Elasticity	76
4.2.4. Flexural Strength and Toughness	77
4.2.5. Failure Modes of Fibres.....	80
4.3. Fibre Characteristics.....	82
4.3.1. Fibre Performance in Concrete.....	82
4.3.2. Fibre Elemental Analysis.....	86
5. Summary and Conclusions.....	90
5.1. Recommendations for Future Research	92
List of References	93
Appendix.....	101

List of Tables

Table 2.1. Selected vegetable fibre types and properties (PCA 1991, *ASM International 1994).....	7
Table 2.2. Properties of synthetic fibres (Cement & Concrete Institute 2010).....	8
Table 3.1. Coarse and fine aggregate properties.....	41
Table 3.2. Group one concrete mix proportions.....	44
Table 3.3. Group two concrete mix proportions.....	44
Table 4.1. Properties of fresh concrete from all batches in Group One.....	53
Table 4.2. Compressive strength (f _c) results of cylinders from all batches in Group One.	54
Table 4.3. Compressive strength (f _c) results of blocks from all batches in Group One.	57
Table 4.4. Flexural strength (FS) results for the beams from all batches in Group One.	67
Table 4.5. Toughness results for the beams from all batches in Group One.....	69
Table 4.6. Properties of fresh concrete from all batches in Group Two.....	73
Table 4.7. Compressive strength (f _c) results for cylinders from the First Sub-group in Group Two.....	73
Table 4.8. Compressive strength (f _c) results for blocks from all batches in Group Two.	74
Table 4.9. Dynamic modulus of elasticity (DME) for the beams from all batches in Group Two.....	77
Table 4.10. Flexural strength (FS) results for the beams from all batches in Group Two.	78
Table 4.11. Toughness results for the beams from all batches in Group Two.....	80

List of Figures

Figure 2.1. Structure of flax stem (Baley 2002).	6
Figure 3.1. Experimental program for Group One specimens	37
Figure 3.2. Experimental program for Group Two specimens	38
Figure 3.3. Coarse aggregate sieve analysis and CSA A23.1-00 constraints.	39
Figure 3.4. Fine aggregate sieve analysis and CSA A23.1-00 constraints.	40
Figure 3.5. Untreated flax fibre.....	42
Figure 3.6. Duralin treated flax fibre.	43
Figure 3.7. Silane treated flax fibre.....	43
Figure 3.8. Freeze-thaw cabinet – beam holders.	47
Figure 3.9. Acceleration test - beam setup.....	49
Figure 3.10. Flexural test – beam setup (dimensions in mm).	50
Figure 3.11. Area under load-deflection curve for flexural toughness calculation.....	51
Figure 4.1. Normalized compressive strengths of Group One cylinders.....	55
Figure 4.2. Normalized compressive strengths of Group One blocks.	58
Figure 4.3. Compressive strengths of cylinders and blocks from all batches in Group One.....	59
Figure 4.4. Dynamic modulus of elasticity (DME) for beams in the second and fourth Sub-groups of Group One.....	61
Figure 4.5. Dynamic modulus of elasticity (DME) for beams in the third and fifth Sub-groups of Group One.....	62
Figure 4.6. Typical acceleration amplitude of beams (a) after 28 day of curing, (b) after first cycle in oven, and (c) after first cycle soaking, as acquired from DME tests. 64	
Figure 4.7. Typical acceleration amplitude of (a) ambient beams after cycling was complete, (b) dry beams on last wet-dry cycle, and (c) soaked beams after the last wet-dry cycle, as acquired from DME tests.....	65
Figure 4.8. Normalized flexural strengths of Group One beams.	68

Figure 4.9. Failure surfaces of beams in the First sub-group of Group One showing (a) flax fibre, (b) Duralin treated fibre, and (c) silane treated fibre.....	70
Figure 4.10. Failure surfaces of beams in the Second sub-group of Group one showing (a) flax fibre, (b) Duralin treated fibre, and (c) silane treated fibre.	71
Figure 4.11. Normalized compressive strengths of Group Two blocks.....	75
Figure 4.12. Normalized flexural strengths of Group Two beams.	79
Figure 4.13. Failure surfaces of beams in the First sub-group of Group Two showing (a) flax fibre, (b) Duralin treated fibre, and (c) silane treated fibre.....	81
Figure 4.14. Rupture failure of (a) a flax fibre at the failure surface, and (b) a Duralin fibre several 100 μm away from the failure surface.	83
Figure 4.15. Possible loss of inner fibres during failure of Duralin fibre resulting in fibres which are (a) hollow, and (b) flat.....	84
Figure 4.16. Evidence of fibres on the failure surface is shown by (a) (silane) fibre imprints in the surface, and (b) (flax) fibre material left on the surface.	85
Figure 4.17. Silane fibre of long length.	86
Figure 4.18. Elemental analysis of cement paste.	86
Figure 4.19. Elemental analysis on the surface of (a) untreated, (b) Duralin treated, and (c) silane treated flax fibre.	87
Figure 4.20. Elemental analysis on the surface of (a) untreated, (b) Duralin treated, and (c) silane treated flax fibre, from the second sub-group in Group One.	88

1. Introduction

1.1. Background

Concrete is one of the few structural materials that is used extensively in the global construction industry today. Among its many important qualities, concrete's universal popularity is partially credited to its ability to carry loads when applied in compression. However, a plain concrete system has nearly no ability to carry loading in tension, once cracking of its cement matrix begins. This makes it essential to add reinforcement to concrete, in order to restrain tensile cracking, and prevent failure of the system.

For primary structural applications, a concrete system's tensile strength is usually completely discounted, and steel reinforcing bars are used to resist tensile forces. In semi-structural applications, like a slab-on-grade, for example, crack prevention and control can be achieved through the use of fibre reinforcement. Fibre reinforcement is able to prevent cracks from forming in a cement matrix, and control cracks from further growth. Synthetic fibres made from steel, polypropylene, and glass are commonly used in today's concrete industry for controlling cement matrix cracking. However, there is growing interest in research studies for the use of natural fibres, or more specifically vegetable fibres, as reinforcement in concrete systems.

Flax is grown extensively on the Canadian prairies, primarily for the purpose of harvesting its oilseed. The straw of the flax plant is not used for many purposes, and is typically destroyed after the oilseed is removed (Ulrich 2008). Flax straw contains a vegetable fibre which exhibits significant tensile strength. Thus, the incorporation of

flax fibre in concrete for reinforcing purposes can open up a new market for this renewable resource.

Concrete is susceptible to two main types of cracking: plastic shrinkage cracking, which occurs as the fluid concrete begins to harden, as well as cracking of the hardened cement matrix. The ability of a concrete system to resist cracking and carry some load once cracking has occurred greatly improves the performance of the system. Recent studies have compared the performance of flax fibre against widely used synthetic fibres in a cement matrix. One study has shown that the resistance to plastic shrinkage cracking in a flax fibre-reinforced concrete (FFRC) member is as good as the best performing synthetic fibre-reinforced concrete member (Boghossian and Wegner 2008).

Since vegetable fibres are a grown biological resource, they are susceptible to decomposition over time. Being subjected to moisture of any kind, for extended periods of time, is detrimental to their mechanical performance. Despite the fact that flax fibre has been shown to be an effective fibre reinforcement for the control of plastic shrinkage cracking, there is some concern that the fibre may deteriorate in a highly alkaline concrete environment and lead to the degradation of FFRC (Wang 2003). The current focus of vegetable fibre-reinforced cement-based composites (VFRC) research is now in the area of long term performance.

Though all types of vegetable fibres are known to degrade when submersed in any liquid, it is currently only theorized that all vegetable fibre types embedded in a cement matrix and subjected to its pore water solution will eventually degrade. Researchers have explored the performance of several types of VFRC, excluding FFRC, by subjecting specimens to rapid cycles of weathering, in order to monitor how the performance of their reinforced and unreinforced specimens are changed over time. After weathering is completed, the mechanical performance of the specimens and the condition of the fibres give an indication of whether certain vegetable fibres are degrading over time in the cement matrix. Of particular concern is the effect of wetting and drying as well as freezing and thawing on the durability of VFRC. Other studies have also experimented with only long periods of specimen immersion in water.

Another area of interest is the possibility of altering the vegetable fibres with certain treatments, before they are used as reinforcement, with the goal of improving their resistance to degradation. Chemicals and heat are two types of treatments which have been performed on vegetable fibres used in VFRC. The treatments are used in order to make the vegetable fibres less susceptible to degradation, when in contact with moisture.

Though some researchers have studied the long-term durability of a few types of VFRC, there has currently been no previous research pertaining to the long-term durability of FFRC systems, or the long-term degradation of flax fibres embedded in a cement matrix. The ability of FFRC systems to show durable properties after being subjected to typical weathering phenomena is of extreme importance before it can be used as a construction material.

1.2. Objectives

The primary objective of this research project was to quantify the long-term durability of flax fibre-reinforced concrete (FFRC) systems. The specific sub-objectives of this research project were:

- to determine the extent to which the mechanical properties of FFRC systems will degrade when subjected to cycles of wetting and drying;
- to determine the extent to which the mechanical properties of FFRC systems will degrade when subjected to cycles of freezing and thawing; and
- to determine whether the inclusion of heat or chemically treated flax fibre will alter the results of the first two specific sub-objectives.

1.3. Scope and Methodology

This research project involved the testing of flax fibre-reinforced concrete (FFRC) cylinders and beams. These specimens were subjected to two types of cyclic weathering scenarios: wetting and drying, and rapid freezing and thawing. Four materials were tested with each weathering scenario. These included unreinforced concrete, untreated flax fibre-reinforced concrete, heat treated flax fibre-reinforced concrete, and chemically treated flax fibre-reinforced concrete. Compression tests were carried out on FFRC cylinders to quantify the ultimate compressive strength. Flexural tests were carried out on FFRC beams to quantify the modulus of rupture and flexural toughness. The flexural tests were conducted under closed-loop displacement controlled conditions, in order to capture the post-peak load-displacement response of the beams.

Two groups of specimens were prepared, each subject to one of the two weathering scenarios. Each group included specimens tested after the 28 day moist curing period and after the weathering cycles were complete.

1.4. Outline of Thesis

The thesis consists of five chapters, in addition to references and appendices. The present chapter presents an introduction to the thesis. Chapter 2 presents a literature review regarding fundamentals of vegetable fibres, the theoretical basis of fibre-reinforced concrete (FRC), and the performance of vegetable fibre-reinforced cement-based composites (VFRC). Chapter 3 details the experimental program and Chapter 4 covers experimental results, analysis and discussion of results. Chapter 5 presents conclusions of this study and recommendations for future research.

2. Literature Review

2.1. Fibres

There are three types of natural fibre which are found in various forms on earth: animal, mineral and vegetable. Natural fibres have been used throughout history for one purpose or another, mainly because of their ability to be easily manipulated for use in different applications. But only recently has there been much research concentrating on the mechanical properties of the vegetable fibre.

This rise in scientific research related to vegetable fibre is mainly attributed to two main factors. The first factor is the large amounts of naturally occurring vegetable fibre around the world which goes unused once vegetation is harvested. The second factor is the increasing knowledge of how well vegetable fibres perform when loaded in tension. An engineering material like vegetable fibre, which is economically feasible and can perform well in engineered applications, is of great interest and importance to design engineers.

This chapter introduces the structure of vegetable fibres and how that structure contributes to their mechanical properties. This chapter also explains how the structure in vegetable fibres can be affected by certain substances, and presents ways of reducing those effects through the use of fibre pre-treatments. In addition, the use of vegetable fibres in concrete is reviewed, as well as the testing and weathering of fibre-reinforced concrete.

2.1.1. Vegetable Fibre Structure

There are several types of vegetable fibres found in nature; these include sisal, jute, coconut, flax, wood and bamboo. The structure of these fibres is similar to the structure of the flax stem shown in Figure 2.1. The flax stem is made up of fibres of varying diameters and lengths. The lengths of the elementary fibre are in the range of 20 to 50 mm and are composed of a polyhedral cross-section, with diameters ranging from 10 to 20 μm . The grouping of the elementary fibres (single plant cells) make up the technical fibre, which is of a size that can easily be incorporated into concrete.

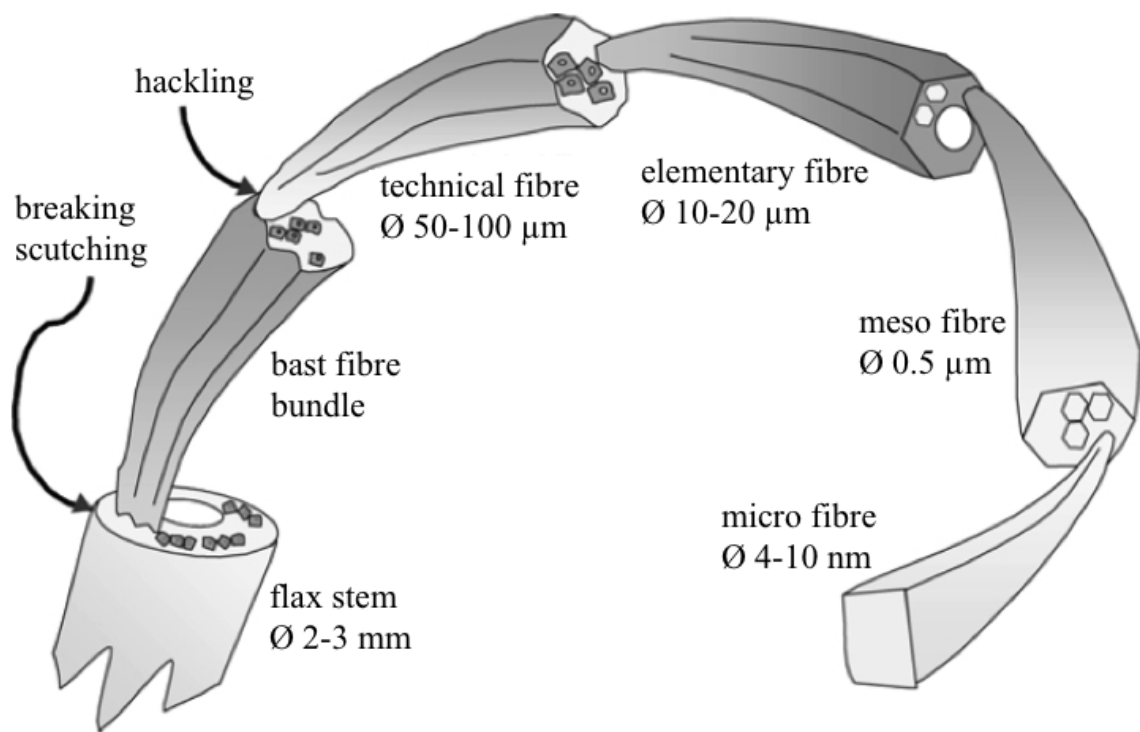


Figure 2.1. Structure of flax stem (Baley 2002).

Vegetable fibres contain three main components: lignin, hemicellulose and cellulose, all of which contribute to the structure of the fibre. All vegetable fibre is made up of these three components, in varied amounts. The cellulose component consists of long chains of glucose molecular units, extended along the length of the elementary fibre, while the hemicellulose and lignin act as binders to keep the fibre together (Gram

1988). The mechanical properties of the fibre are governed by how the cellulose is oriented in the fibre and how much hemicellulose and lignin is present (Bos et al. 1999).

2.1.2. Vegetable Fibre Mechanics

Natural fibres derived from vegetation tend to exhibit high tensile strengths and relatively high stiffnesses, due to the orientation and bond strength between their main components. Table 2.1 shows the varying properties found in some vegetable fibres. Flax fibre exhibits the highest average tensile strength among the natural fibres, making it an ideal candidate for reinforcement in concrete.

Table 2.1. Selected vegetable fibre types and properties (PCA 1991, *ASM International 1994).

Fibre type	Diameter (µm)	Density (10 ³ kg/m ³)	Young's modulus (GPa)	Tensile strength (MPa)	Failure strain (%)
Wood Cellulose	20 - 120	1.5	10 - 40	300 - 900	-
Sisal	< 200	0.75 - 1.07	13 - 26	280 - 565	3 - 5
Coconut	100 - 400	1.12 - 1.15	19 - 26	120 - 200	10 - 25
Bamboo	50 - 400	1.5	33 - 40	350 - 500	-
Jute	100 - 200	1.02 - 1.04	26 - 32	250 - 350	1.5 - 1.9
Flax*	10 - 100	1.5	100	840	1.8

The mechanical properties of some synthetic fibres commonly used for the purpose of reinforcement are shown in Table 2.2. When comparing the mechanical properties of flax fibre with these eleven synthetic fibres, the modulus of elasticity and ultimate tensile strength of flax fibre are similar to the average values achieved by most polymer fibres.

The mechanical properties of vegetable fibres are thought to be influenced by how the plant is grown and harvested. The conditions of the ground and the climate may affect the orientation and amounts of each main fibre component. There are also several processes for extracting fibres from the plants, which involve exposing the plants to water or chemicals. Each process affects the components of the fibre which are later extracted from the plants (Olubayo 2010).

Table 2.2. Properties of synthetic fibres (Cement & Concrete Institute 2010).

Fibre type	Diameter (µm)	Density (10 ³ kg/m ³)	Young's modulus (GPa)	Tensile strength (MPa)	Failure strain (%)
Acrylic	13 - 104	1.16 - 1.18	14 - 19	270 - 1000	7.5 - 50
Aramid I	12	1.44	60	2900	4.4
Aramid II	10	1.44	115	2350	2.5
Carbon, PAN HM	8	1.6 - 1.7	380	2500 - 3000	0.5 - 0.7
Carbon, PAN HT	9	1.6 - 1.7	230	3450 - 4000	1.0 - 1.5
Carbon, pitch GP	10 - 13	1.6 - 1.7	27 - 35	480 - 790	2.0 - 2.4
Carbon, pitch HP	9 - 18	1.8 - 2.15	150 - 480	1500 - 3100	0.5 - 1.1
Nylon	23	1.14	5	970	20
Polyester	20	1.34 - 1.39	17	230 - 1100	12 - 150
Polyethylene	25 - 1000	0.92 - 0.96	5	75 - 590	3 - 80
Polypropylene	-	0.9 - 0.91	3.5 - 4.8	140 - 700	15

2.1.3. Effect of Alkaline Substances on Vegetable Fibres

The concern with placing vegetable fibres in a cement matrix is that they will be subjected to the alkaline pore water, which could break down the fibres over time. An earlier study concluded that the high alkalinity of pore water in concrete, commonly of a pH of 13, reacted with the lignin component in sisal fibre and caused the mechanical performance of the fibre to degrade (Gram 1988). Another study found that after 300 days in an alkaline solution, sisal and coconut fibres lost all of their flexibility and tensile strength (Toledo Filho et al. 2000). A later study stated that after extensive periods of time in pore water solution, all three main components of flax fibres undergo deterioration (Wang 2003). Other tests found the tensile strength of vegetable fibres like sisal and coconut to decrease when exposed to various simulated pore solutions. This study concluded that the loss of tensile strength was a result of a loss in the hemicellulose and lignin components of the fibres (Ramakrishna and Sundararajan 2005a). Another study found that palm fibre exposed to simulated pore water solutions lost more than half their initial strength values (Kriker et al. 2008).

A recent study looked at the mechanical properties of flax fibre after being exposed to a simulated concrete pore water solution (Olubayo 2010). This study

simulated the degradation that flax fibre may undergo when placed in a cement matrix. The flax fibres' tensile strength and elastic modulus were found to decrease as the time of exposure to the pore solution increased. This study showed that the flax fibres lose their ability to carry tensile loads, the longer they are exposed to a simulated concrete pore solution. The loss of strength was attributed to the break down of technical fibres into their component elementary fibres due to the deterioration of the lignin that holds the elementary fibres together.

All studies discussed in this section subjected vegetable fibres directly to simulated pore water solutions, instead of embedding them in cement matrices. It is important to study the degradation of vegetable fibres in cement matrices, as simulated testing cannot realistically quantify the actual degradation.

2.1.4. Vegetable Fibre Treatment

Vegetable fibres have the unique ability to absorb moisture from the surrounding atmosphere and retain water that it comes into contact with. A fibre's abilities to both absorb and retain are a function of how much hemicellulose and lignin are present in the fibre. One study found that hemp fibre had greater moisture absorption as the hemicellulose was reduced and less moisture absorption as lignin was reduced (Pejic et al. 2007). Conversely, the hemp fibre retained less water as the hemicellulose was reduced and retained more water as the lignin was reduced.

Current research on vegetable fibres is focused on pre-treatments. These treatments manipulate the fibres' abilities to absorb and retain moisture, since those very abilities promote the degradation of the fibres. Most of the vegetable fibre research is in the area of polymer-based composites, where small amounts of absorbed moisture into fibres can be detrimental to the composite's performance.

The treatments used on vegetable fibres make use of various chemical and physical conditioning scenarios. All treatments aim to alter the main components of the fibre, in order to decrease its ability to absorb moisture, and improve the chemical bond between the vegetable fibres and the surrounding polymer matrix. Most of the treatments used on the vegetable fibre achieve a reduction in moisture absorption and

create the desired bond characteristics by removing the hemi-cellulose and lignin components from the fibre. Unfortunately, the removal of any amount of these fibre components will result in reducing the fibre's tensile capacity. Invariably, most vegetable fibre treatments are damaging to the fibre's mechanical components, but help increase their resistance to degradation over time (Olubayo 2010).

As illustrated in Section 2.1.3, the mechanical properties of vegetable fibre are diminished when exposed to an alkaline solution. If fibres are able to stay relatively unsaturated, then they are not capable of losing any of their main components, and their mechanical properties will stay intact. Treated vegetable fibre has been successfully used in polymer-based composites, simply because the fibres are not embedded in a saturated matrix environment. However, the matrix environment of a cement-based composite like concrete may be saturated with pore water for most of its life span.

Some common chemical treatments used on vegetable fibre include mercerization, silane, acetylation and acrylation (Olubayo 2010). These treatments are performed by soaking the vegetable fibres in chemical solutions, in order to change the bonding characteristics of their main components or make the fibres react more strongly with a particular polymer matrix. These four chemical treatments are mainly performed on vegetable and man-made fibres used for reinforcement of polymer-based composites.

A heat treatment referred to as Duralin involves pressure heating flax fibres, which causes their hemi-cellulose and lignin components to depolymerise and develop into a water resistant resin, which keeps the cellulose components together (Stamboulis et al. 2001).

One study has shown that sisal and coconut fibres given a mercerization treatment were less susceptible to degradation in a simulated concrete pore solution than untreated fibres (Toledo Filho et al. 2000). Another study performed the Duralin heat treatment on flax fibres, and tested their moisture absorption and tensile strength at 66% relative humidity (Stamboulis et al. 2001). The study found that the treated flax fibres absorbed about 20% less moisture and retained almost 20% more of their mechanical properties when compared to the untreated fibre.

A more recent study treated flax fibre with an assortment of different chemical treatments used on fibres intended for use in polymer-based composites (Olubayo 2010).

These treatments included mercerization, silane, acetylation and acrylation. Once the flax fibre was treated, it was immersed in a simulated concrete pore solution. All five types of fibre, treated and untreated, were found to perform similarly after being subjected to the same testing. The flax fibres' tensile strength, modulus of elasticity, mass loss, water retention, pH and electron paramagnetic resonance (EPR) were found after soaking in the pore solution for several weeks. The tensile strength and elastic modulus decreased by at least 50% in all fibre types. All fibres recorded a loss of mass and a slight increase in water retention. The pH of the pore solution, which all five fibre types were subjected to, decreased slightly over time. The EPR test made the silane treatment stand out among the others, as it was the one fibre type which was least reactive to the simulated pore solution. More details regarding the performance of treated fibre in cement matrices are discussed in Section 2.2.3.

2.2. Fibre-Reinforced Concrete

Cracks can form during the initial curing stages when concrete is rapidly drying after being placed, allowing mix water to evaporate and the concrete surface to form shrinkage cracks (Boghossian and Wegner 2008). Regardless of the cause, once cracking has developed in the cement matrix, more water and other substances may be able to flow more easily through the system, and the degradation of the concrete may increase over time. Therefore, the control or delay of crack growth in a concrete system, through the use of fibre reinforcement, may substantially increase the performance and service life of that system.

Unreinforced concrete fails in a brittle manner. The addition of fibre reinforcement may allow for more tensile loads to be carried after initial cracking of the concrete system occurs, which could increase the system's toughness and durability. Many different combinations of type, size and volume fraction of fibres are used in concrete systems to produce the desired reinforcing effect.

The first published papers studying the effects of fibre reinforcement in concrete date back to the early 1960's, when it was conceived that the strength of concrete would increase with the inclusion of small, closely spaced, fibres (Romualdi and Batson 1963). Much of the fibre-reinforced concrete research has focussed on the use of man-made or synthetic fibres, including steel, glass, and polymers, and their ability to prevent and control cracking in concrete systems. Synthetic fibres are manufactured and non-renewable; however, the inclusion of vegetable fibres creates a market for naturally grown and renewable fibre reinforcement.

The first naturally occurring fibre to be tested and widely used as reinforcement in concrete was the asbestos fibre, which later proved to be hazardous. In fact, the search for a suitable replacement has brought about the interest in studying natural fibres as reinforcement in cement composites (Castro and Naaman 1981).

The mechanical performance of vegetable fibre-reinforced non-cement-based composites is mainly attributed to the orientation of components within the vegetable fibre, but also in fibre bonding technologies (Biagiotti et al. 2004). The durability of these non-cement composite materials is attributed to fibre treatment technologies described in Section 2.1.4, which decrease the fibres' ability to absorb moisture (Olubayo 2010).

2.2.1. Fibre-Reinforced Concrete Performance

Since fibre reinforcement is used to control cracking in a cement matrix, the performance of fibre-reinforced concrete (FRC) is dependant on how well the cracks in the cement matrix are controlled. The performance of an FRC system must therefore be partly attributed to the strength of the fibre-cement bond and type of fibre-cement failure mechanism. The two most common failure mechanisms in FRC are rupture and pull-out. Rupture involves the fibre breaking once a crack in the matrix is formed, whereas pull-out involves the fibre continually bridging the crack as it grows.

The type of bond and failure in an FRC system should then be considered before determining the appropriate type, size, and volume fraction of fibres. One study compared the performance of flax, polypropylene and glass fibres for reinforcing

concrete, at varying sizes and volume fractions (Wang 2003). This study has shown that each unique combination of type, size, and volume fraction of fibres, for the same cement mix, produces a unique bond and failure characteristic in the reinforced concrete.

The fibre-cement bond and fibre-cement failure mechanism are related to one another, since they are both a function of the type and size of fibres used in an FRC system. The type of bond and failure achieved depends on the type of fibre used and the type of matrix the fibre is embedded in. The type of fibre and matrix used determines whether the fibre-cement bond is formed chemically, mechanically, or both. Steel fibres obtain their cement bond mechanically through their corrugated shapes, whereas vegetable fibres like cellulose are able to create chemical bonds as well as mechanical ones (Coutts 1987b). The type and strength of the fibre-cement bond then determine the type of fibre failure mechanism formed in the FRC system.

Sections 2.2.2 through 2.2.6 further explore vegetable fibre-cement bonding and failure mechanisms. These sections describe several studies which explain how vegetable fibre-reinforced concrete performance is affected by different combinations of fibre type, size, and volume fraction, as well as matrix type. Vegetable FRC performance is generally categorized by brittle and ductile fibre-cement failure mechanisms. When the vegetable fibre-cement bond is strong, the fibre ends up rupturing at the face of the crack, resulting in a brittle failure mechanism. When the vegetable fibre-cement bond is not as strong, the fibre is gradually pulled out of the matrix. The gradual pull-out results in a ductile failure of the fibres, and creates the flexural toughness in the system.

2.2.2. Bonding between Vegetable Fibre and Cement Paste

The research pertaining to vegetable fibre bond in cement paste focuses on how the bonds are formed, maintained over time, and changed with respect to environmental conditions. As was explained in Section 2.1, all vegetable fibres are made up of the same main components in varying amounts. These similarities in fibre composition help explain the similarities in fibre-cement bonding and failure of different fibre types.

An extensive early study on VFRC concluded that there are four variables which govern the bond between fibre and cement paste: water/cement ratio, porosity, fibre morphology, and compaction (Coutts 1987b). This study states that these four variables determine the amount of cement particles present in the pore water, which come into contact with the fibres. This study also states that the bonding of cellulose fibres with cement paste is created both chemically and mechanically.

The ingress of cement or hydration particles into the vegetable fibre, by way of the pore water, is referred to as mineralization. This ingress of pore water has been found to decrease the amount of hemicellulose and lignin components in the fibre (Bilba et al. 2003). Various studies have reported that the mineralization of vegetable fibres like sisal, kraft, coconut, and eucalyptus, cause the fibre to create a stronger bond with the surrounding cement paste (Bentur and Akers 1989, de Andrade Silva et al. 2009, Mohr et al. 2005, Rodrigues et al. 2006, Savastano Jr. et al. 2002 and 2009, Soroushian et al. 1994 and 1996, Toledo Filho et al. 2000, Tonoli et al. 2010b and 2010c). These same studies also report that the ingress of cement particles causes the fibres to become stiff and brittle over time, lowering their mechanical performance and durability.

One study explored sisal fibre failure in a cement matrix, and found that debonding between fibre and matrix was dependant on embedment length (Morrissey et al. 1985). The study concluded that an embedment length of 10 mm usually resulted in failure by pullout, whereas an embedment length of 60 mm usually caused the fibre to fail by snapping or rupture. These different failure mechanisms are a result of the critical fibre length, at which the failure mechanism will change from pull-out to rupture. Another study investigated cellulose fibre-reinforced cement-based composites and how their fibre failure mechanisms changed when placed under different moisture conditions (Coutts and Kightly 1982). The failure mechanisms were fibre fracture and pull-out when the specimens were dried or saturated, respectively. Saturated FRC specimens are those which have all of their pores fully saturated. The study concluded that in both types of failures the fibre-cement paste bond was still strong, which meant that the pull-out failures occurred because of the moisture's ability to break down the fibre's internal bonds. A follow up study concluded that oven dried specimens were stronger and more brittle than saturated specimens (Coutts and Kightly 1984). This study also concluded

that specimens neither dried nor saturated achieved the most desirable results. Enhanced bond of hemp fibre to cement paste was achieved when fibres were saturated before mixing, compared to fibres being mixed in a dry state (Li et al. 2006).

Three separate studies tested sisal fibre-reinforced cement-based composites at varying fibre volume fractions (Ramakrishna and Sundararajan 2005b, Savastano Jr. et al. 2005 and 2009). All studies tested their composites under dry conditions and all found the fibres to fail in pull-out.

Another recent study concluded that fibre bond loss was attributed to cycles of volumetric expansion and shrinkage of the fibre due to variation of temperature and moisture conditions (Rodrigues et al. 2006). Another study also found that the ability of vegetable fibres to retain moisture, which then causes volumetric changes in the fibre, contributes to micro cracking of the cement paste and degradation of the fibre paste bond (Tonoli et al. 2007).

An extensive study on sisal and coconut fibre-reinforced cement-based composites looked at the interface between the fibre and cement matrix, also referred to as the transition zone (Savastano Jr. and Agopyan 1999). It was observed that an increase in water-cement ratio caused an increase in the transition zone thickness and that there was a higher porosity in the cement matrix near the transition zone. This creation of porosity in the transition zone resulted in an insufficient fibre-cement bond. Some relationships between the transition zone characteristics and the overall properties of composites were also explored. When the concrete was mixed, fibres collected a large amount of the mix water and increased the size of the transition zones. Since the fibre degradation increased with the age of the specimens, the transition zones became weak points in the composite. In a related study investigating palm fibre-reinforced concrete, voids were found to have formed in the transition zone between the fibre and the cement matrix, when subjected to hot-dry curing conditions (Kriker et al. 2005).

A few studies have concluded that the reduction in flexural toughness of a vegetable fibre-reinforced cement-based composite over time is due an increase in the fibre-matrix bond through mineralization, which causes the fibre to become brittle and fail in rupture (Kim et al. 1999, Toledo Filho et al. 2000). More detail related to how

VFRC mechanical properties are affected by vegetable fibre bonding are presented in Section 2.2.4.

2.2.3. Vegetable Fibre-Reinforced Concrete Performance

Vegetable fibre-reinforced cement-based composites (VFRC) are a fairly new technology, and have seen an increase in research attention within the past three decades. The types of vegetable fibres that have been studied in VFRC include bamboo, cellulose, coconut, cotton, eucalyptus, flax, hemp, kraft, palm, and sisal. Many of these studies focused on measuring the mechanical properties of the VFRC in comparison to synthetic fibre-reinforced cement-based composites (SFRC) or unreinforced cement-based composites, while making variations in fibre volume fraction, fibre lengths, cementitious materials, mixing procedures, and weather scenarios.

As explained in Section 2.2.2, when mixing vegetable fibres in a cement-based composite, the fibres actually lose some of their hemicellulose and lignin. Numerous studies have found that these lost components react with the paste around the fibres and end up slowing down the hydration of the paste (Soroushian and Marikunte 1991, Savastano Jr. et al. 2000, Bilba et al. 2003, Li et al. 2004a, Aamr-Daya et al. 2008, Sedan et al. 2008, Stancato et al. 2005, and Soroushian et al. 2009). Another study has found that the inclusion of cellulose fibre as reinforcement in a cement-based composite created higher early strength than unreinforced composites (Soroushian and Ravanbakhsh 1999).

In fibre-reinforced concrete research, any fibre quantities less than 2% are considered to be low, and all percent volume fractions greater than 2% are considered to be high. Though this research study is focused on a low volume fraction of vegetable fibre, one study has found that flax fibre improved the compressive strength and flexural toughness in cement mortars, with the inclusion of fibre at 5% by volume fraction (Fernandez 2002). Though the fibre size was identified as being that of a bast fibre upon mixing (see Figure 2.1), SEM analysis of the cracked specimens revealed individual fibres the size of elementary fibres, suggesting that the mixing process tended to break the fibre down into elementary fibres.

Flexural toughness of concrete reinforced with palm fibre in amounts ranging from 0.05-0.2% by weight was significant and comparable to that obtained with glass fibre (Al-Oraimi and Seibi 1995). Flexural toughness of concrete reinforced with flax fibre in amounts ranging from 0.1-0.5% by volume fraction was significant and comparable to that obtained with glass fibre (Wang 2003). Flexural toughness was increased when concrete was reinforced with hemp fibre in the range of 0.18% to 0.84% by weight (Li et al. 2004b). A recent study showed that larger flexural strength and toughness were gained in concrete reinforced with hemp fibre, in amounts ranging from 0.18%-1.06% by weight, when fibres were saturated before mixing, as compared to fibres mixed in a dry state. (Li et al. 2006). One study followed the performance of concrete reinforced with palm fibre at 0.6% and 0.8% by volume fraction, and found that over time the flexural toughness slightly decreased due to the ongoing reaction between the fibre and the alkaline pore water (Abdul Razak and Ferdiansyah 2005).

A research topic in VFRC not experimentally undertaken in this current research project, is the influence that supplementary cementitious materials have on the durability and performance of vegetable fibre in the cement matrix. Several studies found that replacing some Portland cement with silica fume caused a reduction in pore water alkalinity and prevented embrittlement of the sisal and coconut fibre in cement-based composites (Gram and Bergstrom 1984, Gram and Nimityongskul 1987, and Toledo Filho et al. 2003). Another study found an increase in compressive and fracture toughness with age in high-volume fly ash concrete reinforced with hemp fibres (Siddique 2005). A most recent study found that replacing a portion of the Portland cement with calcined clay reduced the amount of calcium hydroxide in the paste, and thus decreased the amount of mineralization and degradation experienced by sisal fibres (de Andrade Silva et al. 2009).

Another important research topic in VFRC not experimentally undertaken in this research project, is the ability for VFRC to restrain plastic shrinkage cracking. As stated at the beginning of Section 2.2, controlling cracking in a cement matrix greatly increases its long-term durability. One study found that plastic shrinkage cracking was significantly reduced when a cement composite was reinforced with 0.06% by volume fraction of cellulose fibre (Soroushian and Ravanbakhsh 1998). Two separate studies

with cement composites reinforced with sisal fibre, at 0.2% by volume fraction, found a reduction in free and restrained shrinkage cracking (Toledo Filho and Sanjuan 1999, Toledo Filho et al. 2005). The resistance to plastic shrinkage cracking in concrete reinforced with flax fibre, at 0.3% by volume fraction and 38 mm lengths, was found to be as significant as the best performing synthetic fibre-reinforced concrete (Boghossian and Wegner 2003).

2.2.4. Effect of Weathering on Vegetable Fibre-Reinforced Concrete Performance

Much of the VFRC research is focused on subjecting the composites to various types of weathering scenarios, which typically follow rapid cycles of wetting and drying as well as freezing and thawing. This research is interested in how the fibres react to the constant cyclic migration of pore water as well as temperature variations. Natural weathering has also been undertaken by some researchers. There is also one scenario which does not follow the typical cyclic weathering pattern, but simply involves testing VFRC specimens after being saturated for an extended period of time.

Three separate studies tested high fibre percent volume fraction VFRC specimens to discover any differences in performance between saturated and unsaturated specimens (Mai et al. 1983, Coutts 1987a, and Soroushian et al. 1995). The fibres used in these studies included flax, cellulose, and eucalyptus. All studies found that the flexural toughness was larger for saturated specimens in comparison to specimens tested unsaturated. All studies concluded that the fibre was made less stiff and the fibre-cement bond was weakened when the fibres were saturated, which allowed for a ductile pull-out fibre failure. Two other studies subjected cellulose fibre-reinforced cement-based composites to over 50 days in water at 60°C, and found that the flexural strengths were only slightly reduced (Soroushian and Marikunte 1995, Neithalath 2006).

Flexural tests were performed on cement-based composites, reinforced with kraft fibre at 1-2% by weight, which were saturated for 48 hours before testing (Soroushian and Marikunte 1991). The study concluded that saturating the composites caused a degradation of the fibre-matrix bonding, which changed the fibre's failure mechanism from rupture to pull-out, and caused the specimens' flexural strength to decrease and

toughness to increase. A more recent study claimed that moisture content of cellulose fibre-reinforced cement-based composites, with fibre at 0.6-2% by volume fraction, affected the performance in flexural testing (El-Ashkar et al. 2007). The study found that as the specimens were dried, their flexural toughness decreased and the fibre failure changed from pull-out to a combination of pull-out and fracture.

An early study concluded that maintaining sisal fibre-reinforced concrete in a stable environment, like dry at room temperature or soaking in water, will not affect their flexural performance (Gram 1988). However, introducing cycles of wetting and drying causes a large reduction in flexural toughness. More detail on styles of wetting and drying cycles used in VRFC research will be presented in Section 2.4.2. This same study also stated that frequent changes in temperature and relative humidity in tropical environments cause significant embrittlement of sisal fibre-reinforced concrete when compared to non-tropical environments.

Two separate studies tested high fibre percent volume fraction VRFC specimens to determine if wetting and drying cycles affected the flexural performance of cellulose and sisal VRFC. Both studies found a decrease in flexural toughness after subjecting VRFC specimens to wetting and drying cycles. The first study found that the decrease in toughness may be due to the mineralization of fibres after the composites are aged (Soroushian and Marikunte 1995). The second study found that refinement or beating of the fibres caused fibrillation or roughening of the fibres' outer layer (Tonoli et al. 2007). The decrease in toughness of the composite was thought to come from the increase in mechanical bond between the roughened fibre and the cement paste, which caused the fibres to fail in a more brittle manner.

The flexural toughness of concrete specimens reinforced with cellulose fibre at 0.5% by volume fraction decreased after being subjected to wetting and drying cycles (Sargaphuti et al. 1993). The loss in toughness was thought to be a result of the cycles creating a stronger bond with the cement paste, and also weakening the structure of the fibres. Another early study subjected kraft fibre-reinforced cement-based composites, with 2% by weight of fibres, to wetting and drying cycles (Soroushian et al. 1994). After performing flexural tests on the composites, it was found that the fibre in the weathered specimens failed by rupture whereas the fibre in the un-weathered specimens failed by a

combination of rupture and pull-out. The study concluded that the constant migration of water into the fibres allowed for faster movement of hydration particles into the fibres, also referred to as mineralization, which created a denser transition zone and greater bond between the fibre and the cement matrix. Similar conclusions were established in a study subjecting cement-based composites reinforced with coconut and sisal fibre at 2% to wetting and drying cycles (Toledo Filho et al. 2000).

One study performed 300 rapid freezing and thawing cycles on cement-based composites, reinforced with 2% by mass of kraft fibre, based on the ASTM standard C666a (Soroushian et al. 1994). The study found that unreinforced composites saw a decrease in their dynamic modulus of elasticity, while kraft fibre-reinforced composites remained relatively unchanged. A more recent study performed 100 rapid freezing and thawing cycles on cement-based composites, reinforced with 2.5% by volume fraction of cellulose fibre (Neithalath 2006). The study also found that the reinforced composites showed more damage resistance after dynamic modulus testing. Natural and rapid freezing and thawing were performed on extruded cement-based composites reinforced with 2-8% wood fibre by weight (Shao et al. 2000). The study found that exposing the specimens to five months of winter in Montreal caused a decrease in their flexural strength and an increase in toughness. Other naturally weathered samples were also subjected to four rapid freezing and thawing cycles before testing, and were found to have gained flexural strength and lost toughness. The study concluded that the natural weathering kept the fibres in a saturated and ductile state, whereas the rapid cycles kept drying out the fibres and made them brittle.

An insightful research topic in VFRC, not experimentally undertaken in this research project, is the influence of natural weathering on the performance of VFRC. Two studies tested high fibre percent volume fraction VFRC specimens to determine if weathering in a tropical climate affected their flexural performance. The toughness of sisal and eucalyptus fibre-reinforced cement-based composites, with 3% fibre by volume fraction, decreased after being exposed to four summer months in the Brazilian environment (Roma Jr. et al. 2008). The study concluded that the ease of migration of water through the cement paste's pore system increased the alkaline attack on the fibres, which then lowered the toughness of the specimens. A most recent study examined fique

fibre-reinforced cement-based composites, with 3% fibre by weight, which were exposed to 14 years of natural weathering in the Colombia environment (Tonoli et al. 2011). The specimens experienced a breakdown of fibre-matrix bond that was thought to be due to the cycling of water in and out of the fibres, which caused the fibres to expand and contract.

One study subjected sisal, coconut, and eucalyptus fibre-reinforced cement-based composites, with 2% fibre by volume fraction, to natural and artificial weathering scenarios (Savastano Jr. et al. 2002). The natural weathering scenario was 16 months in the Brazilian environment while the artificial weathering scenario involved 900 cycles following ASTM G53-96, which follows cycles of four hours in air at 50°C and four hours under a water spray. The study found that the artificial weathering produced no damage on the samples, whereas the natural weathering reduced the flexural strength and toughness of the specimens. The loss of mechanical properties in the specimens was thought to be because of mineralization of the fibres and damage of the fibre-matrix transition zone. Two other studies examined cement-based composites reinforced with coconut fibres at 2% by volume fraction, after over 10 years in the Brazilian environment (Agopyan et al. 2005, John et al. 2005). Both studies also found that the fibres became brittle due to mineralization at varying degrees.

Another insightful research topic in VFRC not experimentally undertaken in this research project, is the influence of carbonation on the performance of VFRC subjected to weathering cycles. Providing a carbon rich environment is thought to replicate the processes involved in natural weathering. Two studies have compared the performance of cellulose fibre-reinforced cement-based composites after being weathered naturally and artificially in a carbon rich environment (Bentur and Akers 1989, MacVicar et al. 1999). Both studies found that artificial weathering cycles which featured a carbon rich environment better replicated natural weathering, as compared to normal un-carbonated weathering cycles. The two studies concluded that natural and artificial carbon-rich weathering both produce high mineralization of fibres and high densification of the cement matrix. Two other studies also found that incorporating carbonation on cement-based composites before or during wetting and drying cycles still resulted in high

mineralization of cellulose and sisal fibre, as well as high densification of the cement matrix (Soroshian et al. 1996, Tonoli et al. 2010a).

2.2.5. Effect of Fibre Treatments on Bonding of Vegetable Fibre and Cement Paste

As was discussed in Section 2.1.3, vegetable fibre treatments are generally implemented to reduce the fibres' ability to take on moisture, which can eventually lead to the total destruction of its mechanical properties. Though vegetable fibre treatments change the mechanical properties of fibres to varying degrees, they also change the physical and chemical makeup of the fibres, which governs the type of bonding the fibre will achieve in a cement paste.

Three separate studies reported that an alkaline treatment, also referred to as mercerization, of coconut, hemp, and straw (of unspecified type) fibres resulted in improved bonding with the cement paste compared to untreated fibres (Li et al. 2007, Sedan et al. 2008, and Zheng et al. 2010). One study found that performing a bleaching treatment, also an alkaline treatment, on eucalyptus fibres caused a loss of lignin in the fibre and a rougher fibre surface (Tonoli et al. 2010c). This change in fibre characteristics caused greater mineralization of the fibres once cast in the cement and an improved fibre-cement bond.

One study found that one type of silane treatment on bagasse fibre decreased its ability to retain moisture, while still creating better bond with cement paste (Bilba and Arsene 2008). Another study found that performing different types of silane treatments on cellulose fibre produced distinct bonding scenarios (Tonoli et al. 2009). One type of silane treatment acted much like the untreated fibre, in that there was large ingress of cementitious products into the fibres, creating a strong fibre-paste bond. The other silane treatment allowed less ingress of products, which resulted in a weaker fibre-paste bond.

Pyrolysis treatment, also referred to as a heat treatment, performed on bagasse fibre was found to increase its surface roughness, which was thought to improve the fibre-matrix adhesion (Bilba and Arsene 2008).

2.2.6. Effect of Fibre Treatments on Weathered Vegetable Fibre-Reinforced Concrete Performance

As was explained in Section 2.2.4, VFRC research is mainly focused on subjecting the composites to various types of weathering scenarios, which typically follow rapid cycles of wetting and drying and freezing and thawing, as well as natural weathering and extended periods of saturation. More research is focusing on various treatments for vegetable fibre used as reinforcement in cement-based composites, before being subjected to testing or weathering scenarios.

Three separate studies subjected high percent volume fractions of cellulose, kraft, and eucalyptus fibre to bleaching, which is an alkaline treatment (Mai et al. 1983, Mohr et al. 2005, Tonoli et al. 2010b). The treated fibres were then placed in cement-based composites and subjected to artificial weathering. All three studies found that the bleached fibres allowed for more mineralization and better cement bonding, when compared to unbleached fibres. The composites reinforced with unbleached fibre achieved higher flexural toughness, because of the fibres ability to fail by pull-out, due to the weaker cement bond. Another high fibre percent volume fraction study found that performing a type of silane treatment on kraft fibre allowed for more resistance to deterioration of kraft fibre-reinforced cement-based composites subjected to wetting and drying cycles, as compared to untreated fibre-reinforced composites (Blankenhorn et al. 1999). A most recent high fibre percent volume fraction study found that performing an acid treatment on cellulose fibre produced an increase in flexural toughness of cellulose fibre-reinforced cement-based composites subjected to wetting and drying cycles, as compared to untreated fibre-reinforced composites (Tonoli et al. 2009). The increase in flexural toughness was attributed to the lack of mineralization in the acid treated fibres, as compared to the large amounts of mineralization in the untreated fibre.

One study has shown that mercerization, also referred to as an alkaline treatment, improved the resistance to deicing salt attack of cement-based composites reinforced with cotton fibres at 0.1% by volume fraction (Pichor et al. 2000). The treatment allowed for more ingress of ions into the fibre, because of its high reactivity with the pore water, which actually decreased the fibres' mechanical properties. However, this

decrease in the fibres' mechanical properties did not seem to impede on the composites' resistance to deicing salts.

Performing acid, alkali, or heat treatments on bagasse fibres resulted in varied performance of bagasse fibre-reinforced cement-based composites (Arsene et al. 2007). Cement-based composites reinforced with alkaline or heat treated bagasse fibre at 1-5% by weight had similar flexural strengths as cement-based composites reinforced with the same amount of untreated fibre. However, cement-based composites with acid treated bagasse had much lower flexural strengths compared to those reinforced with alkaline, heat, or un-treated fibre, and performed more like unreinforced systems. The study concluded that the acid treatment was most effective in reducing the tensile strength of the fibres, which led to a reduction in composite performance.

Paraffin wax treated lechuguilla fibre was used as reinforcement in cement-based composites at 1% by volume fraction, and was found to create a more durable composite (Juarez et al. 2007). The study found that after subjecting the treated fibre-reinforced cement composite to wetting and drying cycles, its flexural strength was increased approximately 10% as compared to the untreated fibre-reinforced cement composites.

A most recent study performed wetting and drying cycles as well as long durations of soaking, on flax fibre-reinforced cement-based composites (Aly et al. 2011). The study found that although the fibres were treated in an alkaline solution before mixing, the composites still saw a reduction in their toughness because of fibre embrittlement due to mineralization.

2.3. Flexural Testing

Flexural testing reveals the fibres' contribution to the behaviour of the cracking as well as the flexural properties of the beam. Even though all flexural testing involves the bending of beams, the rate at which the beam is loaded influences the flexural performance achieved. A vegetable fibre-reinforced cement-based composite (VFRC) beam which is loaded at a faster rate will perform differently from a beam which is

loaded at a slower rate. More drastic differences in flexural performance can be found when comparing open-loop and closed-loop testing.

2.3.1. Open and Closed-Loop Testing

The open-loop flexural test has been the only type of test used in VFRC research, with one exception, which is discussed later in this section. The open-loop test involves producing either a constant cross-head displacement rate or loading rate. Open-loop testing is not ideal for testing fibre-reinforced composites in flexure. However, the advanced equipment and technology needed for closed-loop testing usually leaves the open-loop test as the only option.

Closed-loop testing is better suited for fibre-reinforced composites in flexure, because the setup is able to properly record the specimen's behaviour after its maximum load is reached and its first crack is formed. At the point of cracking, the beam releases built up energy and causes instability under open-loop test conditions. However, closed-loop testing compensates for the sudden release (Bernard 2009). The performance of the specimen after its maximum load is reached is also referred to as the post-peak response. The post-peak response can only be accurately recorded with a closed-loop displacement-controlled test (Wang 2003).

For the closed-loop test, a deflection rate is set and controlled using feedback from a displacement sensor to be constant throughout the test, even when the load suddenly drops when the specimen cracks.

The deflection in the closed-loop flexural test is recorded by two displacement reading devices which are placed at mid-span, on either side of the beam. Each device is attached to thin bar, also referred to as a yoke, which has its two ends attached to the beam, over both supports. This setup is shown in Figure 3.8 in Section 3.5.3. The yoke setup allows the devices to record mid-span deflections in the beam. Deflections due to seating and twisting of the beam, as well as elastic displacement of the load frame and supports, are not recorded when the yoke is used (Banthia and Trottier 1995).

Three types of specimens have been used for flexural VFRC research: the beam, the small beam, and the sheet. Beams have a relatively square cross section and follow a

ratio of one to three for specimen height to span length. Small beams follow the same specifications as the regular beams, except that their largest cross sectional dimension ranges from 10 mm to 50 mm. Sheets have cross sections with one cross sectional dimension much smaller than the other and do not follow any set dimensional ratio. The yoke setup has been used to test VFRC beams (Soroushian et al. 1994, Fernandez 2002, Wang 2003, Abdul Razak and Ferdiansyah 2005, Kriker et al. 2005 and 2008), small beams (Soroushian and Marikunte 1991), as well as sheets (Soroushian and Marikunte 1995, Soroushian et al. 1995), but only under open-loop test conditions.

Since all of the VFRC research up until now has only used open-loop flexural testing, there have been studies using both cross-head displacement and load rates to control the testing. Tests conducted on beams have used both types of control rates evenly, whereas small beam and sheets have been mostly conducted using cross-head displacement control. One study performed closed-loop flexural tests on sheets. For these tests, a notch was cut across the bottom of the sheet at its mid-span, and the test rate controlled by recording the instantaneous notch growth due to cracking (Sargaphuti et al. 1993).

Another factor in the setup of the flexural test which affects the results of the test is whether the specimens are under three-point or third-point loading. The three-point loading configuration setup has two supports and one point load on top of the beam at mid-span; this produces a varying moment all along the length of the specimen. The third-point loading setup has two supports and two point loads on the top of the beam, producing a constant moment in the middle third of the specimen. VFRC beam research has been conducted using both setup styles evenly, whereas small beam and sheet research has used the three-point load configuration more extensively than third-point loading.

Once the flexural testing is completed, there are various options for analysing the post-peak response of the specimen. Though most standards have specific steps to follow for the testing of specimens and the analysis of data, most VFRC studies use combinations or pieces of standards for testing, and then follow a specific standard for data analysis.

Two standards which are commonly used in VFRC research for data analysis testing procedures are the ASTM Standard C1018 (Al-Oraimi and Seibi 1995, Fernandez 2002, Abdul Razak and Ferdiansyah 2005, Li et al. 2007, Aly et al. 2011) and the Japanese Standard JSCE-SF (Soroushian et al. 1994, Soroushian and Marikunte 1995, Toledo Filho et al. 2000, Toledo Filho et al. 2003). Both standards define the flexural toughness of a beam by first calculating the area under the load-deflection curve, but both standards present their toughness in different formats. ASTM C1018 provides toughness indexes which are a ratio of the entire area under the load-deflection curve at a specific deflection to the area under the load-deflection curve before reaching the peak load. JSCE-SF provides a toughness factor which relates the entire area under the load-deflection curve and the dimensions of the beam itself.

One study investigated these two standards and outlined how their procedures create incorrect results for flexural toughness (Banthia and Trottier 1995). The study then proposed a test setup and data analysis procedure for acquiring proper toughness results. The closed-loop displacement controlled test was suggested for recording the true beam displacement, as well as keeping the post-peak response from becoming unstable. The study also suggested not using the data before the peak load for calculating the toughness, as there is human error related to identifying the point where the matrix first cracks.

Only one VFRC study has specifically followed the ASTM Standard C1399-98 method directly for testing beams (Wang 2003). This standard is used to obtain the post-peak response of the specimen, using the residual strength method, with an open-loop testing setup. Beams are placed in third-point loading, on top of a steel plate, and loaded until the first crack is formed. The beam is unloaded and then reloaded without the plate, until failure. The use of the plate is to minimize the damage sustained by the specimen when it cracks, so that an accurate post-peak response may be measured using open-loop conditions.

An updated method for testing fibre-reinforced concrete beams in flexure, ASTM Standard C1609-07, incorporates the closed-loop testing setup. This method is described in greater detail in Section 3.5.3.

2.4. Weathering

As was explained in Section 2.1.3, water or alkaline substances are detrimental to the mechanical performance of vegetable fibres. The current research strategy for determining the performance and limitations of vegetable fibre-reinforced cement-based composites (VFRC) involves subjecting specimens to weathering cycles, as presented in Sections 2.2.4 and 2.2.6. As shown in these sections, there are four types of weathering used in VFRC research: rapid wetting and drying, rapid freezing and thawing, periods of saturation, and natural weathering.

Apart from the type of fibre and weathering scenario used on an VFRC specimen, there are two factors which may influence the specimen's performance: the mix design and the duration of weathering cycles. Both of these factors influence the amount of pore water migrating in and out of the cement matrix, which could be potentially damaging to the vegetable fibres.

2.4.1. Porosity of a Cement Matrix

When air is introduced into concrete during the mixing stage, a network of pore pathways is generated in the finished concrete. This system of connected pores in the cement matrix, which can vary in volume depending on the mix design, allow for water and other solutions to travel into the concrete throughout its life span.

The porosity of any cement-based composite is a function of its water/cement ratio. The use of admixtures in the composite, like air entrainment or superplasticizer, also influences the formation of its pore structure. One publication found that cement-based composites with high water/cement ratios were able to take on more water over time, than similar composites with lower water-cement ratios (Maekawa et al. 1999).

There is still more detail to the pores themselves, which dictates the rate at which a cement-based composite matrix takes on or gives off pore water. The size and shape of the pores in a cement matrix generate a capillary suction when partially saturated, which aids in the taking on of moisture and hinders the release of moisture. This means that a cement matrix with smaller pores will take on more water more quickly when

submerged, than a composite with larger pores. Therefore, a composite with larger pores should be able to dry out more quickly than a composite with smaller pores.

However, as composites are subjected to repeated wet-dry cycles, which cause them to constantly take on and give off pore water, their pore system may be at risk of becoming damaged and their capillary suction lowered as a result. For composites with smaller pores, this means that the rate at which they would take on moisture begins to decrease, and longer soak times may be required to take on the amounts generated by their previously higher capillary suction.

The performance of a cement-based composite is not only at risk because of the degradation of the pores, but also from the structure of the pore system itself. One study reported a relationship between the compressive strength of the cement-based composite and its porosity, finding that as the porosity of the matrix decreased, the strength increased, and vice versa (Roy et al. 1993). This was attributed to the fact that creating more pores in the matrix also created more voids for cracks and stress concentrations to form. The study revealed that composites with compressive strengths around 30 MPa tend to have approximately 40% of their volumes occupied by capillary pores.

2.4.2. Wetting and Drying Cycles

The difference in cross sectional dimensions between beams and sheets, as defined in Section 2.3.1, may lead to a variation in the performance of specimens subjected to weathering cycles. With identical mix designs and weathering conditions, the entire pore system of a sheet may become saturated and dried during short periods of submersion and drying, while a beam may only have its outer thickness exposed to cycling of the moisture content, leaving the centre volume of the beam potentially untouched by the weathering process. This occurrence would make the comparison of performances between beams and sheets difficult, and the effect of weathering on sheets rather extreme compared to beams.

One study has performed wetting and drying cycles on VFRC beams, whereas all other similar studies considered sheets instead (Juarez et al. 2007). This beam study incorporated two different styles of weathering, with both having a total of 15 cycles.

The first style subjected the samples to 24 hours in a humid oven and 24 hours in a dry oven, while the second style subjected the samples to 24 hours in water and 24 hours in a dry oven.

There are two standards used in VRFC research which focus specifically on wetting and drying cycles for cement-based composite sheets: the British Standard EN 494 and ASTM C1185. One researcher has used the British Standard EN 494 for testing VRFC, and did so using two separate scenarios over four studies. The first study involved cycles of 18 hours in water at 20°C and 6 hours in an oven at 60°C, with a total of 100 cycles performed (Tonoli et al. 2007). The other three studies cycles involved only 170 minutes in water at 20°C and 170 minutes in an oven at 70°C, but performed 200 total cycles (Tonoli et al. 2009, Tonoli et al. 2010a, and Tonoli et al. 2010b).

Two studies have followed ASTM C1185 for testing VRFC sheets. The first study performed two scenarios. One involved 25 cycles of 175 minutes in water at 30°C, 5 minutes in air at 20°C, 175 minutes in an oven at 60°C, and five minute in air at 20°C. The other involved only soaking of samples for 56 days in water at 60°C (Soroushian and Marikunte 1995). The second study performed the same soaking as the previous study, except the length of time was extended from 56 days to 100 days (Neithalath 2006).

Some researchers have experimented with the lengths of cycle times in order to find a length which best cycled the moisture in and out of the samples. One study's cycles involved 24 hours in water at 18°C and six days in air at 23°C and 40.1% relative humidity (Toledo Filho et al. 2000). This cycling scenario was chosen because 72% of the water retained in 24 hours was lost after sitting for six days. A different study used cycles of 23.5 hours in water at 20°C, half an hour in air at 22.5°C and 60% relative humidity, 23.5 hours in an oven at 65°C and 20% relative humidity, and 0.5 hours in air at 22.5°C and 60% relative humidity (Mohr et al. 2005). This cycling was chosen based on testing which monitored the mass gain and loss during wetting and drying of the specimens. The time allotted to wetting and drying was said to allow for less than a 1% change in mass after a three hour period.

There have been numerous studies which used wetting and drying cycles similar to those found in standards and from past research, but do not make reference to either. Two such studies are almost identical in the cycling scenarios they used, with the first going 30 minutes in water at 10°C and 330 minutes in an oven at 105°C for 120 cycles (Gram 1988), and the second going 30 minutes in water and 330 minutes in an oven at 80°C for 120 cycles (Soroushian et al. 1994).

Some of the wetting and drying cycle studies also incorporated air drying into their cycling along with oven drying. One study used cycles of 20 hours in water at 20°C, four hours in air at 20°C, 20 hours in an oven at 100°C, and four hours again in air at 20°C (Sargaphuti et al. 1993). Another study performed 25 cycles of 72 hours in water at 27°C, 24 hours in air at 27°C and 72 hours in heated air at 70°C (Aggarwal 1995). Other studies on wetting and drying cycles left out oven drying and only considered air drying. One researcher performed cycles of seven days in water at 25°C and seven days in air at 40°C and 30% relative humidity (Blankenhorn et al. 1999). Another study used 100 cycles of 24 hours in water at 30°C and 48 hours in a chamber with 36°C air being blown at 0.5 m/s (de Andrade Silva et al. 2009).

Another modification to the typical wetting and drying scenario, which is not covered in this research project, is the incorporation of accelerated carbonation. One study performed 25 cycles of eight hours in water, one hour in an oven at 80°C, five hours in a rich carbon dioxide environment, nine hours in an oven, and one hour of cooling, to help generate results which more closely follow the process of natural weathering (Soroushian et al. 1996).

The purpose of wet-dry cycling is to produce an effect in a specimen similar to that produced by natural weathering. Though the different styles of wet-dry cycles described in this section all produce degradation on cement-based composites, it can not be said whether one style of weathering is superior to the other, since different fibre and mix designs were used in each study.

2.4.3. Freezing and Thawing Cycles

The expansion of water when frozen has proven to be detrimental to cement matrixes, as expanding pore water produces tensile stresses in the surrounding paste. Vegetable fibres may also be susceptible to degradation when saturated and frozen, due to this same build up of stresses. Thus, rapid freeze-thaw cycles are performed on VFRC in order to study the effects on the composite's mechanical performance.

There is only one standard used in VFRC research which focuses specifically on freezing and thawing cycles for cement-based composite beams, ASTM C666 – Resistance of Concrete to Rapid Freezing and Thawing. Only one VFRC study has utilized this standard, performing cycles which followed ASTM C666a, and started after 14 days of moist curing (Soroushian et al. 1994). This version of the standard keeps the specimens under water while they are thawed and frozen. This standard also subjects the beams to 300 cycles of 4°C to -18°C to 4°C in two to five hours.

There have been three other studies reported in the literature which performed freezing and thawing cycles but did not reference any particular standardized test. The first study performed cycles of 24 hours in water at 20°C, 24 hours in air at -17°C, two hours in air at 20°C and 22 hours in a blowing air oven at 80°C (MacVicar et al. 1999). The second study performed four cycles consisting of 18 hours in water at 40°C, six hours in air to reach -40°C, 18 hours at -40°C, and then 6 hours in water to reach 40°C (Shao et al. 2000). The third study submerged its specimens in water before cycling, with cycling started after 14 days of moist curing (Neithalath 2006). The cycles used were five hours at -16°C, then the raising of temperature at 6.3°C per hour until 22°C was reached, and then five hours at 22°C. Two different rates were used for lowering the temperature after 5 hours at 22°C; the first was 7.5°C per hour until -8°C was reached and the second was 1.5°C per hour until -16°C was reached.

The purpose of freeze-thaw cycling is to produce an effect in a specimen similar to that produced by natural weathering. Though the different styles of freeze-thaw cycles described in this section all produce degradation on cement-based composites, it can not be said whether one style of weathering is superior to the other, since different fibre and mix designs were used in each study.

2.4.4. Dynamic Modulus of Elasticity

The dynamic modulus of elasticity (DME) uncovers changes in the stiffness of VFRC beams, through non-destructive testing. ASTM standard C215 – Fundamental Transverse, Longitudinal, and Torsional Resonant Frequencies of Concrete Specimens, presents a method for measuring the natural frequencies of concrete beams and calculating the DME as a function of the natural frequency. The stiffness of the beams is directly related to its recorded natural frequency. The natural frequencies of the VFRC beams are found by first impacting the beams with a hammer and measuring their acceleration time histories. Then, a Fourier transform is performed on the acceleration signals and a natural frequency is found for each specimen. As the stiffness of the specimens changes, due to the weathering cycles, the dynamic modulus will reflect these changes through the change in natural frequency. ASTM Standard C215 also states that as the beams degrade over the weathering cycle period, their damping becomes greater. This means that the acceleration amplitude impact response should become shorter as the weathering cycles progress.

No studies have documented the use of ASTM Standard C215 on VFRC beams. However, one study used ASTM Standard C666, and presented values of relative DME on VFRC beams, generated from the transverse mode every 20 cycles (Soroushian et al. 1994). This study found that VFRC beams retained their DME when subjected to rapid freezing and thawing cycles, while unreinforced beams experienced a reduction.

Two other studies performed non-destructive tests on VFRC beams, in order to obtain a DME. The first study used ASTM Standard E1876 for generating the transverse or out-of-plan flexure mode on beams. ASTM Standard E1876 and C215 are identical in their procedure for determining the DME, although each standard uses different specimen sizes, so the calculation of correction factors for the DME are slightly different (Neithalath 2006). The second study used ASTM Standard C597 for generating the longitudinal mode on beams, which is a different mode than that explored in the previous two studies (Aamr-Daya et al. 2008). ASTM Standard C597 uses a different method for determining the natural frequency of beams, but it references C215 for the

calculation of the DME. Unreinforced beams were found to have twice the value of DME than 10% flax fibre-reinforced beams.

2.5. Literature Review Summary

Past research focusing on the capability of flax fibre-reinforced cement-based composites (FFRC) has shown that the flax fibre can add as much plastic shrinkage cracking restraint as the fibres used in industry. But one factor these studies have not taken into consideration is the possibility that flax fibres will degrade over time.

Some research has shown that the degradation of flax fibres is a possibility, especially when the fibres come into contact with a highly alkaline substance like concrete pore water. These studies have shown that when flax fibre is subjected to a simulated pore water solution, it experiences degradation of the fibres' lignin component, which causes the mechanical properties of the fibres to decrease.

Other research has sought to reduce the degradation of flax fibre in highly alkaline substances like concrete pore water. These studies have investigated the use of treatments to change the physical and chemical make up of the flax fibre. One study imposed a heat treatment which caused the flax fibre to take on less moisture, when compared to untreated fibre. Another study found that one type of silane treated flax fibre was less reactive to a simulated pore water solution, when compared to acid and alkaline treated fibres, as well as untreated fibres. Though these studies have shown that flax fibres may become more durable, they have not subjected the treated flax fibres to cement matrixes for the purpose of long-term durability analysis.

One recent study has performed wetting and drying cycles on alkaline treated FFRC specimens. The study found that the composite's toughness was reduced because of fibre embrittlement, caused by mineralization. This study did not consider the use of heat or silane treated flax fibres, nor did it consider a weathering scenario like freezing and thawing.

Past studies have subjected other types treated and untreated vegetable fibre-reinforced cement-based composites (VFRC) to wet-dry cycles, and the majority have found that the flexural toughness increases and the dynamic modulus of elasticity remains stable. Thus, flax fibre should be no exception to the trend that vegetable fibres do not significantly degrade in cement paste over time, and VFRC can maintain its mechanical properties after being weathered. But these weathering conditions must be administered on FFRC in order to reinforce this hypothesis.

The current study was undertaken to determine the extent to which the mechanical properties of heat and chemically treated FFRC systems degrade, when subjected to cycles of freezing and thawing as well as wetting and drying, and compared them with untreated FFRC.

3. Description of Experimental Study

3.1. Overview

Two types of test specimens were used in this project: flax fibre-reinforced concrete (FFRC) beams with dimensions 75 x 100 x 400 mm, and FFRC cylinders with a diameter of 100 mm and length of 200 mm. This beam size was chosen to accommodate the rapid freeze-thaw cabinet used in this study.

For the purpose of performance comparisons, four different materials were used, including concrete with no flax fibre, untreated flax fibre, heat treated flax fibre, and chemically treated flax fibre. The heat and chemical treatments employed were Duralin and silane, respectively. These treatments are described in detail in Section 3.2.2.

Two groups of specimens were prepared, each subject to one of the following weathering scenarios: wet-dry cycling and freeze-thaw cycling. Within each group, specimens were tested after the 28 day moist curing period and after the weathering cycles were completed.

Group one contained five sub-groups of 16 beams and 16 cylinders each, all of which were cast in the Structures lab at the University of Saskatchewan. All five sub-groups included four beams and four cylinders for each of the four different types of concrete used in this study. The first sub-group of 16 beams and 16 cylinders was tested after the 28 day moist curing period. This sub-group provided a baseline for the properties of each type of concrete at 28 days. The second sub-group of 16 beams and 16 cylinders was tested after they had been subjected to 50 four day cycles of wetting and drying. The third sub-group of 16 beams and 16 cylinders was tested after 25 eight day cycles of wetting and drying. More details on the wet-dry cycle times and procedures are presented in Section 3.4. The dynamic modulus of elasticity was also

found for all beams after every soaking and drying period, in order to monitor changes in beam stiffness. The second and third sub-groups provided an indication of how weathering affected the performance of each type of concrete. The fourth and fifth sub-groups of 16 beams and 16 cylinders were set aside in the ambient laboratory environment while the second and third sub-groups were weathered, and then tested when the second and third sub-groups were tested. The fourth and fifth sub-groups provided a basis for comparison of the properties of the weathered specimens tested at the same age. Before each of the 80 beams from all five sub-groups were tested in flexure, its dynamic modulus of elasticity was measured. After all 80 beams were tested in flexure, each beam had both of its ends sawed off at lengths of 150 mm, and the beam end prisms of 75 x 100 x 150 mm were tested in compression. The experimental program for the Group One specimens is presented in Figure 3.1.

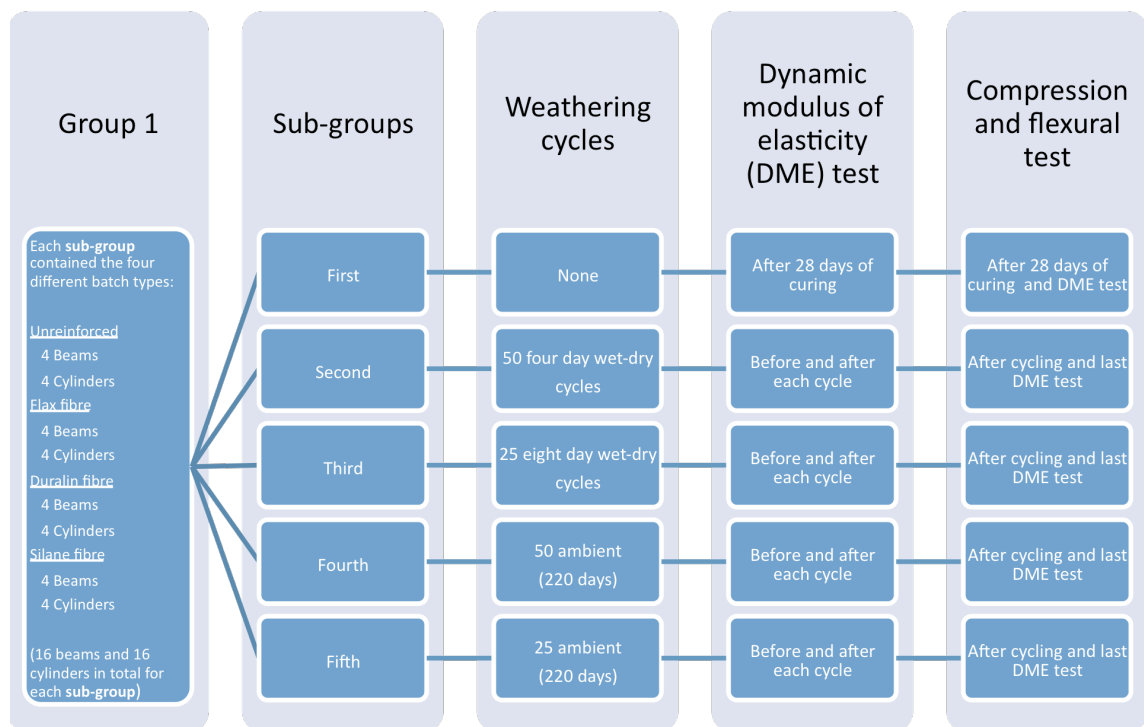


Figure 3.1. Experimental program for Group One specimens

Group Two contained three sub-groups, all of which had 16 beams, and one of which also had 16 cylinders. All of the specimens in group two were cast at Lafarge's research laboratory in Richmond, B.C. All three sub-groups in group two included four

beams for each of the four different types of concrete being used in this study. The only exception was that the first sub-group also had four cylinders for each of the four different types of concrete. The first sub-group, which consisted of 16 beams and 16 cylinders, was sent to the Structures lab at the University of Saskatchewan and tested after the 28 day moist curing period. This sub-group provided a baseline for the properties of each type of concrete at 28 days. The second sub-group of just 16 beams was tested after they had been subjected to 300 cycles of rapid freezing and thawing. This sub-group provided an indication of the influence of freezing and thawing on the properties of each type of concrete. The third sub-group of 16 beams was set aside in ambient laboratory conditions while the second sub-group was weathered, and then tested when the second sub-group was tested. This sub-group provided a basis for comparison of the properties of the weathered specimens tested at the same age. Before each of the 48 beams from all three sub-groups were tested in flexure, their dynamic modulus of elasticity was measured. After all 48 beams were tested in flexure, each beam had both of its ends sawed off at lengths of 150 mm, and the beam end prisms of 75 x 100 x 150 mm were tested in compression. This type of compression specimen was chosen since the rapid freeze-thaw cabinet used could not accommodate cylindrical specimens. The experimental program for the Groups two specimens is presented in Figure 3.2.

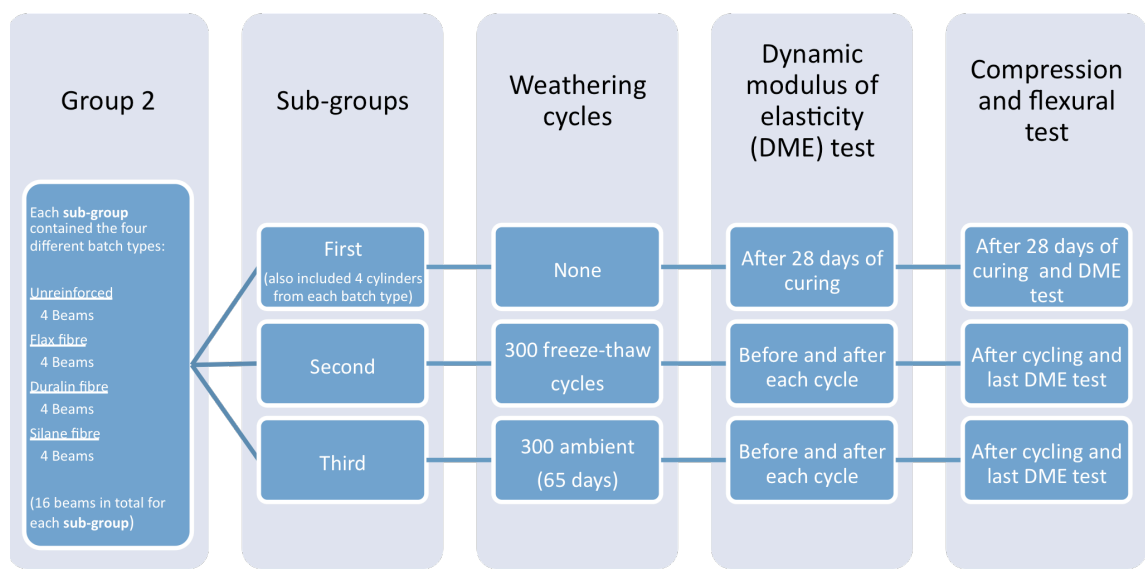


Figure 3.2. Experimental program for Group Two specimens

3.2. Materials

3.2.1. Concrete Ingredients

Since the two groups of specimens used in this study were mixed in different provinces, different coarse and fine aggregates were used to produce each group. The methods used to perform a sieve analysis for all coarse and fine aggregates followed CSA Standard A23.1-00 (Concrete Materials and Methods of Concrete Construction); results can be seen in Figures 3.3 and 3.4, along with the specified range given in the standard. The coarse aggregate from both groups had a 14 mm nominal maximum size. The coarse aggregate used in the concrete for group one followed the sieve constraints, as shown in Figure 3.3.

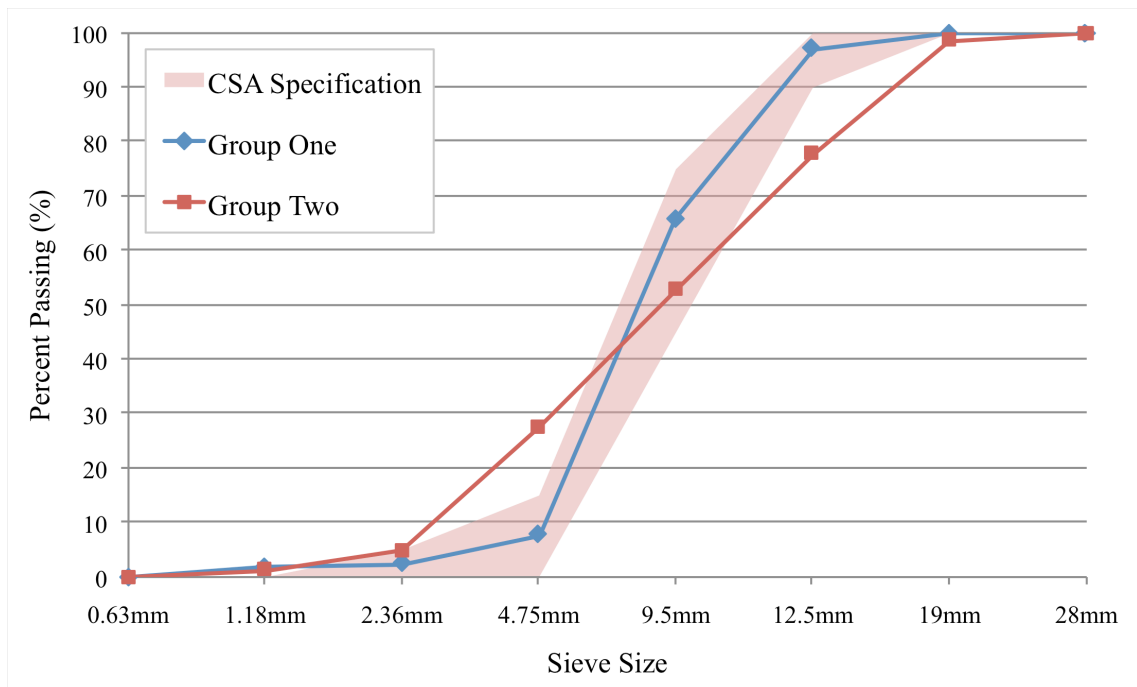


Figure 3.3. Coarse aggregate sieve analysis and CSA A23.1-00 constraints.

For group two, there was no single aggregate type available which followed the gradation sieve constraints, so two different coarse aggregate types were combined, referred to as 14 mm and 5 mm. However, as shown in Figure 3.3, the best combination

of the two types, consisting of 48% of the 14 mm and 52% of the 5 mm, was still significantly out on the 4.75 and 12.5 mm sieve constraints. The two different types of fine aggregate used for the group one and two concrete mixes were both within the specified sieve constraints, as shown in Figure 3.4.

The properties of aggregates used in group one were measured in the geotechnical laboratory at the University of Saskatchewan, whereas the properties of the group two aggregates were provided by the Lafarge staff in Richmond B.C. All aggregate properties can be seen in Table 3.1.

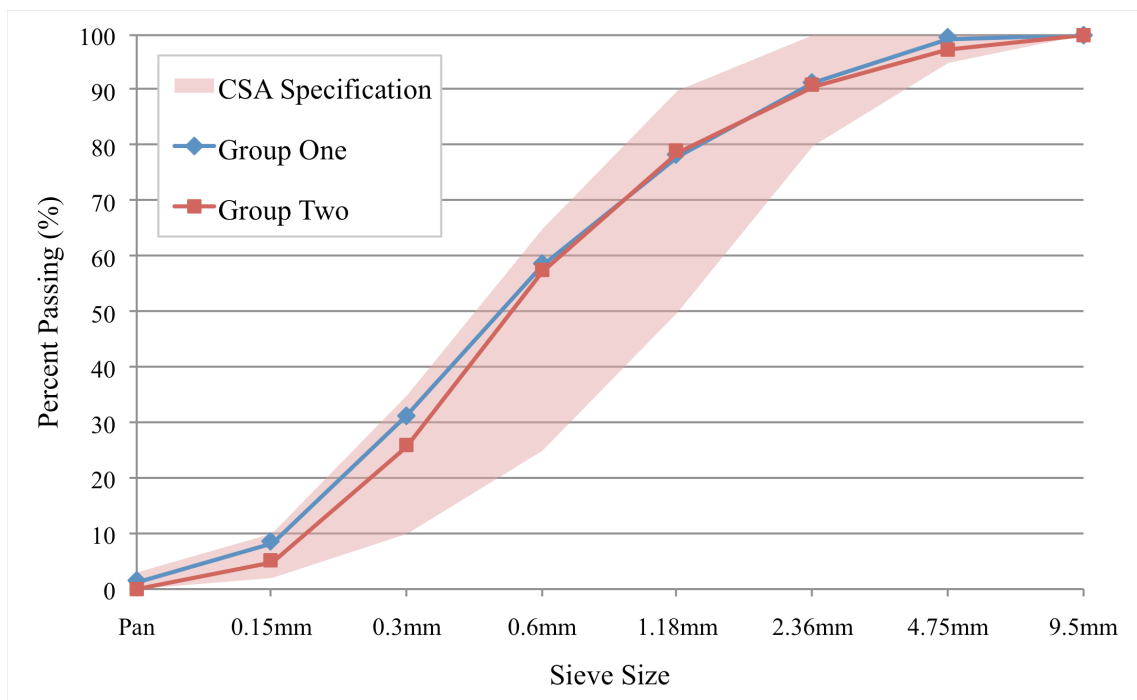


Figure 3.4. Fine aggregate sieve analysis and CSA A23.1-00 constraints.

The cement used for both groups was the standard Type 10 Portland cement. The water used for both groups was the tap water provided in each laboratory. The air-entraining admixture and superplasticizer used for both groups were MB AE 90 and Glenium 7101, respectively.

Table 3.1. Coarse and fine aggregate properties.

Aggregate		Bulk relative density	Bulk relative density (SSD*)	Apparent relative density	Absorption (%)	Moisture content (%)
Group One	Coarse	2.546	2.600	2.691	2.113	0.021
	Fine	2.548	2.589	2.658	1.618	0.016
Group Two	14 mm	2.711	2.746	2.811	1.036	2.110
	5 mm	2.578	2.629	2.718	2.006	2.015
	Blend sand	2.651	2.669	2.700	0.682	5.570

* SSD=saturated surface-dry

3.2.2. Fibre Types

The flax fibre used in this study was extracted from flax straw grown in Saskatchewan and supplied by Biolin Research Inc. in Saskatoon. The fibre was processed mechanically using equipment in the Agricultural and Bioresources laboratory at the University of Saskatchewan. Three machines were used to progressively clean the fibre: a picker (model PKR, Belfast Mini Mills, Prince Edward Island), small fibre separator (model SFS, Belfast Mini Mills, P.E.I.), and large carder (model LCR, Belfast Mini Mills, P.E.I.). This process removed virtually all shives from the fibre. After cleaning, the fibres were cut to 38 mm lengths using a slicing machine (model CTR, Belfast Mini Mills, P.E.I.) located in the same laboratory. After these processes, approximately 2.5 kg of cleaned and chopped flax fibre was available for use.

The two treatments performed on this raw flax fibre included Duralin and silane treatments. Duralin is a treatment which required an autoclave for high pressure heating, and the silane treatment required first subjecting the fibres to an alkaline solution and then a silane solution.

The Duralin treatment described in Stamboulis et al. (2001) was performed by subjecting the cleaned flax fibre to steam at a temperature of 160°C for 30 minutes in an autoclave (scientific pre-vacuum sterilizer, model SV-120, Steris Corporation, Mentor, OH). Then the fibre was dry heated at a temperature of 150°C for two hours in an oven (Iso Temp Oven model 630G, Fisher Scientific, Hampton, NH).

The silane treatment was performed by washing the flax fibre in a solution with 2% clothing detergent, rinsing it in distilled water and then drying it at 70°C for 24 hours. The fibre was then immersed in a 5% sodium hydroxide solution for one hour, followed by rinsing in distilled water and then drying at 70°C for 24 hours. This step is also referred to as mercerization as described in Olubayo (2010). The fibre was then immersed in a mixture of ethanol and water at 60:40, with the addition of the coupling agent triethoxysilane, at 2.5% by weight. While the fibres were immersed for 30 minutes, the solution was continuously adjusted to keep the pH between 3.5 and 4. The fibres were then removed from the solution, rinsed in distilled water and then dried at 70°C for 24 hours.

The differences in surface texture between the three types of fibres used in this study are shown in the SEM images presented in Figures 3.5, 3.6, and 3.7. The surface of the untreated fibre seems to be rough, whereas both the Duralin and silane treated fibres seem to have smoother surfaces. This may be caused by the loss of wax and impurities as a result of the treatment processes. As shown in these figures, the fibres were a mix of technical and elementary fibres before being mixed into the concrete. The SEM images in Chapter 4, in Sections 4.1.5, 4.2.5 and 4.3.1, show evidence that after mixing, only elementary fibres could be found on the crack surface of the concrete.

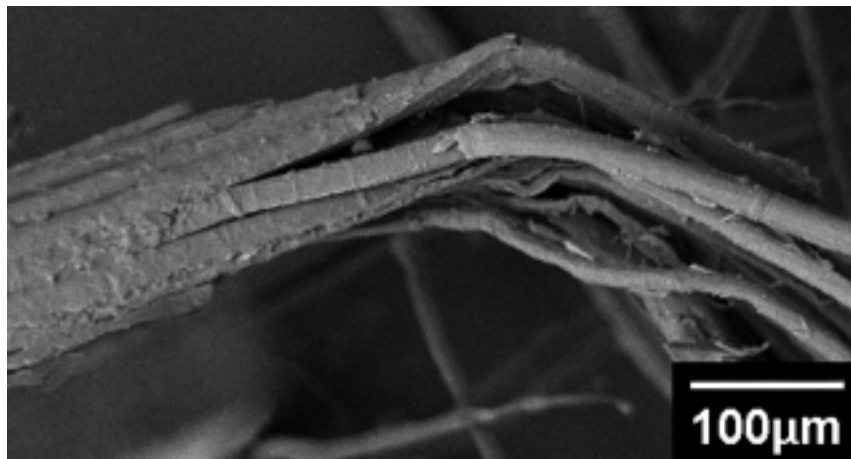


Figure 3.5. Untreated flax fibre.

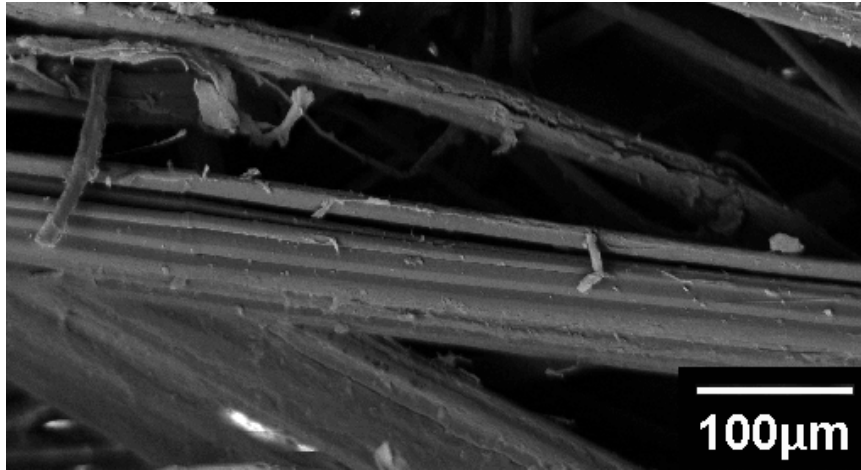


Figure 3.6. Duralin treated flax fibre.

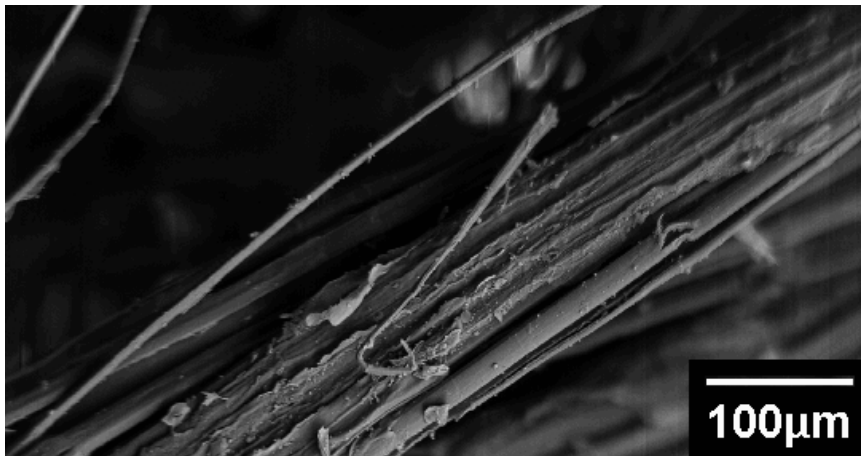


Figure 3.7. Silane treated flax fibre.

3.2.3. Concrete Mix Portions

The concrete mix design for this study was selected to have 32 MPa minimum specified compressive strength after a 28 day curing period, which corresponds to exposure class C-2 from CSA Standard A23.1-00. This mix design was ideal for this study, because it is typically used for concrete in slab or pavement design – structures which are typically subjected to much natural weathering and small tensile loads.

The concrete mix proportions for this study were modelled after a previous study of flax fibre-reinforced concrete (Wang 2003), and are presented in Tables 3.2 and 3.3. The previous study gave recommendations for mix proportions, based on the outcomes

of the research. The study recommended that a 50% sand to total aggregate ratio be used with the inclusion of flax fibre, in order to increase the amount of fibre to cement matrix bond in the concrete system. The study also recommended the use of a water-cement ratio of 0.40. The air-entrainment and superplasticizer were added in varying amounts to establish reasonable air content and workability, respectively.

Table 3.2. Group one concrete mix proportions.

Material	Portion
Cement	540 kg/m ³
Water	215 kg/m ³
Coarse aggregate	825 kg/m ³
Fine aggregate	825 kg/m ³
Superplasticizer	325 – 1250 mL/100 kg cement
Air-Entrainment	16 – 260 mL/100 kg cement
Flax fibre (38 mm lengths)	0.3% by volume fraction

Table 3.3. Group two concrete mix proportions.

Material	Portion
Cement	540 kg/m ³
Water	215 kg/m ³
Coarse aggregate (14 mm)	396 kg/m ³
Coarse aggregate (5 mm)	429 kg/m ³
Fine aggregate	825 kg/m ³
Superplasticizer	325 – 1250 mL/100 kg cement
Air-Entrainment	16 – 260 mL/100 kg cement
Flax fibre (38 mm lengths)	0.3% by volume fraction

3.3. Specimen Preparation

Since the two groups of specimens in this study were weathered in separate locations, the concrete for each group was also prepared in different laboratories. The

mixing procedure for both groups followed the procedure of the CSA Standard A23.1-00 for preparing concrete in a rotary mixer. The mixers used for both groups were motorized and had capacities of 0.15 m³. The mixing procedure used for both groups involved the following steps:

1. Add coarse and fine aggregate to the mixer;
2. Mix for 30 seconds;
3. While mixer is running, add half the batch water, and all the air-entrainment;
4. After the water and air-entrainment have been mixing for one minute, stop mixing;
5. Add all the cement, begin mixing again and run for one minute;
6. While mixer is running, add the rest of the water and admixtures, and mix for three minutes;
7. Stop mixing for three minutes;
8. Begin mixing again for another two minutes; and
9. Test for fresh concrete properties

For the three fibre-reinforced batches, the fibres were added during step eight of the mixing procedure. If the fibres seemed to be balling up in the concrete, the superplasticizer was added and the concrete was mixed for at least 10 more minutes.

Once mixing was completed, the batches were tested for slump and air content, and then cast in forms. For all four batch types in group one, 20 beams of dimensions 75 x 100 x 400 mm and 20 cylinders of dimensions 100 x 200 mm were cast in forms made of PVC. For all four batch types in group two, the 12 beams of dimensions 75 x 100 x 400 mm and four cylinders of dimensions 100 x 200 mm were cast in forms made of steel and PVC, respectively.

The general procedure for forming and curing the concrete followed ASTM Standard C192 - Making and Curing Concrete Test Specimens in the Laboratory. Once the concrete was cured in a humid environment for 24 hours, the specimens were removed from their forms, and placed in a curing pool of water saturated with calcium hydroxide at 3 g/L, at a temperature of 25°C (+/- 3°C). The group one specimens were

removed from their curing pool after 27 days, to begin testing and the wet-dry weathering cycles. Group two specimens were also removed from their curing pool after 27 days, but the first sub-group was shipped to the Saskatoon laboratory in order to be tested. The second and third sub-groups remained in the Richmond laboratory to undergo the freeze-thaw weathering cycles conducted by the Lafarge staff, and were shipped to Saskatoon for final testing, once weathering was completed.

3.4. Weathering

The two weathering scenarios used in this study included wetting and drying cycles as well as freezing and thawing cycles. The wetting and drying cycles were carried out in the Structures and Geotechnical laboratories at the University of Saskatchewan. The freezing and thawing cycles were carried out in Lafarge's research laboratory in Richmond, B.C.

The wetting and drying cycles were performed on the second and third sub-groups of group one. The second sub-group was subjected to 50 cycles while the third sub-group was subjected to 25 cycles. The first nine of the 50 cycles consisted of three days in water at 25°C and one day in a dry oven at 100°C (SHEL LAB High Performance Oven, model 1685, Sheldon Manufacturing Inc., Cornelius, OR) located in the Geotechnical Laboratory at the University of Saskatchewan. The remaining 41 cycles involved two days in water at 25°C and two days in a dry oven at 100°C. The first five of the 25 cycles involved seven days in water at 25°C and one day in a dry oven at 100°C. The remaining 20 cycles involved six days in water at 25°C and two days in a dry oven at 100°C. This change in cycle time was made in order to provide the specimens with more time to dry out. Specimens were weighed before and after each cycle.

The rapid freezing and thawing cycles were performed on the second sub-group of group two. The cabinet (model H-3185, Humboldt Manufacturing Co., Schiller Park, IL) used for the cycling followed the ASTM Standard C666 - Resistance of Concrete to

Rapid Freezing and Thawing (Procedure A), which calls for 300 cycles. The inside of the cabinet is shown in Figure 3.8.

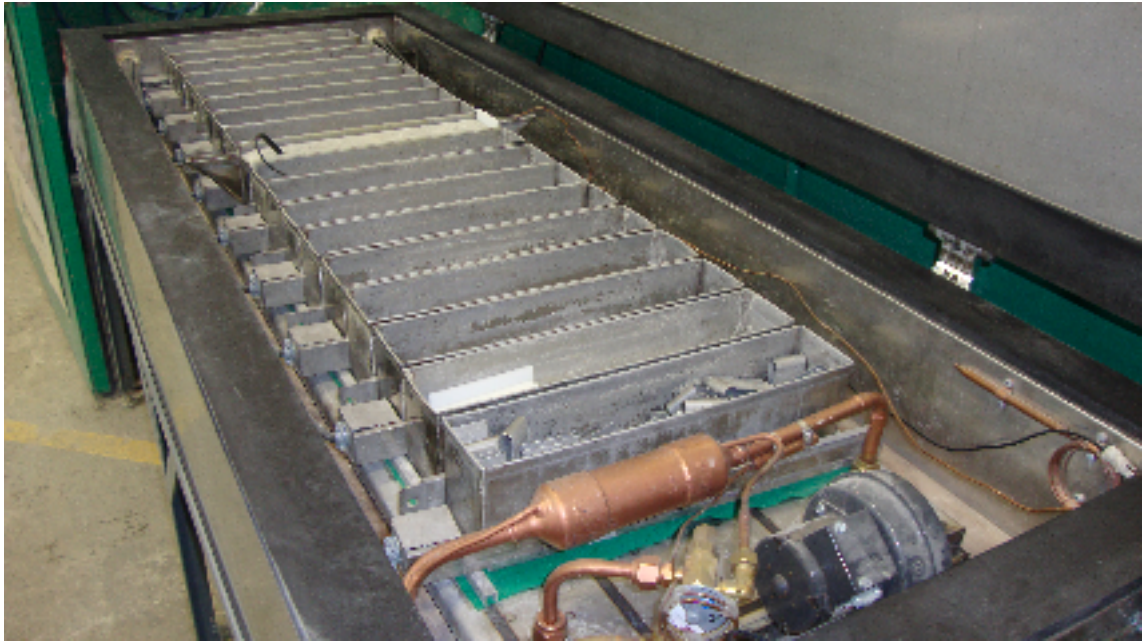


Figure 3.8. Freeze-thaw cabinet – beam holders.

Once the beams were set inside the beam holders within the cabinet and submerged in water, each of the 300 cycles involved changing the temperature of the beams from 4°C to -18°C , and then from -18°C to 4°C , in a time lapse between 2 and 5 hours. Two dummy beams which contained temperature sensors were used to control cycling. The beams were removed from the cabinet after each set of between 25 and 41 cycles, to clean out the beam holders and replace the water. Details on the freeze-thaw cycling periods are summarized in Table A.30 in the Appendix.

3.5. Test Procedures

The testing of both groups of specimens was conducted in the Structures laboratory at the University of Saskatchewan. Once the 28 day moist curing period was

over, the first sub-group from both group one and two were tested. The beams were weighed, tested for their dynamic modulus of elasticity, and then tested in flexure to obtain their flexural strength and toughness. The cylinders were weighed and then tested for their compressive strength. Also, once the 28 day moist curing period was over, the remaining sub-groups from both group one and two had their weathering cycles started.

When the weathering of both groups was completed, final testing of the specimens was performed. All of these tests were conducted in the Structures lab, in the Engineering building at the University of Saskatchewan. Once all the beams were tested in flexure, their ends were sawed off at lengths of 150 mm, and the beam end prisms of 75 x 100 x 150 mm were tested in compression.

The specimens tested after 28 days of curing were tested in a saturated surface-dry state. The specimens subjected to weathering cycles were also tested in a saturated surface-dry state. However, the specimens which were not subjected to weathering were tested after air drying for the duration of the weathering cycles.

3.5.1. Compressive Strength

Compression tests on cylinder specimens were performed following ASTM Standard C39 - Compressive Strength of Cylindrical Concrete Specimens. Tests were conducted under load control on a Universal Testing Machine (model 600DX, Instron, Norwood, MA), at a loading rate of 0.2 kN/s. In addition to the 80 cylinders tested from group one and 16 from group two, 256 beam end prisms of 75 x 100 x 150 mm were tested under the same compression test setup, with the compressive force applied parallel to the largest specimen dimension. Cylinders were capped with sulphur mortar.

3.5.2. Dynamic Modulus of Elasticity

The dynamic modulus of elasticity (DME) was measured for all beams, before they were tested in flexure. All sub-groups in group one, besides the first, also had their DME recorded after every wet-dry cycle. The procedure for obtaining the DME followed ASTM Standard C215-08 – Fundamental Transverse, Longitudinal, and Torsional Resonant Frequencies of Concrete Specimens.

The setup for finding the DME followed the transverse natural frequency approach. As shown in Figure 3.9, the beams rested flat wise on two rubber supports and an accelerometer (model 4112B, Dytran Instruments Inc., Chatsworth, CA) was attached to the top of the beam, at the end of its span. The beams were impacted on the top face and at the middle of the span with a ball-peen hammer. The longer cross sectional dimension of the beams was oriented vertically for all tests. The accelerometer recorded vertical acceleration amplitudes at 20,000 Hz for a two second period.



Figure 3.9. Acceleration test - beam setup.

For each separate beam, five impact tests were performed, and the resulting Fourier spectra were averaged and used to identify the fundamental natural frequency. The natural frequency, along with the mass and dimensions of the beams, was then used to find the DME using an equation found in ASTM C215-08.

3.5.3. Flexural Strength and Toughness

Flexural tests were performed on all beam specimens following ASTM Standard C1609 - Flexural Performance of Fibre-Reinforced Concrete. Standard C1609 calls for beam specimens with square cross sections, and cross section widths to be three times the length of the longest fibre. The beams used in this study did not have square cross

sections and the fibre length used was longer than one third the cross section width. Although these two requirements were not followed, the standard was still implemented.

A closed-loop third-point flexural test was performed on all beams using a Universal Testing Machine (model 60HVL, Instron, Norwood, MA). The longer cross sectional dimension of the beams was oriented vertically for all tests, as shown in Figure 3.10. Two linear variable differential transformers (LVDT), one on either side of the specimen, were mounted at mid-span with a yoke, to record the true mid-span deflection during the test. This procedure eliminated extraneous displacements due to seating of the specimen and elastic displacement of the loading frame. The signal from one of the LVDTs was used to control the displacement rate, and tests were run with a target displacement rate of 0.1 mm/min.

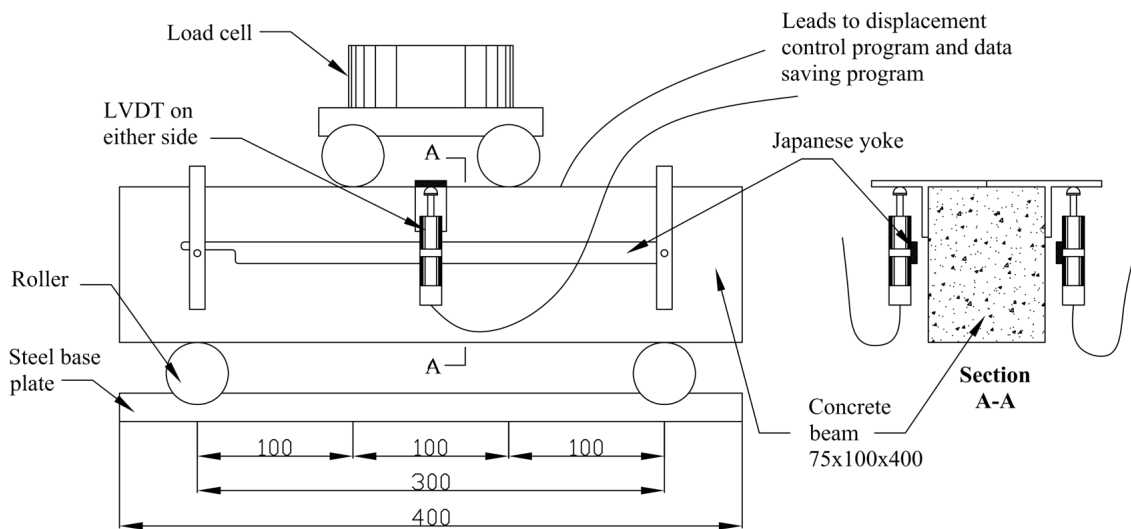


Figure 3.10. Flexural test – beam setup (dimensions in mm).

The deflections found by both LVDTs, as well as the load, were recorded at a sampling rate of 10 Hz. From this recording, the average mid-span deflection of the beams was calculated and the actual deflection rate was found. The range of deflection rates needed to satisfy the standard was 0.05-0.1 mm/min. The actual rates from the wet-dry and freeze-thaw tests varied from 0.05 to 0.23 mm/min and 0.05 to 0.25 mm/min, respectively.

Once each beam had failed in flexure, the largest load obtained during the testing was used, along with the dimensions of the beam, to calculate the flexural strength of the beam. Since the post-cracking response of the beams was highly variable, and often not achieved, a pre-cracking and post-cracking toughness value was calculated for each beam, based on the area under the flexural curve. Figure 3.11 shows an example of the load-deflection curves generated from each of the flexural tests. Once the average deflection was calculated from the two LVDTs placed on either side of the beam, the area under the average deflection curve was calculated before and after the peak load. The area obtained up until the peak load was considered the pre-cracking toughness, and the area obtained after the peak load until failure was the post-cracking toughness.

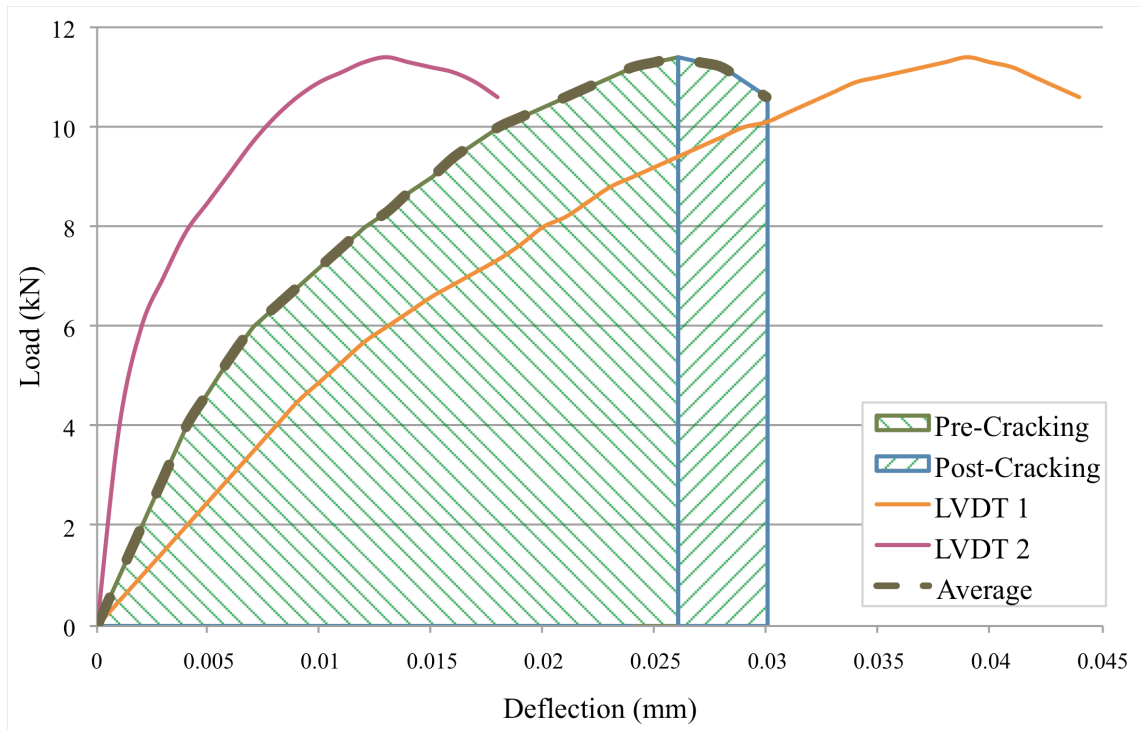


Figure 3.11. Area under load-deflection curve for flexural toughness calculation.

3.5.4. Scanning Electron Microscope

In order to better understand the failure mechanisms of the fibres that failed in the flexural tests, a scanning electron microscope (SEM) (JEOL 840A), located in the

Geology Department at the University of Saskatchewan, was used to analyze the fibres on the crack surface, to see how each type of fibre failed after being subjected to the different weathering conditions.

The samples used for the SEM analysis were taken off the crack surface of the beams, after they were tested in flexure. The samples were cut out of the bottom corners of each beam's crack surface, with an area of approximately 400 mm². One sample was taken from each of the three different fibre batches to be analyzed. Since the fourth and fifth sub-groups in group one underwent the same type of weathering, only three samples were analyzed between the two of them, resulting in a total of 12 samples from group one. Nine samples from the three sub-groups in group two were also analyzed.

Since the samples needed to be enclosed in a vacuum chamber within the SEM, they were placed in a vacuum chamber before being analyzed, to removed any excess moisture or air. Once the samples seemed to be emitting very small amounts of excess, they were then covered in a gold coating in order to produce images in the SEM.

3.5.5. Energy-Dispersive X-Ray Spectroscopy

In order to find out how the fibres chemically reacted with the cement paste before and after wet-dry cycling, energy-dispersive x-ray spectroscopy (EDS) analysis was performed using a superprobe electron microprobe analyser (EMPA) (JEOL 8600), located in the Geology Department at the University of Saskatchewan.

While the SEM analysis gave an actual physical picture of the failed fibres, the EDS analysis provided a spectrum of elements present on the surface of the failed fibres, as well as the paste surrounding the embedded fibres, which helped explain the characteristics of the failed fibres.

4. Experimental Results and Discussion

In this chapter, the results of all tests are presented, and the effect that wet-dry and freeze-thaw cycles have on the mechanical properties of flax fibre-reinforced concrete (FFRC) are examined. The mechanical properties of FFRC presented here include the compressive strength, dynamic modulus of elasticity, flexural strength, and flexural toughness. Fracture modes and chemical composition of embedded fibres are also observed. All statistical analyses can be viewed in Section A of the Appendix.

4.1. Group One – Wetting and Drying Cycles

4.1.1. Fresh Concrete Properties

The fresh concrete properties from all batches in group one are presented in Table 4.1. All batches were fabricated to similar slumps and air contents to rule out the possibility that either property could be responsible for differences in performance.

Table 4.1. Properties of fresh concrete from all batches in Group One.

Batch Type	Slump (mm)	Percent Air (%)
Unreinforced	120	9.1
Flax Fibre	105	9.9
Duralin	95	9.7
Silane	90	8.4

4.1.2. Compressive Strength

The compressive strength results for cylinders from all batches in group one are presented in Table 4.2. The data from all cylinder tests were included in the analysis, since none of the specimens broke prematurely due to eccentric loading.

The compressive strengths of cylinders from each of the five sub-groups, relative to their 28 day compressive strengths, are shown in Figure 4.1. The error bars in the plots signify one standard deviation from the mean values.

Table 4.2. Compressive strength (f_c) results of cylinders from all batches in Group One.

Sub-group	Batch Types	N*	f_c (MPa)	SD* (MPa)	COV* (%)
First (28 days curing)	U	4	24.7	0.8	3.1
	R	4	25.2	1.5	5.9
	D	4	25.7	1.4	5.4
	S	4	26.8	0.5	2.0
Second (50 cycles)	U	4	24.8	0.5	1.9
	R	4	25.1	1.9	7.4
	D	4	26.0	1.5	5.7
	S	4	27.0	1.5	5.7
Third (25 cycles)	U	4	24.0	0.3	1.3
	R	4	25.6	1.1	4.4
	D	4	26.4	1.4	5.3
	S	4	28.5	0.3	1.2
Fourth (50 ambient‡)	U	4	31.1	1.1	3.7
	R	4	33.7	2.0	5.9
	D	4	34.4	2.0	5.8
	S	4	36.2	2.2	6.0
Fifth (25 ambient‡)	U	4	33.0	1.2	3.7
	R	4	32.0	1.2	3.9
	D	4	34.7	1.1	3.1
	S	4	35.0	1.8	5.0

* N=number of specimens; SD=standard deviation; COV=coefficient of variation

+ U=unreinforced; R=flax fibre; D=Duralin; S=silane

‡ 50 ambient and 25 ambient specimens are subjected to ambient laboratory conditions and tested at the same time as the specimens subjected to 50 and 25 cycles, respectively.

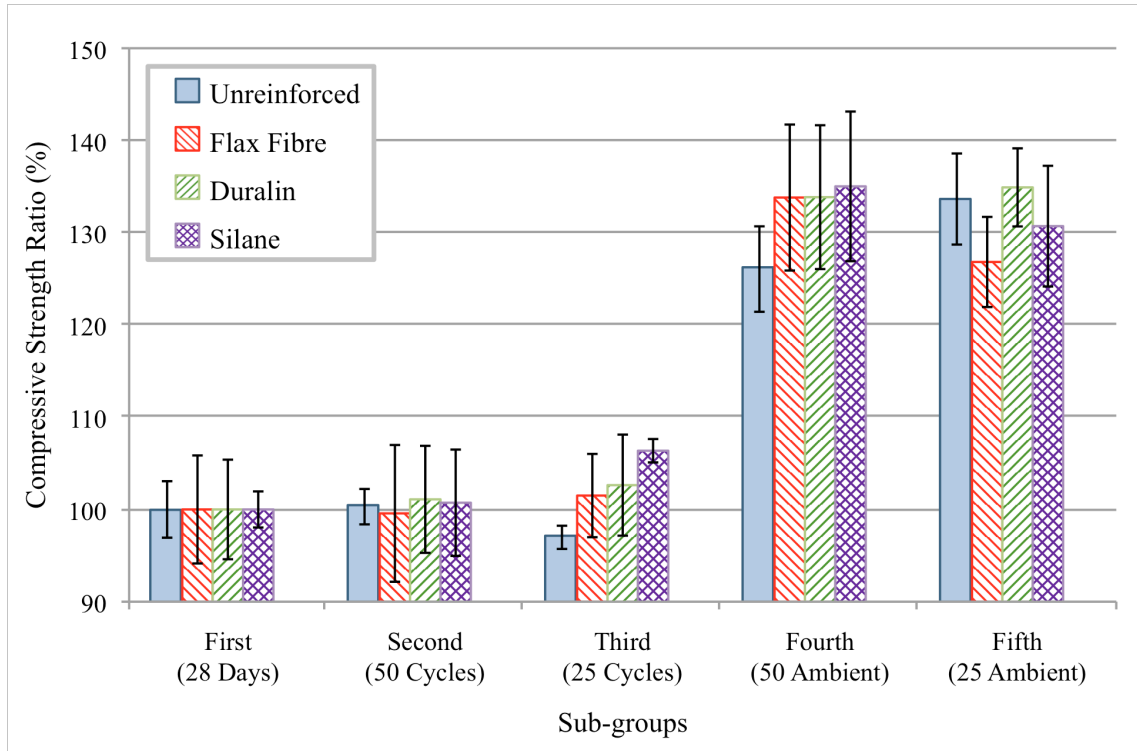


Figure 4.1. Normalized compressive strengths of Group One cylinders.

A visible trend in the relative compressive strengths of cylinders, shown in Figure 4.1, was that the fourth and fifth sub-groups out-performed the other three sub-groups, at a 99% level of confidence. The mean compressive strengths of the fourth and fifth sub-groups are not significantly different from each other at a 90% level of confidence.

The ability for the fourth and fifth sub-groups to out-perform the first sub-group is partly attributed to the fact that the fourth and fifth sub-groups had seven more months to harden and gain strength. The ability for the fourth and fifth sub-groups to out-perform the second and third sub-groups is partly attributed to the fact that the second and third sub-groups were subjected to wet-dry cycles while the other two were not. However, the difference in relative compressive strengths may also be attributed to the fact that the second and third sub-groups were tested in a saturated state, while the fourth and fifth sub-groups were tested in a natural air dried state. This may also explain the difference in performance between the first sub-group and the fourth and fifth sub-

groups. As shown in Section 2.2.2, previous research has also reported this phenomenon (Coutts and Kightly 1984).

Another visible trend in the relative compressive strengths of cylinders was the lack of difference in strengths between the first three sub-groups. Even though the second and third sub-groups endured wet-dry cycling, their difference in strength from the first sub-group was not statistically significant. The only batch which obtained a statistically significant difference in relative compressive strengths, at a 90% level of confidence, was the silane batch from the third sub-group. This batch's strength was greater than that achieved by the first sub-group, which means that the wet-dry cycling improved the strength.

All three fibre-reinforced batches in the second and third sub-groups performed as well as or better than the unreinforced batch, showing that the presence of each fibre type was not detrimental to the specimens performance after being weathered.

Since there was not a statistically significant difference in the strengths between batches in each sub-group, it can not be concluded that one batch type performed better than another in compression, after being subjected to wet-dry cycles.

The compressive strength results for blocks from all batches in group one are presented in Table 4.3. Not all of the batches provided eight blocks for test results, either because the beams they were cut from failed outside the middle third of their span, or because one or more outliers were identified. The compressive strengths of blocks from each of the five sub-groups, normalized by their respective 28 day strengths, are plotted in Figure 4.2. The error bars in the plots signify one standard deviation from the mean values.

A visible trend in the relative compressive strengths of blocks, shown in Figure 4.2, is that the fourth and fifth sub-groups out-perform the second and third sub-groups, at a 99% level of confidence. This trend was also found in the relative compressive strengths of cylinders. The fourth and fifth sub-groups also out-perform the first sub-group, at a 99% level of confidence.

Another visible trend in the relative compressive strengths of blocks, which was different from that found in the cylinder strengths, was that the second and third sub-groups had smaller strengths when compared to the first sub-group. This decrease in

relative compressive strength was only statistically significant for the silane batch, at a 99% level of confidence. This decrease in strength can be attributed to variability that is expected from different batches.

Table 4.3. Compressive strength (fc) results of blocks from all batches in Group One.

Sub-group	Batch Type	N*	fc (MPa)	SD* (MPa)	COV* (%)
First (28 days curing)	U ⁺	8	26.5	1.8	6.9
	R ⁺	8	27.1	2.6	9.4
	D ⁺	8	28.1	3.2	11.4
	S ⁺	5{3}	32.8	2.7	8.3
Second (50 cycles)	U	7	24.3	1.4	5.6
	R	8	26.4	2.1	7.9
	D	8	25.7	2.1	8.3
	S	8	28.7	1.3	4.7
Third (25 cycles)	U	7{1}	22.3	2.8	12.6
	R	7{1}	26.6	1.9	7.1
	D	6{1}	25.5	2.8	10.9
	S	7	28.9	3.0	10.5
Fourth (50 ambient‡)	U	8	31.0	3.0	9.6
	R	8	34.8	2.1	6.1
	D	8	36.8	2.0	5.4
	S	4{3}	37.7	3.0	8.0
Fifth (25 ambient‡)	U	7	29.8	2.1	7.0
	R	8	32.1	2.6	8.0
	D	7{1}	33.1	2.0	6.0
	S	7{1}	34.9	1.7	4.8

* N=number of specimens; SD=standard deviation; COV=coefficient of variation

+ U=unreinforced; R=flax fibre; D=Duralin; S=silane

‡ 50 ambient and 25 ambient specimens are subjected to ambient laboratory conditions and tested at the same time as the specimens subjected to 50 and 25 cycles, respectively.

{ }=number of outliers

All three fibre-reinforced batches in the second and third sub-groups performed as well or better than the unreinforced batch, showing that the presence of each fibre type was not detrimental to the specimens performance after being weathered.

The main reason for testing the beam ends of group one specimens in compression was to see if there was a correlation between the compressive strength of the cylinders and blocks. The compressive strengths of cylinders and blocks from each of the four batch types are plotted together in Figure 4.3. The error bars in the plots signify one standard deviation from the mean values.

As can be seen in Figure 4.3 in most cases, the strengths obtained from the two specimen types were similar. Neither the flax nor the Duralin fibre-reinforced batches produced compressive strengths that were statistically different at a level of confidence greater than 90%, so their cylinder and block strengths were statistically not different.

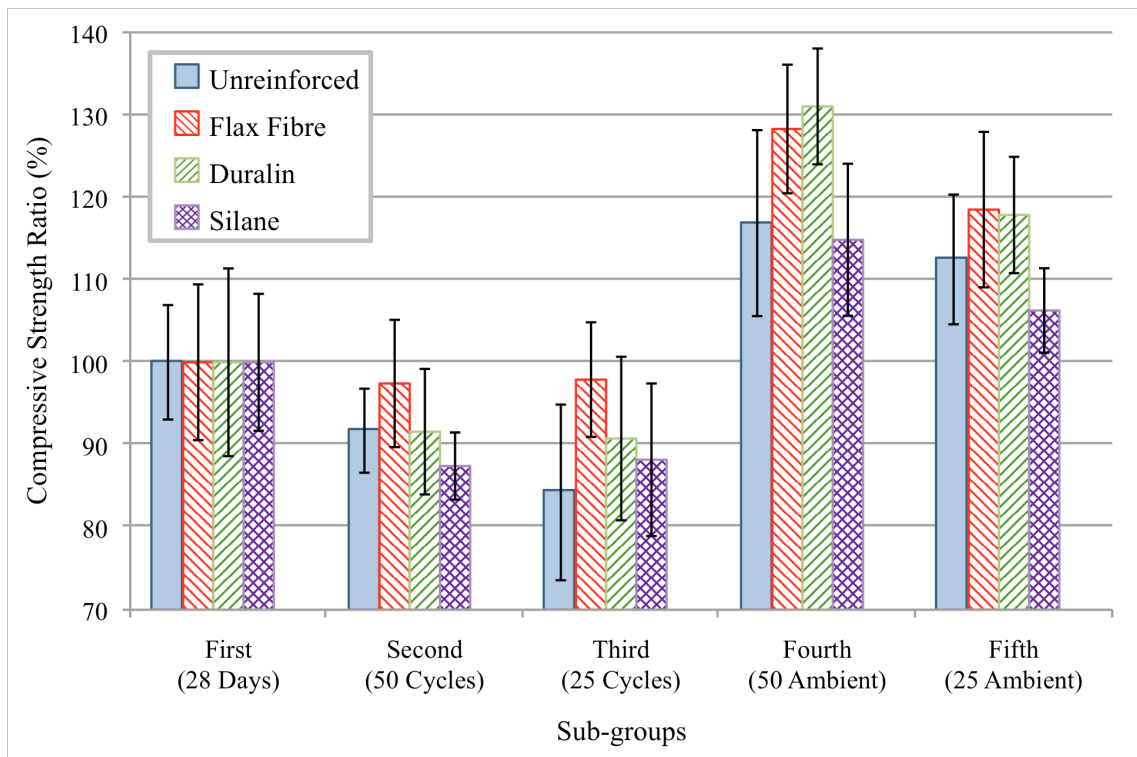


Figure 4.2. Normalized compressive strengths of Group One blocks.

Both the unreinforced and silane fibre-reinforced batches had strengths which were statistically different at a 90% level of confidence, and the two cases are identified by an asterisk beneath the sub-group number in Figure 4.3. The most obvious of these different strengths was the first sub-group of the silane batch, for which the block compressive strength was more than 25% higher than that found in the cylinder.

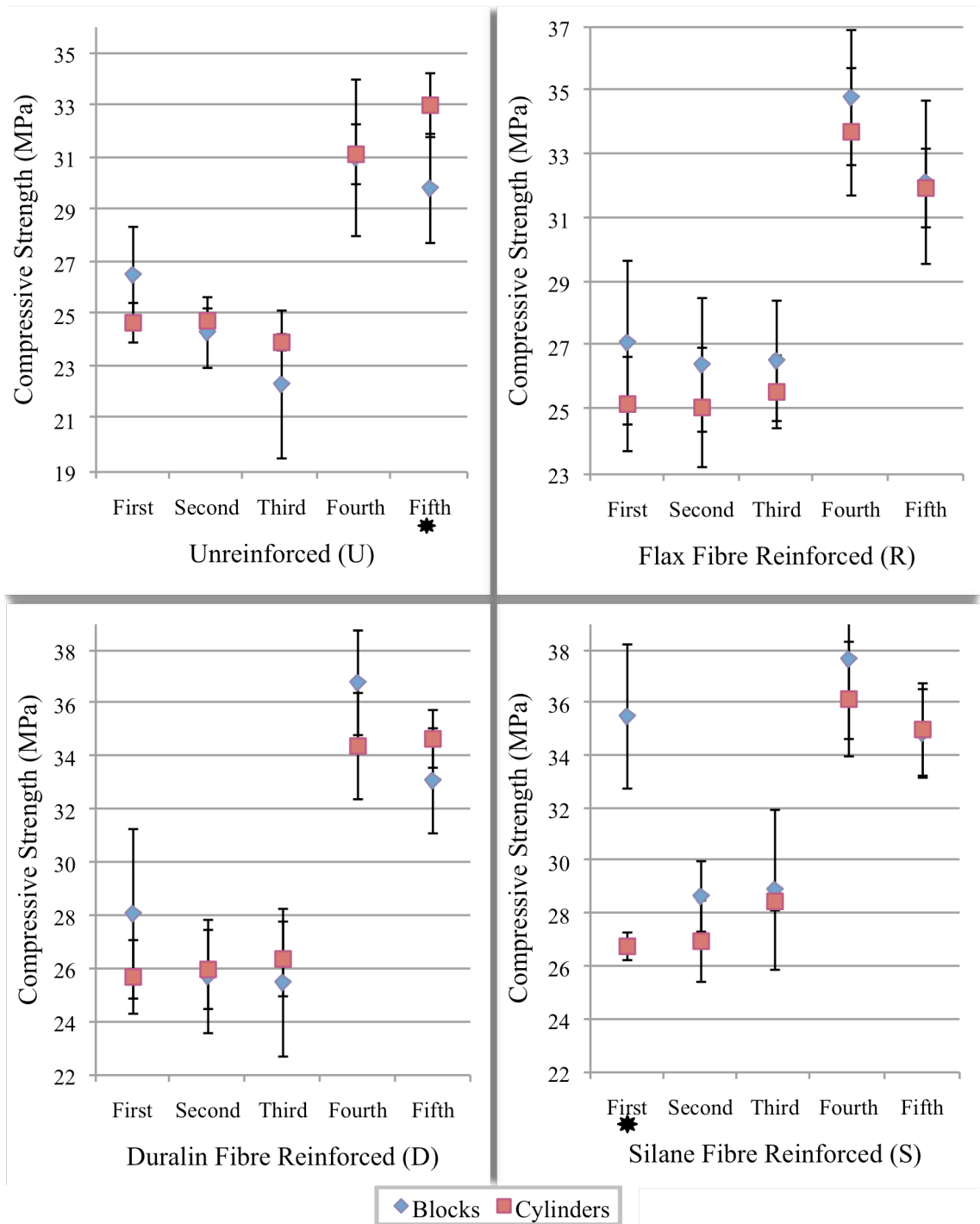


Figure 4.3. Compressive strengths of cylinders and blocks from all batches in Group One.

The block specimens used in this research did not conform to any particular standard. However, they produced results remarkably close to those of the cylinders.

One factor that may have contributed to the differences that were found is the fact that the blocks may have experienced eccentric loading, since they were tested without using a capping compound, which could have produced a lower average strength value. This is reflected in the sizeable number of removed outlier block specimens.

The ability for blocks to properly determine the compressive strength of concrete was needed for the concrete in group two, for which cylinder specimens could not be subjected to rapid freezing and thawing.

4.1.3. Dynamic Modulus of Elasticity

The dynamic modulus of elasticity (DME) of beams from the second and fourth sub-groups is plotted in Figure 4.4. The dynamic modulus of elasticity of beams from the third and fifth sub-groups is plotted in Figure 4.5. The legend on the sides of these plots shows that each batch type from each sub-group was tested in two states, wet and dry. This was true for the second and third sub-groups since they underwent 50 and 25 wetting and drying cycles, respectively. The DME was found in these beams once they were removed from soaking in water and again after oven drying. However, the fourth and fifth sub-groups were set aside during the cycles, so their designation as wet or dry only corresponds to state of the cycling sub-group it was being tested with.

The trend followed by both the fourth and fifth sub-groups was that they lost approximately 4% of their original DME. This is most likely due to the loss of pore water as a result of evaporation over time. Degradation of fibres over time does not explain this decrease in DME, since the unreinforced batches followed the same trend.

The trend followed by both the second and third sub-groups was that their wet and dry state DME started off at different values, and eventually got closer to the same value over time. The amount of water that the beams could take on or lose over time did not change, but the natural frequency of the beams was constantly changing. The natural frequency of the wet beams was constantly getting lower, while the natural frequency of the dry beams was progressively getting higher.

For the second sub-group, the change in natural frequency can not be attributed to any particular batch type, because all batches followed the same trend for DME.

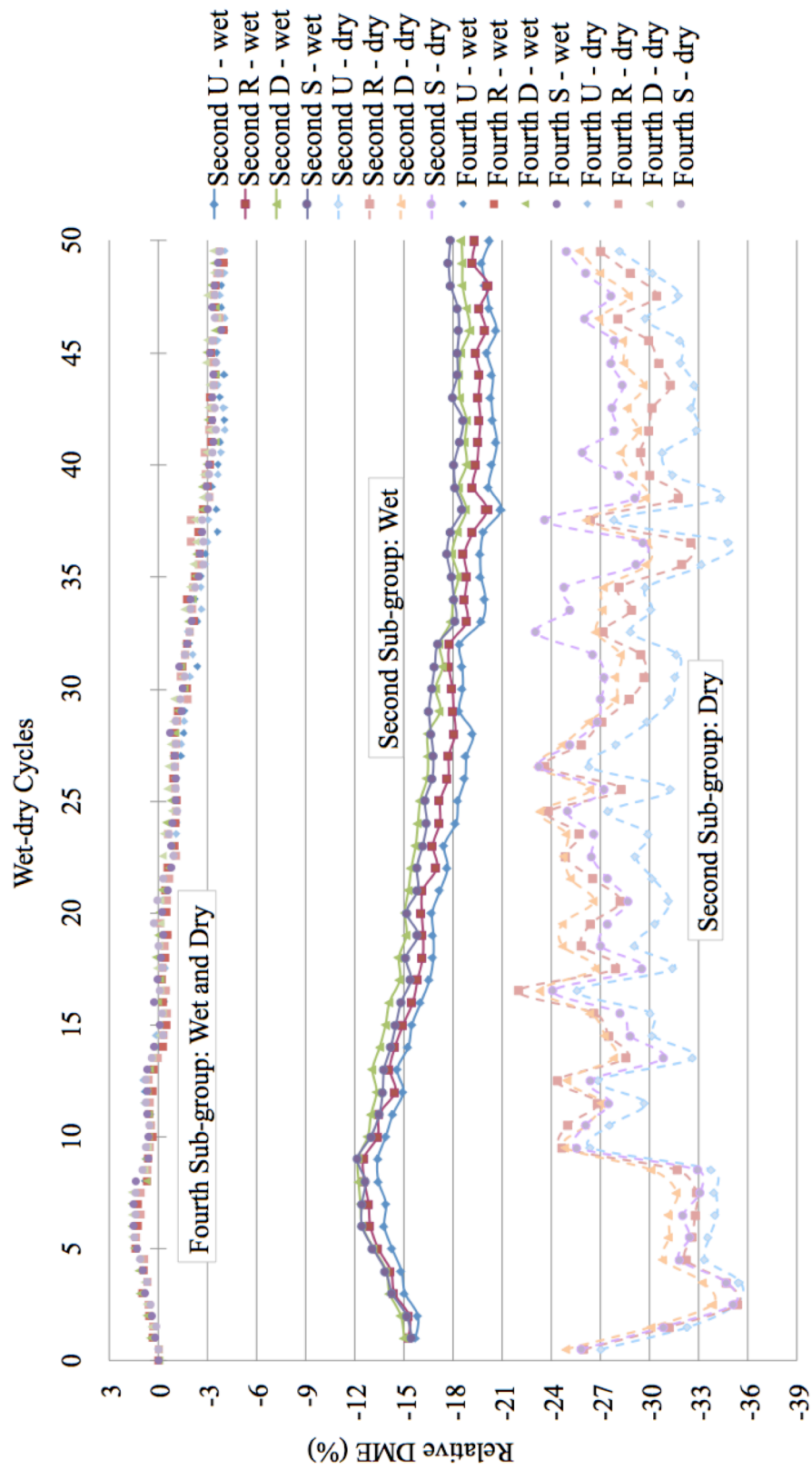


Figure 4.4. Dynamic modulus of elasticity (DME) for beams in the second and fourth Sub-groups of Group One.

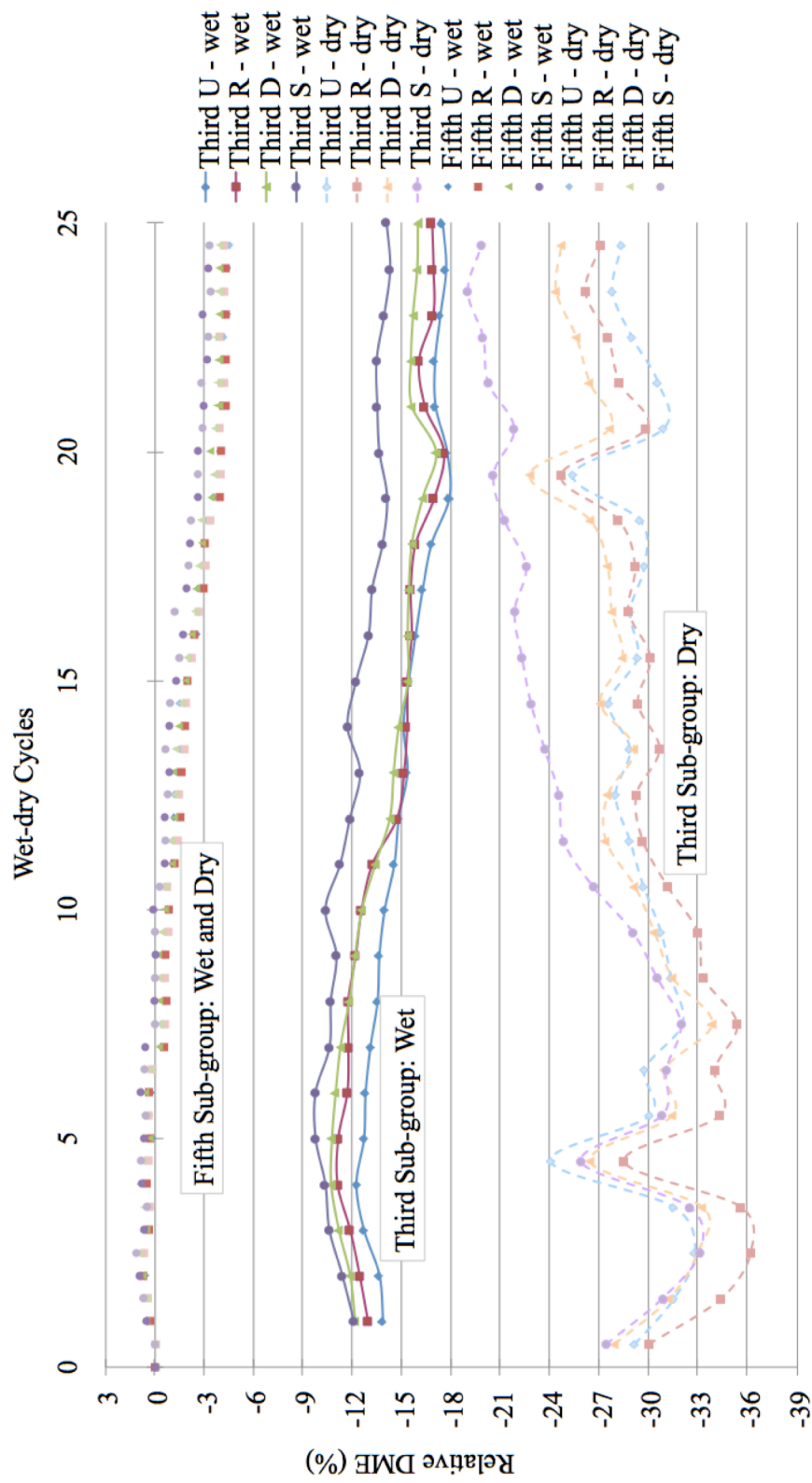


Figure 4.5. Dynamic modulus of elasticity (DME) for beams in the third and fifth Sub-groups of Group One.

However, for the third sub-group, the change in dry natural frequency in the silane fibre-reinforced batch produced a DME trend which seems slightly more accelerated than the other batches. It is still not clear whether the change in natural frequency was brought on by the silane treated fibre or the length of the weathering cycle. It does seem plausible that the cycles were producing an effect on the cement paste, which in turn was affecting the natural frequency of the beams over time.

Typical acceleration amplitude plots for beams at various stages in the wet-dry cycling process are shown in Figures 4.6 and 4.7. After analysing the acceleration amplitude plots from the four different batches at various stages in the cycling process, it became clear that there were not large variations in beam behaviour from batch to batch, at specific stages. The analysis also showed that the type of cycling, 50 wet-dry cycles versus 25 wet-dry cycles, did not create large variations in beam behaviour from batch to batch, at specific stages.

The typical acceleration amplitude plots for beams which were at the beginning of the wet-dry cycling are shown in Figure 4.6. Acceleration data from each beam was taken after 28 days of curing (Figure 4.6(a)), after the first drying period (Figure 4.6(b)), and after the first soaking period (Figure 4.6(c)). Though the beams lost 25-30% of their initial DME after the first drying period, the plots do not show a great change in the amplitudes or damping experienced by the beams. However, once the first soaking period was complete, the vibration of the beam was damped out noticeably faster. This is possibly due to the transformation of cement paste within the beams during their initial drying period. Then, once the beams were soaked and regained their initial mass of moisture, they were able to damp the vibrations faster than before.

The typical acceleration amplitude plots for beams which were finishing the wet-dry cycling are shown in Figure 4.7. Acceleration data was taken from the ambient beams after cycling was complete (Figure 4.7(a)), the dried beams on the last wet-dry cycle (Figure 4.7(b)), and the soaked beams after the last wet-dry cycle (Figure 4.7(c)). The ambient beams seemed to have lost much of their damping capabilities after losing approximately 4% of their initial mass. The weathered beams did not seem to gain or lose their damping capabilities in a dried or soaked condition. However, they did seem

to lose some amplitude to their vibration, which may have been due to the deterioration of the specimens over time.

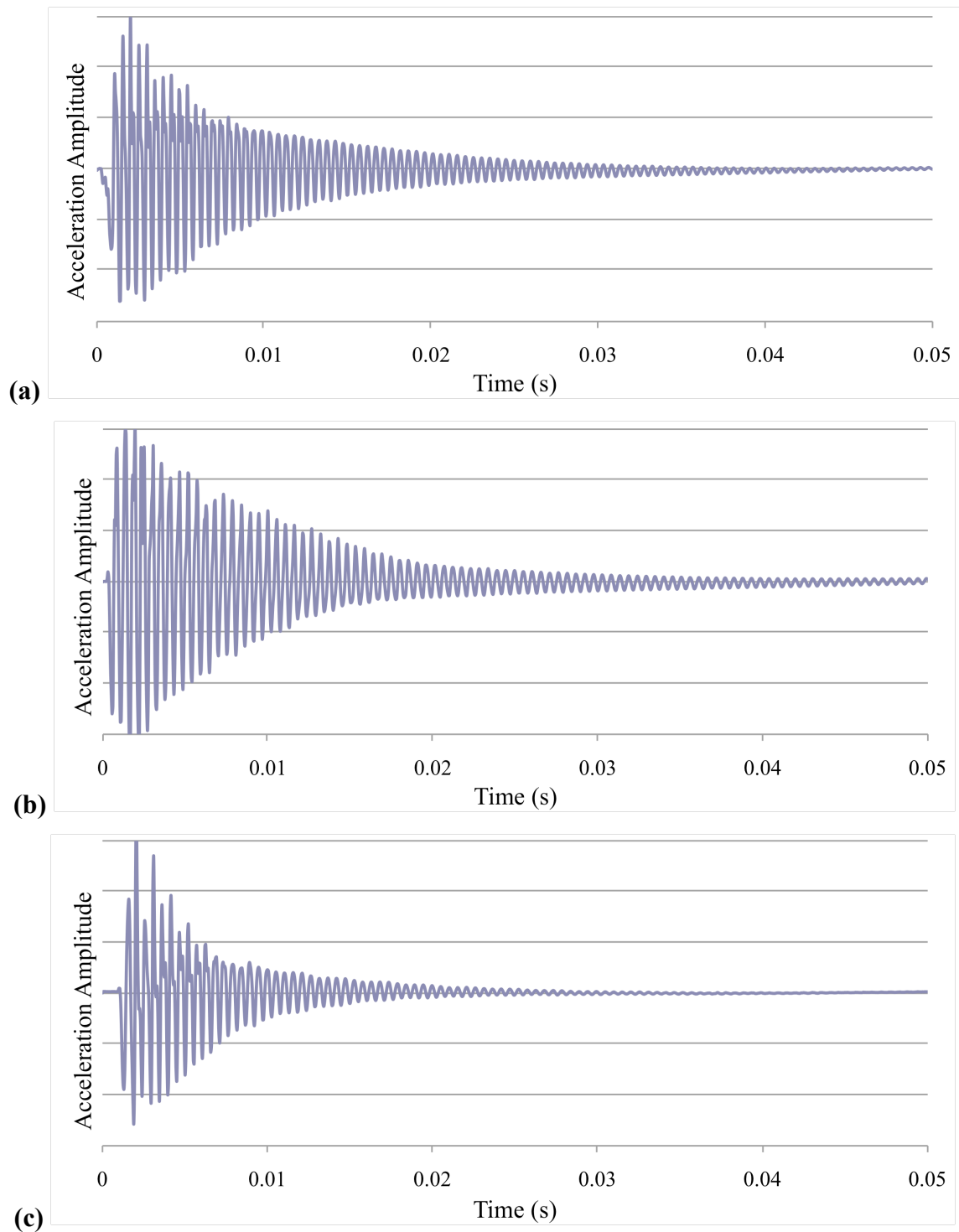


Figure 4.6. Typical acceleration amplitude of beams (a) after 28 day of curing, (b) after first cycle in oven, and (c) after first cycle soaking, as acquired from DME tests.

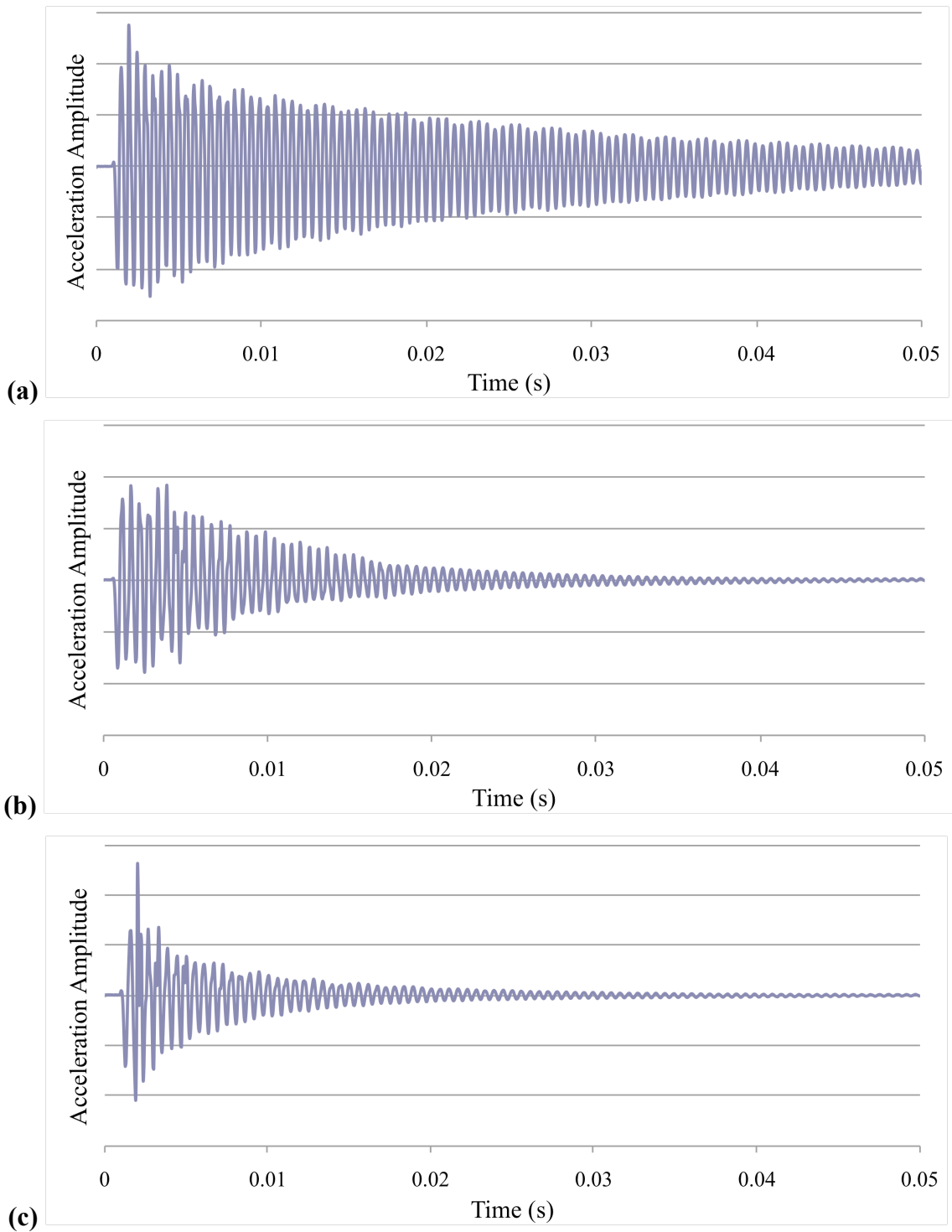


Figure 4.7. Typical acceleration amplitude of (a) ambient beams after cycling was complete, (b) dry beams on last wet-dry cycle, and (c) soaked beams after the last wet-dry cycle, as acquired from DME tests.

As was explained in Section 2.4.4, ASTM Standard C215 states that as beams are subjected to weathering cycles, they begin to degrade, and tend to experience an increase to their damping. As a result, the acceleration amplitude impact response becomes shorter, which is evident in Figures 4.7(b) and 4.7(c).

4.1.4. Flexural Strength and Toughness

The flexural strength results for beams from all batches are presented in Table 4.4. Not all of the batches include the test results for all four beams, because some of the beams failed outside the middle third of their span. The relative flexural strengths of beams from each of the five sub-groups are plotted in Figure 4.8. The error bars in the plots signify one standard deviation from the mean values.

A visible trend in the relative flexural strengths of beams, shown in Figure 4.8, was that the fourth and fifth sub-groups out-performed the other three sub-groups, at a 99% level of confidence, with exception to the silane batch in the fifth sub-group. This trend is similar to that shown by the relative compressive strengths (see Figure 4.1).

Another visible trend in the relative flexural strengths of beams, was that the strengths of the second and third sub-groups were smaller than those of the first sub-group. This decrease in relative flexural strength is only statistically significant, at a 95% level of confidence, for the unreinforced and silane batches in the second subgroup and the unreinforced batch in the third sub-group. In most cases, therefore, this decrease in strength can be attributed to variability that is expected from different batches. As will be shown in Section 4.1.5, the SEM analysis uncovered no significant differences in fibre condition or failure mode between each fibre type in these sub-groups.

All three fibre-reinforced batches in the second and third sub-groups performed as well or better than the unreinforced batch, showing that the presence of each fibre type was not detrimental to the specimens performance after being weathered.

Since there was not a statistically significant difference between the strengths of the different batches in each sub-group, it appears that none of the batch types performed better than any other in flexure, after being subjected to wet-dry cycles.

Table 4.4. Flexural strength (FS) results for the beams from all batches in Group One.

Sub-group	Batch Type	N*	FS (MPa)	SD* (MPa)	COV* (%)
First (28 days curing)	U ⁺	4	3.87	0.14	3.7
	R ⁺	4	3.79	0.21	5.5
	D ⁺	4	3.62	0.33	9.2
	S ⁺	4	4.20	0.17	4.1
Second (50 cycles)	U	3	3.21	0.12	3.7
	R	4	3.42	0.44	13.0
	D	4	3.20	0.70	22.0
	S	4	3.24	0.53	16.5
Third (25 cycles)	U	4	3.27	0.32	9.7
	R	4	3.59	0.24	6.7
	D	4	3.52	0.65	18.4
	S	3	3.71	0.44	11.8
Fourth (50 ambient‡)	U	4	4.57	0.32	7.1
	R	4	5.08	0.57	11.2
	D	4	4.53	0.44	9.7
	S	3	4.98	0.23	4.6
Fifth (25 ambient‡)	U	4	4.92	0.42	8.4
	R	4	4.66	0.29	6.2
	D	4	4.51	0.28	6.3
	S	4	4.35	0.29	6.7

* N=number of specimens; SD=standard deviation; COV=coefficient of variation
+ U=unreinforced; R=flax fibre; D=Duralin; S=silane

‡ 50 ambient and 25 ambient specimens are subjected to ambient laboratory conditions and tested at the same time as the specimens subjected to 50 and 25 cycles, respectively.

The flexural toughness results for beams from all batches are presented in Table 4.5. Again, not all of the batches include the test results for all four beams, because some of the beams failed outside the middle third of their span. A visible trend in the pre-cracking toughness of beams, was that all three fibre batch types, in all five sub-groups, had higher pre-cracking toughness values when compared to the unreinforced batch. The post-cracking toughness values only accounted for approximately 10-30% of the total toughness recorded.

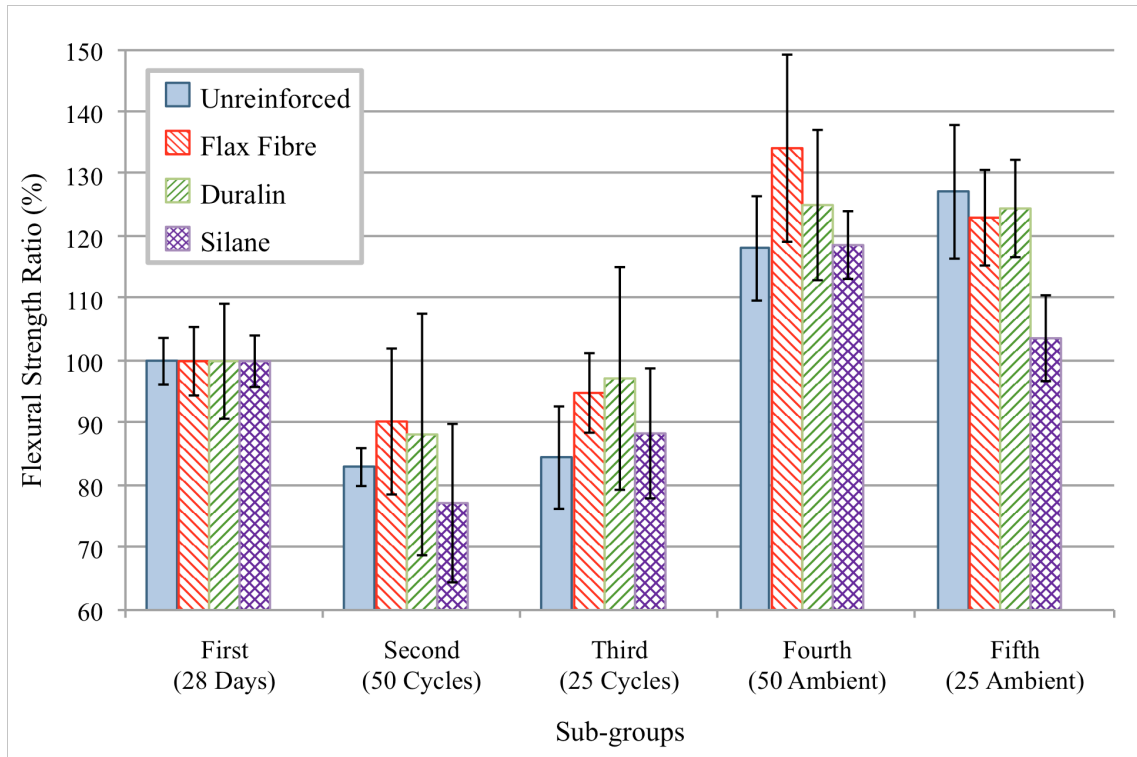


Figure 4.8. Normalized flexural strengths of Group One beams.

The large variation in toughness values recorded makes it impractical to perform analysis to distinguish trends in the mean toughness values. Therefore, the presence of each fibre type was not detrimental to the specimens' performance after being weathered, and the treated fibres provided no greater performance.

The closed-loop flexural testing setup may be the cause for such large variations in the toughness. A previous study which employed open-loop flexural testing allowed for load to be taken off at the moment the first crack appears. When load was re-applied, it started from zero again and increased (Wang 2003). However, the closed-loop test setup may not have allowed the fibre to slowly redistribute the load after cracking, as the open-loop setup would. As a result, the flexural plots created by an open-loop test would generate a gradual descending deflection curve, whereas the closed-loop plots show evidence of brittle failure soon after cracking, as illustrated in Figure 3.9 in Section 3.5.3.

Table 4.5. Toughness results for the beams from all batches in Group One.

Sub-group	Batch Type	Number of specimens	Toughness			SD*	COV*
			Pre-cracking (J)	Post-cracking (J)	Total (J)		
First (28 days curing)	U ⁺	4	0.16	-	0.16	0.05	29.0
	R ⁺	4	0.17	0.04	0.21	0.07	32.3
	D ⁺	4	0.18	0.03	0.21	0.09	44.9
	S ⁺	4	0.24	0.03	0.27	0.04	14.8
Second (50 cycles)	U	3	0.09	-	0.09	0.02	20.9
	R	4	0.13	0.03	0.17	0.06	35.6
	D	4	0.13	0.02	0.15	0.08	50.6
	S	4	0.12	0.02	0.14	0.05	33.3
Third (25 cycles)	U	4	0.10	-	0.10	0.06	59.0
	R	4	0.16	0.05	0.20	0.06	29.1
	D	4	0.13	0.05	0.18	0.12	68.9
	S	3	0.17	0.05	0.21	0.01	5.53
Fourth (50 ambient‡)	U	4	0.16	-	0.16	0.04	25.5
	R	4	0.26	0.03	0.28	0.05	17.0
	D	4	0.23	0.02	0.26	0.08	32.3
	S	3	0.23	0.04	0.27	0.07	25.6
Fifth (25 ambient‡)	U	4	0.14	-	0.14	0.01	7.07
	R	4	0.16	0.02	0.18	0.06	31.2
	D	4	0.16	0.05	0.21	0.09	45.2
	S	4	0.17	0.07	0.24	0.10	42.2

* SD=standard deviation; COV=coefficient of variation

+ U=unreinforced; R=flax fibre; D=Duralin; S=silane

‡ 50 ambient and 25 ambient specimens are subjected to ambient laboratory conditions and tested at the same time as the specimens subjected to 50 and 25 cycles, respectively.

4.1.5. Failure Modes of Fibres

Scanning electron microscope (SEM) images of failed fibres from the first and second sub-groups of group one are shown in Figure 4.9 and Figure 4.10, respectively. As shown in Figure 4.9, all three types of fibres showed lengths ranging from 0.1 to 0.5 mm, which indicates that all fibre types experienced a brittle fracture failure mechanism. These pull-out lengths indicate that beams may become unstable after crack widths

ranging from 0.1 to 0.5 mm are reached, since the fibres typically failed at these lengths. The stiff and brittle nature of all three types of fibres does not allow for larger pull-out lengths, most likely due to the strong bond held between the fibres and the cement paste.

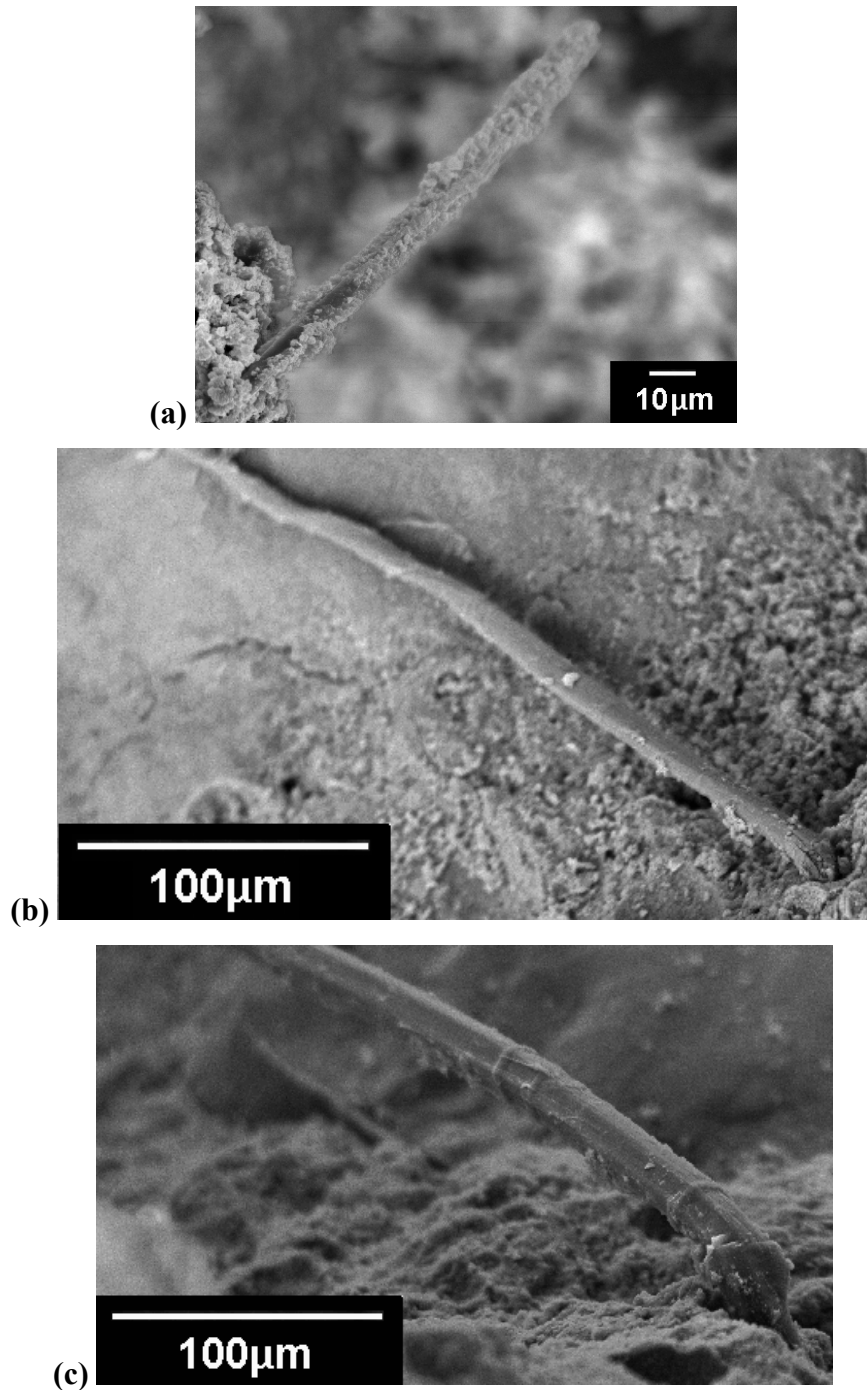


Figure 4.9. Failure surfaces of beams in the First sub-group of Group One showing (a) flax fibre, (b) Duralin treated fibre, and (c) silane treated fibre.

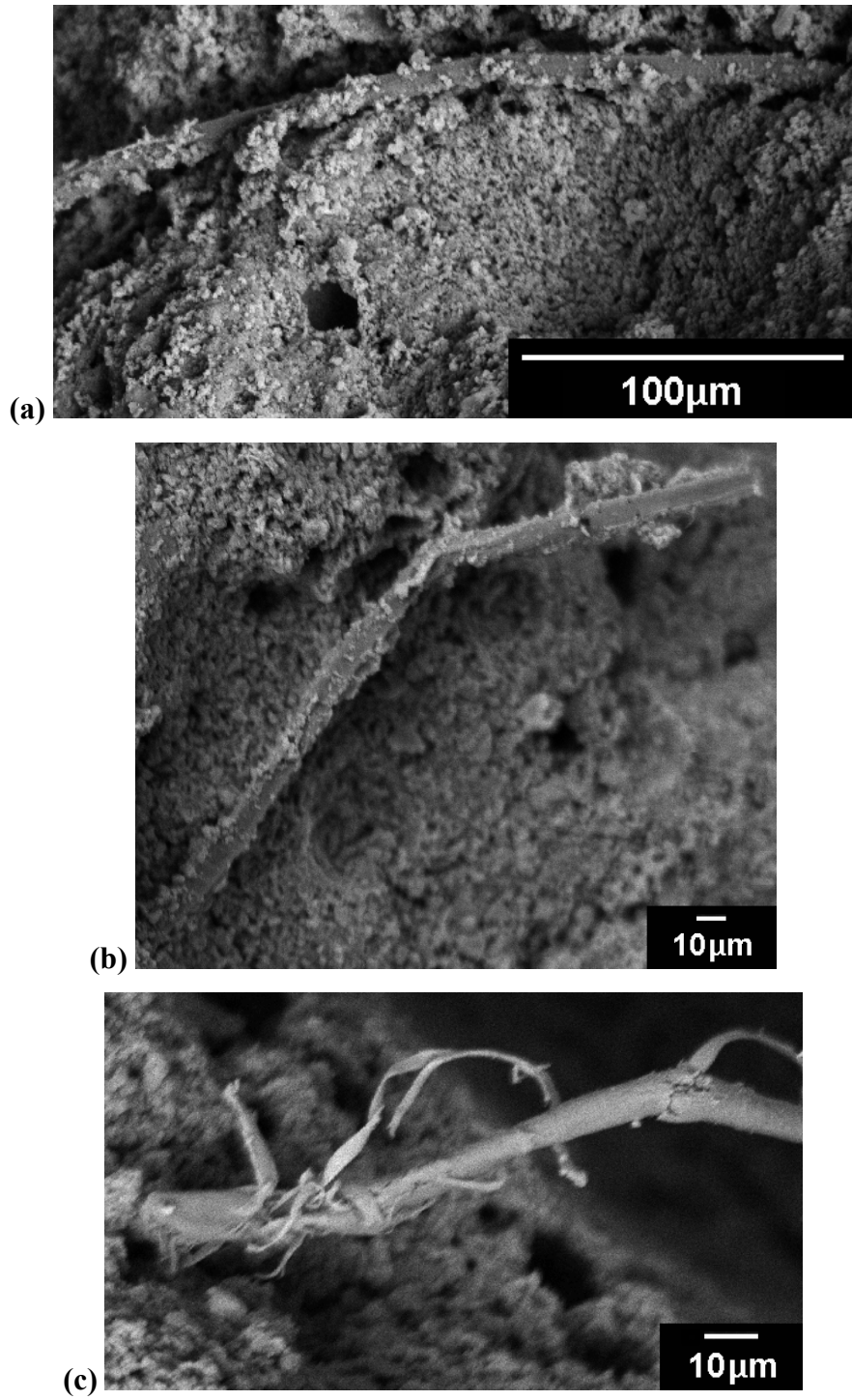


Figure 4.10. Failure surfaces of beams in the Second sub-group of Group one showing (a) flax fibre, (b) Duralin treated fibre, and (c) silane treated fibre.

It can also be seen from Figure 4.9 that some of the flax fibre seems to be covered in cement paste, whereas the Duralin and silane fibres seem relatively clean of paste. An example of this paste coverage, however, was found on all three types of fibre, from every sub-group.

Scanning electron microscope (SEM) images of failed fibres from the second sub-group are shown in Figure 4.10. No signs of fibre degradation are apparent, as the fibres resemble the condition of those found in the first sub-group. Any cracks found in the cement paste around the fibres were not considered degradation of the paste due to fibre interaction. In the de-gassing phase of the SEM sample preparation, as concrete samples begin to give off stored up moisture, cracks tend to form during the change in volume. The samples tested from the third and fourth sub-groups showed similar traits to those in the first and second sub-groups; therefore, it can not be concluded that one batch type performed better than the other in flexure, after being subjected to wet-dry cycles. The images from the third and fourth sub-groups can be viewed in Section B of the Appendix. All of the fibre types showed similarly short pull-out fibre lengths, which constitutes a brittle failure.

4.2. Group Two – Freezing and Thawing Cycles

4.2.1. Fresh Concrete Properties

The properties of fresh concrete for all batches used for the freeze-thaw study are presented in Table 4.6, along with the amount of superplasticizer used. Due to balling of the fibres during the mixing stage, superplasticizer was used in each batch at varying amounts. The variations in superplasticizer, mixing time, and initial moisture content of the aggregate, may account for the varied slump and air content of the fresh concrete.

Table 4.6. Properties of fresh concrete from all batches in Group Two.

Batch Type	Slump (mm)	Percent air (%)	Super-plasticizer (mL)
Unreinforced	110	7.2	0
Flax Fibre	150	4.5	80
Duralin	55	7.8	40
Silane	110	12	30

4.2.2. Compressive Strength

The compressive strength results for cylinders from all batches are presented in Table 4.7. It is recalled that cylinders were not produced for the second and third subgroups, since they could not be accommodated in the freeze-thaw chamber. The data from all cylinder tests are represented in this table, since none of the specimens broke prematurely due to eccentric loading. There was no trend in the strengths which directly relate to the types of fibres used in these specific batches. However, there was a definite relationship between the compressive strength and the air content of each batch. The flax fibre-reinforced batch had the lowest percent air and highest strength, and the silane fibre-reinforced batch had the highest percent air and lowest strength. The unreinforced and Duralin batches had similar air contents, and their compressive strengths did not differ significantly at the 90% level of confidence.

Table 4.7. Compressive strength (f_c) results for cylinders from the First Sub-group in Group Two.

Sub-group	Batch Type	N*	f_c (MPa)	SD* (MPa)	COV* (%)
First (28 days curing)	U ⁺	4	39.5	0.7	1.8
	R ⁺	4	59.8	1.2	2.0
	D ⁺	4	43.4	5.3	12.3
	S ⁺	4	28.5	2.3	8.0

* N=number of specimens; SD=standard deviation; COV=coefficient of variation
+ U=unreinforced; R=flax fibre; D=Duralin; S=silane

The compressive strength results for blocks from all batches are presented in Table 4.8. Only one batch did not provide eight blocks for testing, because one of the four beams failed outside the middle third of its span.

Table 4.8. Compressive strength (f_c) results for blocks from all batches in Group Two.

Sub-group	Batch Type	N*	f_c (MPa)	SD* (MPa)	COV* (%)
First (28 days curing)	U ⁺	8	41.5	4.0	9.6
	R ⁺	8	> 63.2	1.2	1.9
	D ⁺	8	45.2	5.4	12.0
	S ⁺	8	32.6	2.6	8.1
Second (Freeze- thaw cycles)	U	8	36.9	3.0	8.2
	R	8	> 62.8	0.3	0.4
	D	8	45.0	2.8	6.3
	S	8	28.5	2.3	8.1
Third (Ambient)	U	8	47.3	4.5	9.5
	R	8	> 64.0	0.2	0.4
	D	7	50.9	5.1	10.0
	S	8	32.7	2.6	8.0

* N=number of specimens; SD=standard deviation; COV=coefficient of variation
+ U=unreinforced; R=flax fibre; D=Duralin; S=silane

Many of the flax fibre-reinforced blocks reached the maximum load of the testing machine before they failed, so the batch strengths presented in Table 4.8 are signified as being greater than their reported values. The relative compressive strengths of blocks from each of the three sub-groups, normalized by their respective 28 day strengths, are plotted in Figure 4.11. The error bars in the plots signify one standard deviation from the mean values.

Since cylinders were only cast for the first sub-group, the blocks were used to determine how freeze-thaw cycling affected the compressive strength of the batches. As was observed for the cylinder test results, batches with higher air contents had lower compressive strengths. This is to be expected as the more air voids are introduced to the paste, the higher the stress concentrations and the more areas there are for larger cracks to propagate through.

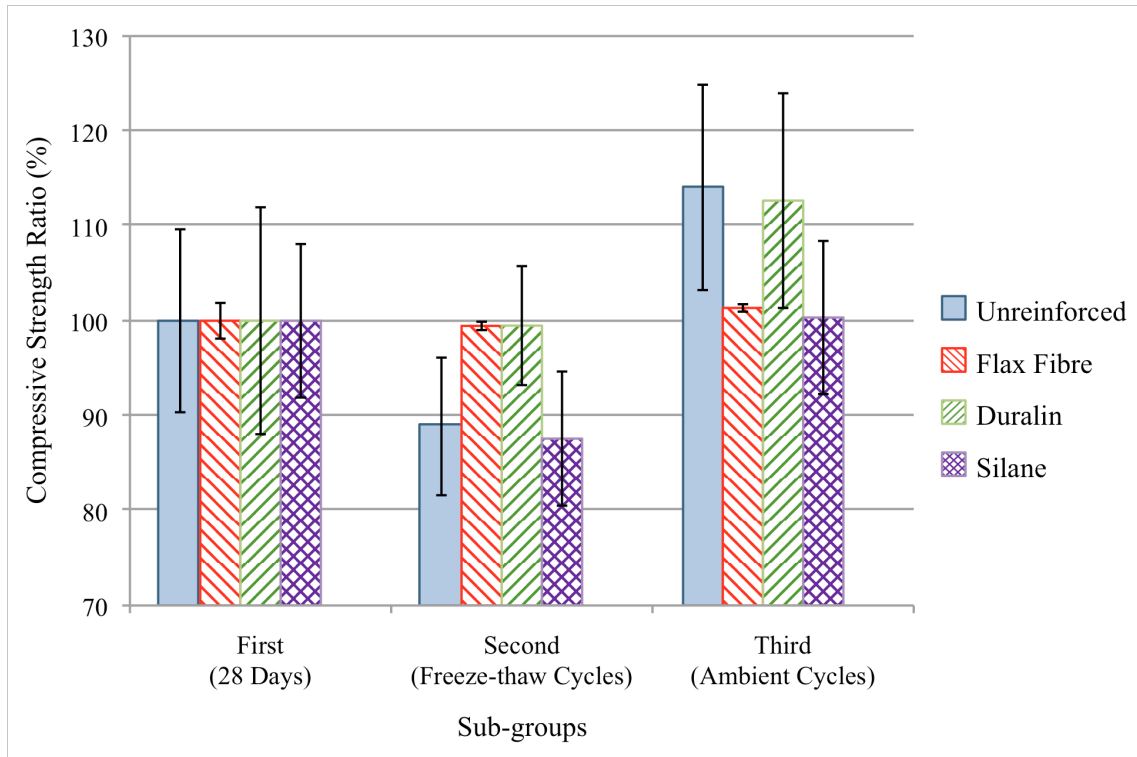


Figure 4.11. Normalized compressive strengths of Group Two blocks.

The compressive strengths of unreinforced and Duralin fibre-reinforced batches, in both cylinder and block forms, were not significantly different at a 90% level of confidence. Therefore, the compressive strengths of both batch types, in cylinders or blocks, were statistically similar. On this basis, a comparison of the compressive strengths of the unreinforced and Duralin fibre-reinforced batches in the second and third sub-groups should provide a realistic representation of their relative performance after weathering. The compressive strengths of blocks from these batches in the third sub-group, like the first sub-group, were not significantly different at a 90% level of confidence. However, the compressive strengths of blocks from these two batches in the second sub-group were significantly different at a 99% level of confidence, with the Duralin batch having a larger strength than the unreinforced batch. Since the two batches had similar strengths in all sub-groups except for the second, it can be concluded that the Duralin batch better retained its compressive strength after freeze-thaw cycling, when compared to the unreinforced batch.

Both the flax and silane fibre-reinforced batches were significantly different than the unreinforced batch at a 99% level of confidence. In every sub-group, the flax fibre-reinforced batch had larger strengths than the unreinforced batch, whereas the silane fibre-reinforced batch had lower strengths than the unreinforced batch.

A visible trend in the relative compressive strengths of blocks, which was also presented in Group one specimens (see Section 4.1.2), is that the beams in the third sub-group out-perform those in the second sub-group, at a 99% level of confidence.

All three fibre-reinforced batches in the second sub-group performed as well as or better than the unreinforced batch, showing that the presence of each fibre type was not detrimental to the specimens' performance after being weathered.

4.2.3. Dynamic Modulus of Elasticity

The dynamic modulus of elasticity (DME) of beams from all batches is shown in Table 4.9. The DME was found in these beams before they were tested in flexure. As was explained in Chapter 3, each of the three sub-groups was shipped in sealed containers from the lab in Richmond, once their weathering was completed.

The trend followed by all batch types, except for the Duralin batch, was that their DME decreased after subjecting the beams to rapid freezing and thawing cycles. There is no definite trend to be found for DME between batches, because of the large variation in DME. This large variation in DME between batches in the same sub-group is mainly due to the large variation in their compressive strengths presented in Tables 4.7 and 4.8. Variation in the performance of one fibre type relative to another could be more easily detected if the compressive strengths were similar between batches. Since there are significant differences in the DME between batches in each sub-group, it can not be concluded whether one batch type out-performed another, after undergoing freeze-thaw cycles.

Table 4.9. Dynamic modulus of elasticity (DME) for the beams from all batches in Group Two.

Sub-group	Batch Type	N*	DME (GPa)	SD* (GPa)	COV* (%)
First (28 days curing)	U ⁺	4	36.6	0.8	0.02
	R ⁺	4	45.0	0.7	0.01
	D ⁺	4	37.4	0.5	0.01
	S ⁺	4	30.8	0.4	0.01
Second (Freeze- thaw cycles)	U	4	34.9	0.5	0.01
	R	4	44.0	0.8	0.02
	D	4	37.5	0.4	0.01
	S	4	29.6	0.5	0.02
Third (Ambient)	U	4	33.9	0.3	0.01
	R	4	44.7	0.9	0.02
	D	4	36.0	0.3	0.01
	S	4	27.3	0.6	0.02

* N=number of specimens; SD=standard deviation; COV=coefficient of variation
+ U=unreinforced; R=flax fibre; D=Duralin; S=silane

4.2.4. Flexural Strength and Toughness

The flexural strength results for beams from all batches are presented in Table 4.10. Only one batch did not provide four beams for test results, because the beam failed outside the middle third of its span. The flexural strengths of beams from each of the three sub-groups, normalized by their respective 28 day strengths, are plotted in Figure 4.12. The error bars in the plots signify one standard deviation from the mean values.

Like the compressive strengths shown in Tables 4.7 and 4.8, there was a large variation in the flexural strengths between batches, as shown in Figure 4.15. This, once again, is attributed to the large variation in air contents between the batches.

Table 4.10. Flexural strength (FS) results for the beams from all batches in Group Two.

Sub-group	Batch Type	N*	FS (MPa)	SD* (MPa)	COV* (%)
First (28 days curing)	U ⁺	4	4.50	0.57	12.57
	R ⁺	4	6.43	0.21	3.30
	D ⁺	4	5.50	0.36	6.47
	S ⁺	4	4.48	0.15	3.34
Second (Freeze- thaw cycles)	U	4	5.90	0.30	5.01
	R	4	7.27	0.15	2.11
	D	4	6.12	0.12	2.04
	S	4	4.61	0.19	4.16
Third (Ambient)	U	4	6.74	0.36	5.32
	R	4	8.47	0.49	5.77
	D	3	7.55	0.24	3.23
	S	4	5.52	0.27	4.91

* N=number of specimens; SD=standard deviation; COV=coefficient of variation
+ U=unreinforced; R=flax fibre; D=Duralin; S=silane

One trend in the flexural strengths, which is different from the one found for the compressive strengths, was that the flexural strength of beams in the second sub-group out-performed the beams in the first sub-group. The compressive strength results show the opposite trend, in which the freeze-thaw cycles led to a decrease in the compressive strengths. The increase in flexural strength from the first sub-group to the second was statistically significant in the first three batch types, at a 95% level of confidence. The specimens from group one experienced a general decrease in flexural strength after being weathered in wetting and drying cycles. An interesting difference between the beams from group one and two, however, was the change in DME from before weathering to after weathering. The beams tested in group two seemed to lose less of their original DME, when compared to the loss of DME in the weathered beams in group one. This larger percent of original DME reflects the idea that the freeze-thaw weathered specimens retain more of their mechanical properties than the wet-dry weathered specimens.

All three fibre-reinforced batches in the second sub-group performed as well as or better than those batches in the first sub-group, showing that the presence of each fibre type was not detrimental to the specimens' performance after being weathered.

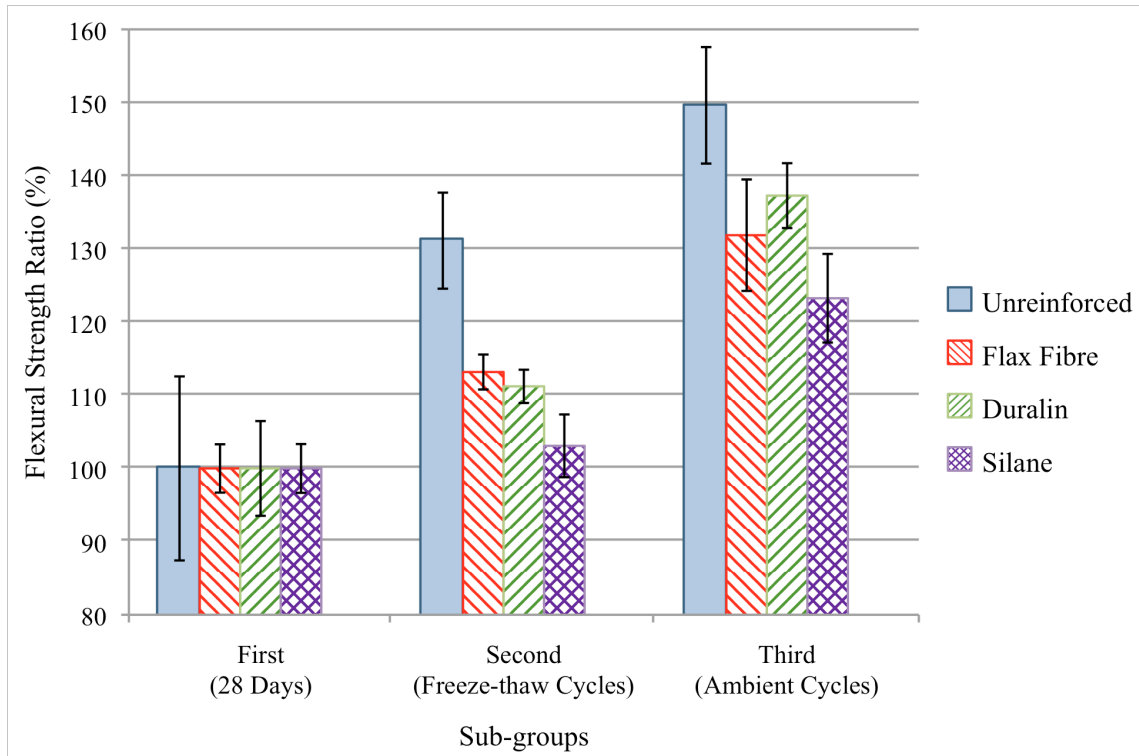


Figure 4.12. Normalized flexural strengths of Group Two beams.

The flexural toughness results for beams from all batches are presented in Table 4.11. As stated before, one Duralin fibre-reinforced beam strength was not used in the analysis, because the beam failed outside the middle third of its span. The post-cracking toughness values accounted for approximately 1-24% of the total toughness recorded. Similarly large variations in toughness were observed in group one beams. As was explained in Section 4.1.4, the high variability in toughness values makes it impractical to perform analysis to distinguish trends in the mean toughness values. Therefore, the presence of each fibre type was not detrimental to the specimens performance after being weathered, and the treated fibres provided no greater performance.

Table 4.11. Toughness results for the beams from all batches in Group Two.

Sub-group	Batch Type	Number of specimen	Toughness			SD*	COV*
			Pre-cracking (J)	Post-cracking (J)	Total (J)		
First (28 days curing)	U ⁺	4	0.21	-	0.21	0.05	23.5
	R ⁺	4	0.37	0.12	0.49	0.11	22.5
	D ⁺	4	0.34	0.02	0.35	0.08	21.6
	S ⁺	4	0.23	0.03	0.26	0.03	12.5
Second (Freeze-thaw curing)	U	4	0.32	-	0.32	0.07	20.6
	R	4	0.29	0.01	0.30	0.05	16.7
	D	4	0.34	0.01	0.35	0.04	12.4
	S	4	0.22	0.01	0.23	0.08	36.1
Third (ambient)	U	4	0.47	-	0.47	0.07	13.7
	R	4	0.35	0.03	0.37	0.21	55.3
	D	3	0.40	0.003	0.40	0.14	35.6
	S	4	0.30	0.004	0.30	0.08	27.9

* SD=standard deviation; COV=coefficient of variation

+ U=unreinforced; R=flax fibre; D=Duralin; S=silane

4.2.5. Failure Modes of Fibres

Like the fibres observed in group one, all three types of fibres experienced brittle fracture failures, at lengths ranging from 0.1 to 0.5 mm. These pull-out lengths indicate that beams may become unstable after crack widths ranging from 0.1 to 0.5 mm are reached, since the fibres typically failed at these lengths. The stiff and brittle nature of all three types of fibres does not allow for larger pull out lengths, most likely due to the strong bond held between the fibres and the cement paste. Scanning electron microscope (SEM) images of failed fibres from the first sub-group are plotted in Figure 4.13.

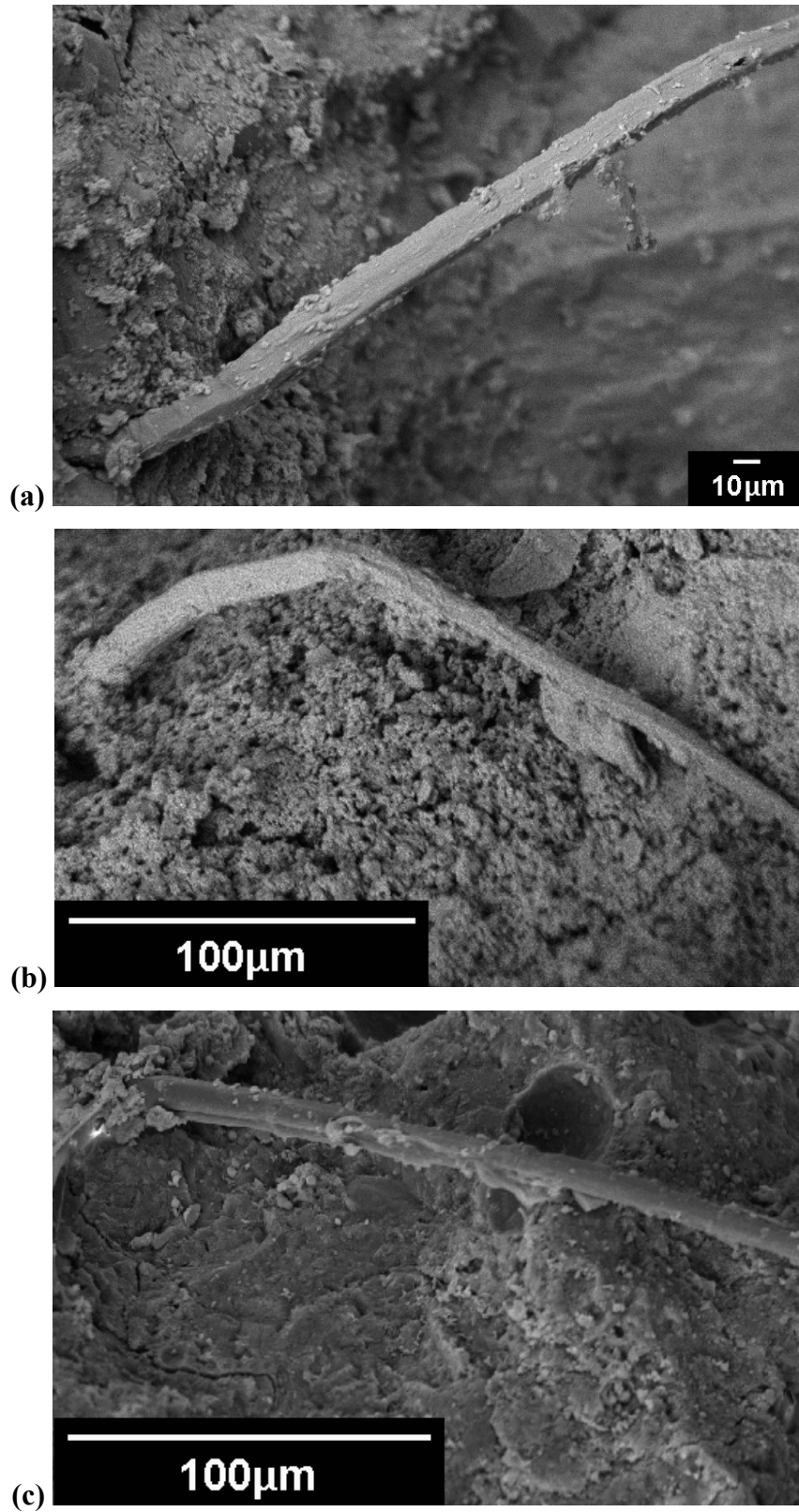


Figure 4.13. Failure surfaces of beams in the First sub-group of Group Two showing (a) flax fibre, (b) Duralin treated fibre, and (c) silane treated fibre.

Similar to the fibres observed in group one, all fibre types and sub-groups in group two contained both clean fibre and fibre covered in cement paste, as well as fibres of varying lengths. Thus, there were no trends found between the batch types or subgroups. The images of the first and second sub-groups can be viewed in Section B of the Appendix. Again, all of the fibre types showed similarly short pull-out fibre lengths, which constitutes a brittle failure.

4.3. Fibre Characteristics

4.3.1. Fibre Performance in Concrete

As was stated in Section 3.2.2, the SEM analysis of the fibres indicated that a combination of technical and elementary fibre sizes was present at the concrete mixing stage. However, evidence from the SEM analysis described in this Section, Sections 4.1.5 and 4.2.5, as well as Section B of the Appendix, indicates that the only fibre size left after the mixing and curing stages corresponded to elementary fibres. The mixing process was thought to have broken down all technical fibres into their elementary fibre components. Previous research has also reported this same phenomenon (Fernandez 2002).

Though there were no trends developed from the SEM analysis for either group of failed specimens, as discussed in Sections 4.1.5 and 4.2.5, there were many types of failed fibre found in beams from all batch types and sub-groups. This variety of failure types makes it more challenging to understand which mechanism causes flax fibre to fail in a brittle manner, when embedded in a cement paste.

One failure type prevalent in several of the samples observed is rupture, as shown in Figure 4.14. This failure type involved fibres which experienced no signs of pull-out from the cement paste and seem to fail right at the failure surface of the beams, as shown in Figure 4.14(a). This is most likely due to a strong bond developed between the cement paste and the fibres, caused by mineralization of the fibre.

A similar form of rupture was observed in fibres which appeared to fail from pull-out. Though these fibres extended out several 100 μm from the failure surface, as

shown in Figure 4.14(b), their ends resembled a ruptured failure which may have occurred inside the cement matrix to initiate pull-out.

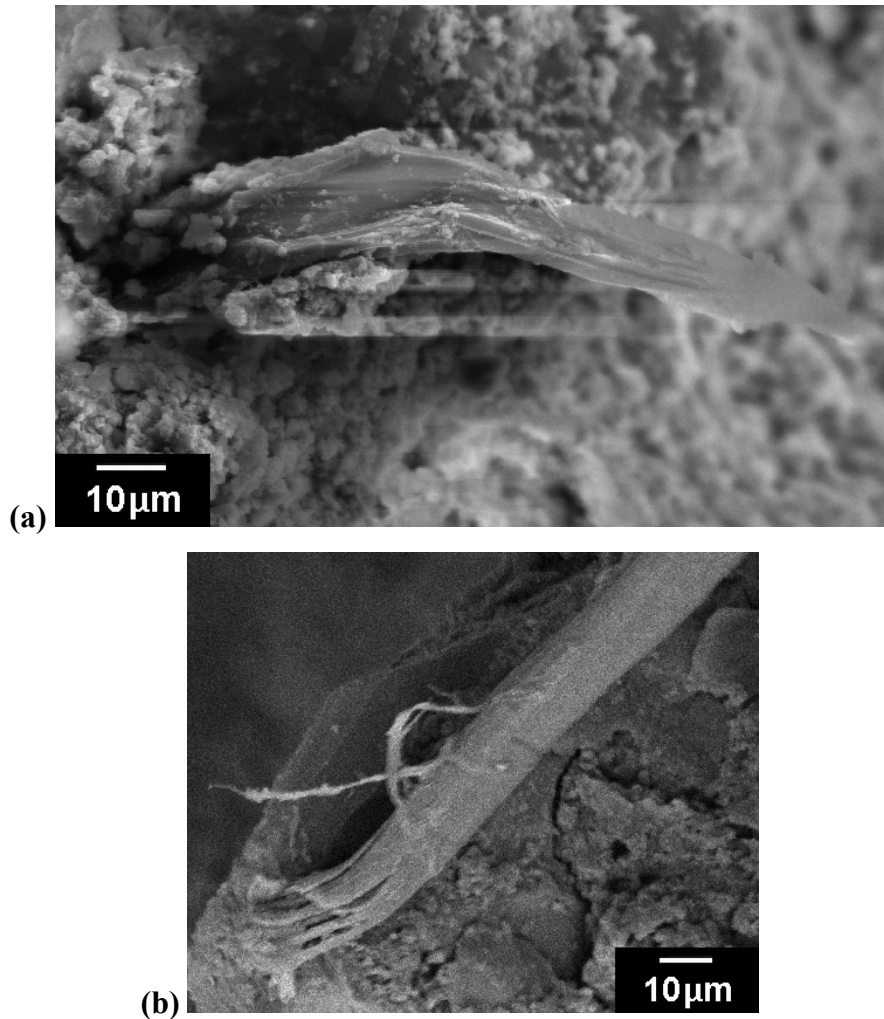


Figure 4.14. Rupture failure of (a) a flax fibre at the failure surface, and (b) a Duralin fibre several 100 µm away from the failure surface.

Another type of rupture failure found through SEM analysis was the loss of inner micro fibres from the elementary fibre, as shown in Figure 4.15. The hollow fibre shown in Figure 4.15(a) may have been the result of rupture of the outer fibre wall and inner micro fibres at different places along the fibre. Further possible evidence of fibres becoming hollow after failure is shown in Figure 4.15(b), where the fibre is shown to be flattened after losing its inner micro fibres.

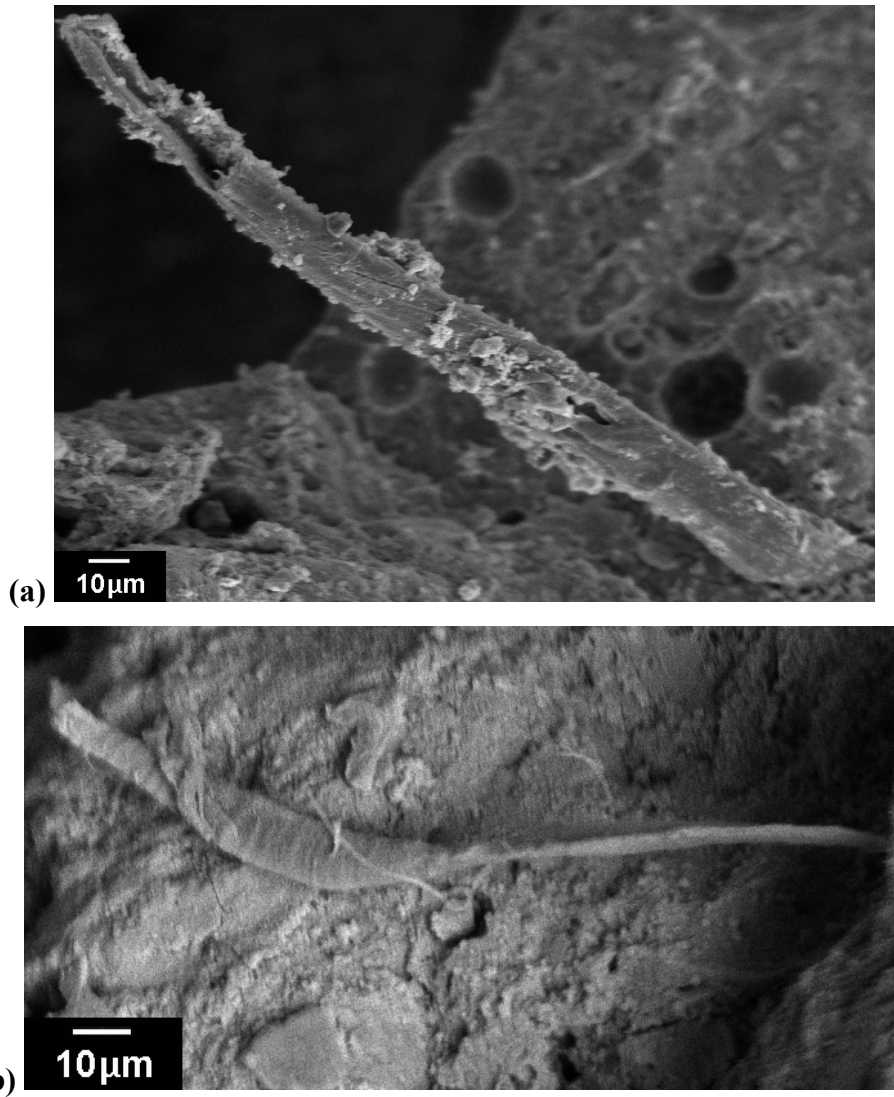


Figure 4.15. Possible loss of inner fibres during failure of Duralin fibre resulting in fibres which are (a) hollow, and (b) flat.

Another occurrence taking place along the crack surface of beams, as shown in Figure 4.16, is the propagation of flexural cracks along fibres. Fibres not situated perpendicular to the flexural crack surface, as shown by the fibre imprint on the failure surface in Figure 4.16(a), may have created weak spots in the matrix which assisted the propagation of the cracks. More evidence of fibres being situated parallel to the failure surface of beams is shown in Figure 4.16(b). Here, the remains of the outer fibre wall are shown, having been peeled off the rest of the fibre, and left on the failure surface.

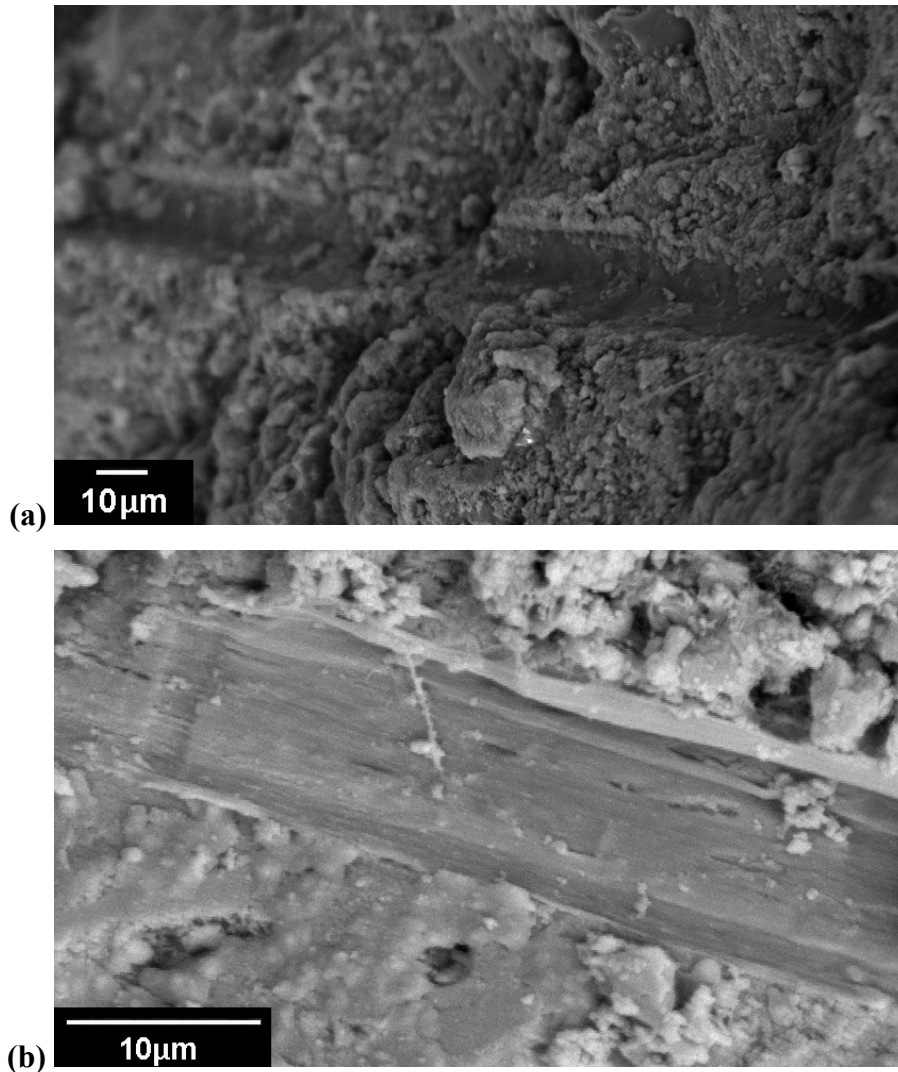


Figure 4.16. Evidence of fibres on the failure surface is shown by (a) (silane) fibre imprints in the surface, and (b) (flax) fibre material left on the surface.

The rare and final failure mechanism found in this study was that of the true fibre pull-out, shown in Figure 4.17. This fibre was the longest found on the failure surface of any sample observed by SEM in this study. This fibre is a true pull-out failure because it allows for large widening of the flexural crack, and potentially large energy absorption as the beam fails. Apart from this fibre, the longest fibres found in this study were approximately half the size of this one, which would explain the lack of post-cracking toughness found in all beams tested in this study.

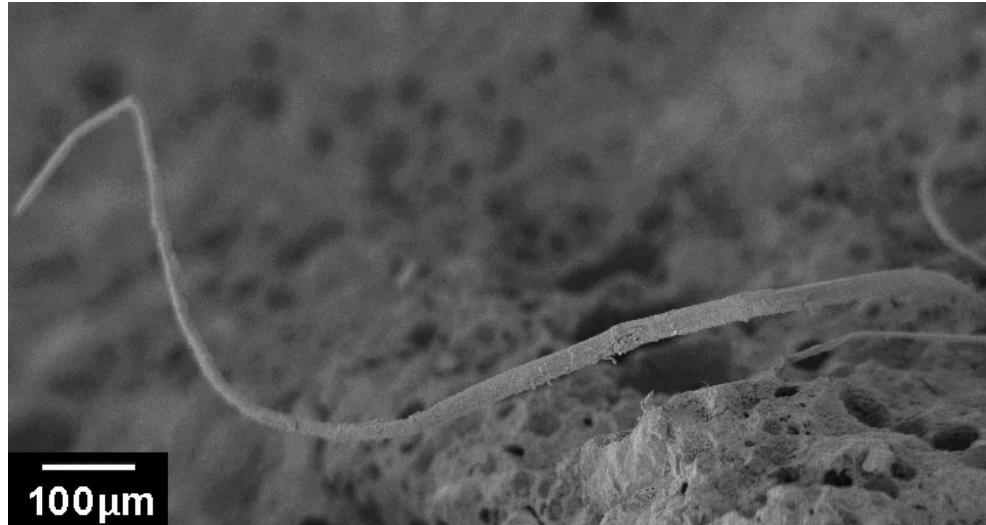


Figure 4.17. Silane fibre of long length.

4.3.2. Fibre Elemental Analysis

Elemental analysis was performed on the cement paste from each batch; a representation of all batches is shown in Figure 4.18. The dominant elements present in all paste analysed, as illustrated, were calcium and silicon. In order to understand how the different fibre types were affected by the concrete paste, elemental analysis was performed on the fibres before and after being placed in concrete, as shown in Figures 4.19 and 4.20, respectively.

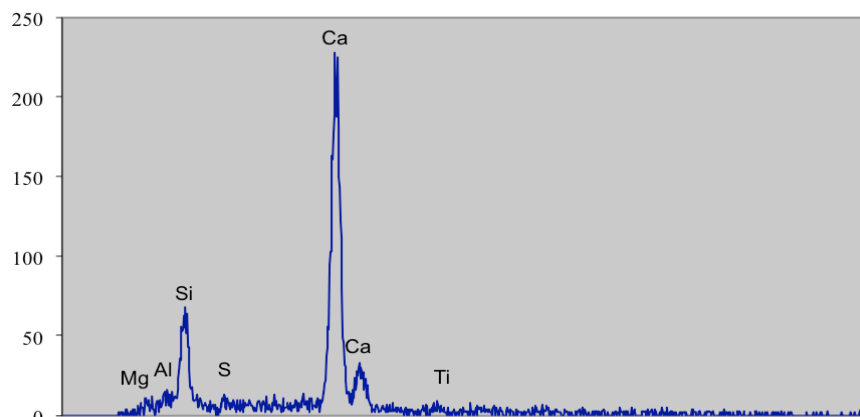


Figure 4.18. Elemental analysis of cement paste.

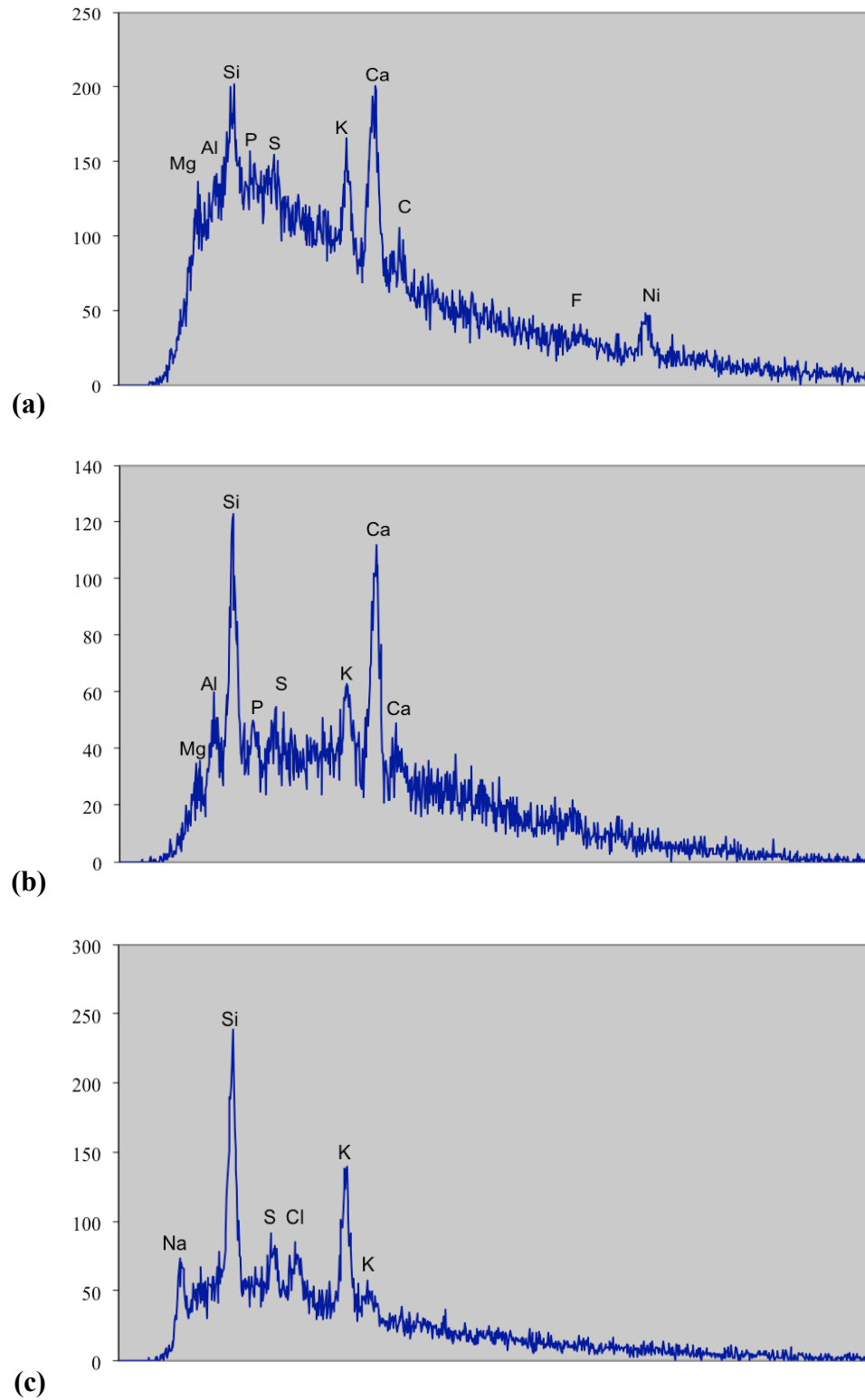


Figure 4.19. Elemental analysis on the surface of (a) untreated, (b) Duralin treated, and (c) silane treated flax fibre.

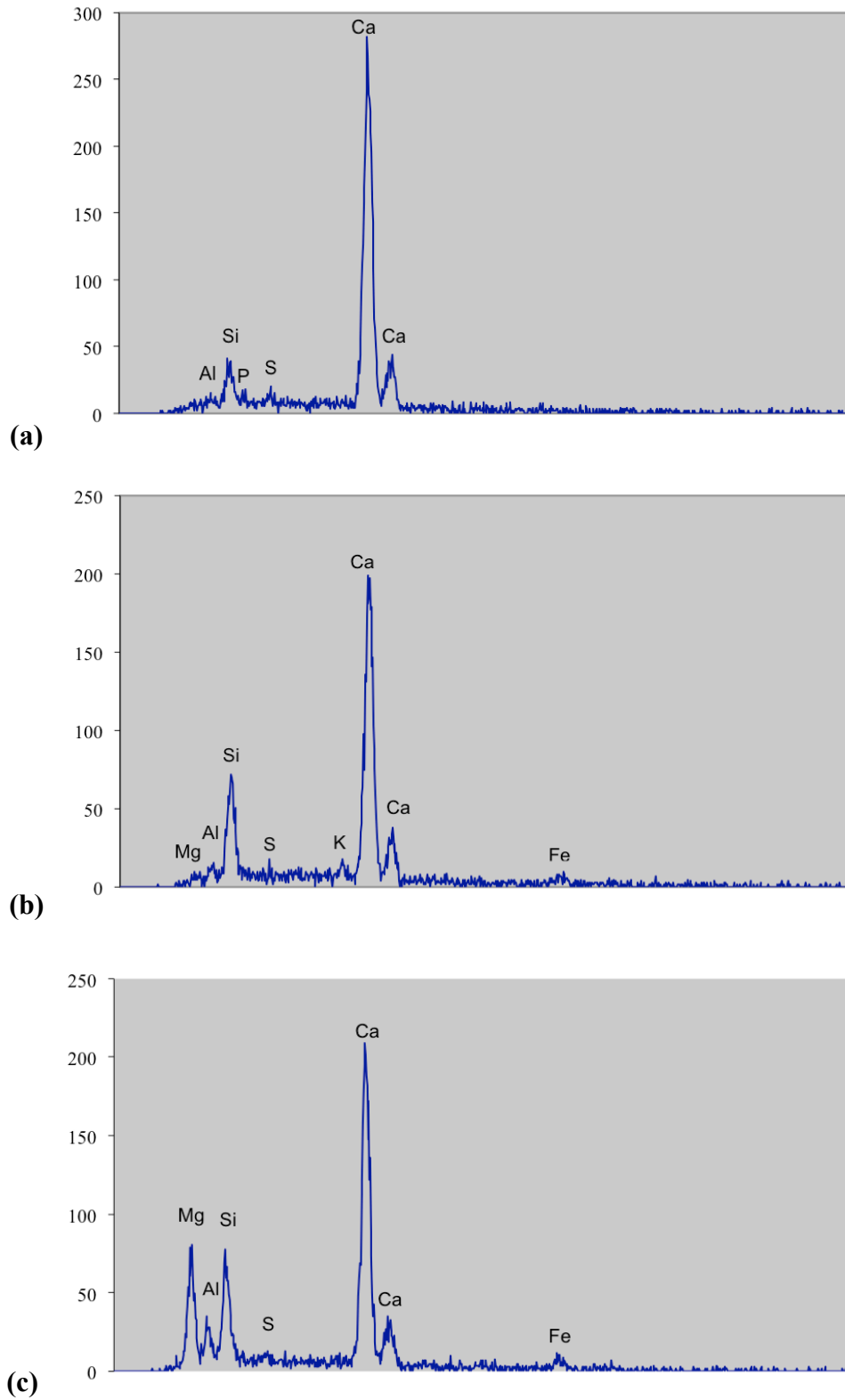


Figure 4.20. Elemental analysis on the surface of (a) untreated, (b) Duralin treated, and (c) silane treated flax fibre, from the second sub-group in Group One.

The elemental analysis of the surfaces of three fibre types, before being placed in the cement paste, show varied chemical compositions. The silane treated fibre was the most chemically different, simply because it was the only fibre of the three to be chemically treated. The elemental analysis of the surfaces of three fibre types, after being placed in the cement paste, show similar chemical compositions. All three fibre types show chemical compositions which are very similar to that of cement paste, which includes calcium as the main compound being generated from the analysis.

The elemental analysis shows that the surface of the fibres took on the chemical elements of the cement paste after being placed in it, most likely through the dissolving of these elements from the cement paste into the pore water and then onto the surface of the fibre. It should be noted that the elemental analysis only focused on the surface of the fibres, so the degree to which each fibre type experienced mineralization was not found.

5. Summary and Conclusions

Flax fibre-reinforced concrete (FFRC) was subjected to wet-dry cycling in order to determine the extent to which its mechanical properties degraded as a result of the weathering cycles. Two types of treated flax fibre (heat treated using the Duralin process and chemically treated with silane) were also tested to compare their performance with that of untreated flax fibre. Compression and flexural tests were performed on FFRC cylinders and beams, respectively. These tests were conducted both before and after approximately 220 days of wet-dry cycling was conducted, in order to determine whether degradation of the specimens took place as a result of the wet-dry cycles. The compressive strength of FFRC did not degrade after being subjected to wet-dry cycling, when compared to unreinforced concrete. The flexural strength of FFRC was also found not to degrade after being subjected to wet-dry cycling. The flexural toughness of FFRC was found to be highly variable, due to the strong bond between the fibre and cement paste, which created a brittle failure mode in the beams. As a result, a clear determination of whether the flexural toughness was degraded after being subject to wet-dry cycles could not be found. However, the flax fibre was not capable of adding a significant level of toughness to the concrete.

Flax fibre-reinforced concrete (FFRC) was also subjected to freeze-thaw cycling in order to determine the extent to which its mechanical properties degraded as a result of the weathering cycles. The performance of untreated flax fibre-reinforced concrete was tested along with the two types of treated flax fibre for comparison. Compression and flexural tests were performed on FFRC blocks and beams, respectively. In order to determine whether specimens degraded as a result of the freeze-thaw cycles, compression and flexural tests were conducted both before and after approximately 65 days (300 cycles) of freeze-thaw cycling. The compressive strength of FFRC did not

degrade after being subjected to freeze-thaw cycling, when compared to unreinforced concrete. The flexural strength of FFRC was also found not to degrade after being subjected to freeze-thaw cycling. The flexural toughness of FFRC was again found to be highly variable and small. Again, the strong bond between the fibre and cement paste created a brittle failure mode in the beams and did not permit the achievement of significant levels of flexural toughness. Therefore, it could not be concluded whether or not the flexural toughness was degraded after being subject to freeze-thaw cycles. Again, the flax fibre was not capable of adding a significant level of toughness to the concrete.

The mechanical properties of the Duralin and silane fibre-reinforced concrete batches were slightly different than the unreinforced batch for several tests in both Group one and two. However, the differences in strength and toughness values between the three batches were not statistically significant enough to conclude whether the treatment of flax fibre improves or impedes the performance of concrete.

Non-destructive testing was also carried out on specimens both during the weathering cycles and after testing, in order to track the change in properties over time. Dynamic modulus of elasticity (DME) was monitored during the wet-dry cycling, and the trends showed that as cycling went on, the beams experienced a reduction in their DME, presumably due to slight changes in the microstructure of the cement paste as it lost and took on moisture.

Other non-destructive tests used to examine the FFRC included scanning electron microscope (SEM) imaging and energy-dispersive x-ray spectroscopy (EDS) analysis. Analysis of the SEM images showed that the bulk of the failed fibres exposed on the flexural crack surfaces had a protruding length of 0.1-0.5 mm, which was too small to be regarded as pull-out failures. There was also no clear correlation between the condition of the fibres and the type of weathering they were subjected to. The EDS analysis showed that elements from the cement paste had adhered the surface of the fibres after they had been placed in the concrete, but the extent of mineralization inside the fibres was not found.

The presence of flax fibre does not seem to have a negative effect of the long-term performance of concrete.

5.1. Recommendations for Future Research

Future study is required to determine whether other forms or durations of weathering cycles would cause different types of flax fibre-reinforced concrete to degrade over time.

It is necessary to study the effect that moisture content has on the mechanical properties found in this study to determine whether or not a beam which has hardened in a laboratory for 7 months will perform differently dry or after being soaked in water for a short period of time.

Studies should focus on the distribution of fibres on the crack surfaces of the beams. This kind of study could generate a correlation between the distribution of fibres on the fracture surface and the strength and toughness values found in the beam.

Studies should also focus on mix designs or fibre treatments which could reduce the bond between fibre and cement paste, in order to improve the toughness of flax fibre-reinforced beam specimens.

List of References

- ASM International (1994). ASM Engineering Materials Reference Book, 2nd edition, edited by M. Baucchio, ASM International, Materials Park, OH, 74-880.
- Aamr-Daya, E., Langlet, T., Benazzouk, A., and Queneudec, M. (2008). Feasibility study of lightweight cement composite containing flax by-product particles: Physico-mechanical properties. *Cement and Concrete Composites*, 30(10): 957-963.
- Abdul Razak, H. and Ferdiansyah, T. (2005). Toughness characteristics of arenga pinnata fibre concrete. *Journal of Natural Fibers*, 2(2): 89-103.
- Aggarwal, L.K. (1995). Bagasse reinforced cement composites. *Cement and Concrete Composites*, 17(2): 107-112.
- Agopyan, V., Savastano Jr., H., John, V. M., and Cincotto, M. A. (2005). Developments on vegetable fibre-cement based materials in Sao Paulo, Brazil: An overview. *Natural Fibre Reinforced Cement Composites*, 27(5): 527-536.
- Al-Oraimi, S. and Seibi, A. C. (1995). Mechanical characterisation and impact behaviour of concrete reinforced with natural fibres. *Composite Structures*, 32(1-4): 165-171.
- Aly, M., Hashmi, M.S.J., Olabi, A.G., and Messeiry, M. (2011). Durability of waste glass flax fiber reinforced mortar. *AIP Conference Proceedings*, 1315, 241-246.
- Arsene, M.-A., Okwo, A., Bilba, K., Soboyejo, A.B.O., and Soboyejo, W.O. (2007). Chemically and thermally treated vegetable fibers for reinforcement of cement-based composites. *Materials and Manufacturing Processes*, 22(12): 214-227.
- Baley C. (2002). Analysis of the Flax fibres tensile behaviour and analysis of the tensile stiffness increase. *Composites: Part A* (33): 939-948.
- Banthia, N. and Trottier, J.F. (1995). Test methods for flexural toughness characterization of fiber reinforced concrete: some concerns and a proposition. *ACI Materials Journal*, 92: 48-57.

Bentur, A. and Akers, S.A.S. (1989). The microstructure and aging of cellulose fibre reinforced cement composites cured in a normal environment. *The International Journal of Cement Composites and Lightweight Concrete*, 11(2): 99-109.

Bernard, E.S. (2009). Influence of test machine control method on flexural performance of fiber reinforced concrete beams. *Journal of ASTM International*, 6(9).

Biagiotti, J., Puglia, D., and Kenny, J. M. (2004). A review on natural fibre-based composites - part I: Structure, processing and vegetable fibres. *Journal of Natural Fibers*, 1(2): 37-68.

Bilba, K., Arsene, M.-A., and Ouensanga, A. (2003). Sugar cane bagasse fibre reinforced cement composites. Part I. Influence of the botanical components of bagasse on the setting of bagasse/cement composite. *Cement and Concrete Composites*, 25(1): 91-96.

Bilba, K. and Arsene, M.-A. (2008). Silane treatment of bagasse fiber for reinforcement of cementitious composite. *Composites Part A: Applied Science and Manufacturing*, 39(9): 1488-1495.

Blankenhorn, P.R., Silsbee, M.R., Blankenhorn, B.D., Dicola, M. and Kessler, K. (1999). Temperature and moisture effects on selected properties of wood fiber-cement composites. *Cement and Concrete Research*, 29(5): 737-741.

Boghossian, E. and Wegner, L.D. (2003). Plastic shrinkage properties of flax fibre reinforced concrete. *Proceedings of the CSCE Annual Conference, Moncton, NB, June 4-7, 2003*, 1180-1118.

Boghossian, E. and Wegner, L.D. (2008). Use of flax fibres to reduce plastic shrinkage cracking in concrete. *Cement and Concrete Composites*, 30(10): 929-937.

Bos H. L. and Donald A.M. (1999). In situ ESEM study of the deformation of elementary flax fibres. *Journal of Material Sciences*, 34(13): 3029-3034.

Castro, J. and Naaman, A.E. (1981). Cement Mortar Reinforced with Natural Fibers. *Journal of Ferrocement*, 11(4): 285-301.

Cement & Concrete Institute (2010). *Fibre Reinforced Concrete*. Cement & Concrete Institute, Midrand, 2010.

Coutts, R.S.P. and Kightly, P. (1982). Microstructure of autoclaved refined wood-fibre cement mortars. *Journal of Materials Science*, 17(6): 1801-1806.

Coutts, R.S.P. and Kightly, P. (1984). Bonding in wood fibre-cement composites. *Journal of Materials Science*, 19(10): 3355-3359.

Coutts, R.S.P. (1987a). Eucalyptus wood fibre-reinforced cement. *Journal of Materials Science Letters*, 6(8): 955-995.

Coutts, R.S.P. (1987b). Fibre-matrix interface in air-cured wood-pulp fibre-cement composites. *Journal of Materials Science Letters*, 6(2): 140-142.

de Andrade Silva, F., Fairbairn, E.M.R., de Almeida Melo Filho, J., and Filho, R.D.T. (2009). Durability of compression molded sisal fiber reinforced mortar laminates. *Construction & Building Materials*, 23(6): 2409-2420.

El-Ashkar, N.H., Nanko, H., and Kurtis, K.E. (2007). Effect of moisture state on mechanical behavior and microstructure of pulp fiber-cement mortars. *Journal of Materials in Civil Engineering*, 19(8): 691-699.

Fernandez, J. E. (2002). Flax fiber reinforced concrete - A natural fiber biocomposite for sustainable building materials. *High Performance Structures and Composites*, 4: 193-207.

Gram, H.E. and Bergstrom, S.G. (1984). Durability of alkali-sensitive fibres in concrete. *International journal of cement composites and lightweight concrete*, 6(2): 75-80.

Gram, H.E. and Nimityongskul, P. (1987). Durability of Natural Fibers in Cement-based Roofing Sheets. *Journal of Ferrocement*, 17(4): 321-327.

Gram, H.E. (1988). Durability of natural fiber in concrete, in *Natural Fiber Reinforced Cement and Concrete*, Swamy, R.N. editor, Blackie, Glasgow and London, 143-172.

John, V. M., Cincotto, M. A., Sjostrom, C., Agopyan, V., and Oliveira, C. T. A. (2005). Durability of slag mortar reinforced with coconut fibre. *Natural Fibre Reinforced Cement Composites*, 27(5): 565-574.

Juarez, C., Duran, A., Valdez, P., and Fajardo, G. (2007). Performance of "Agave lecheguilla" natural fiber in Portland cement composites exposed to severe environment conditions. *Building and Environment*, 42(3): 1151-1157.

Kim, P.J., Wu, H.C., Lin, Z., Li, V.C., Delhoneux, B. and Akers, S.A.S. (1999). Micromechanics-based durability study of cellulose cement in flexure. *Cement and Concrete Research*, 29(2): 201-220.

Kriker, A., Debicki, G., Bali, A., Khenfer, M. M., and Chabannet, M. (2005). Mechanical properties of date palm fibres and concrete reinforced with date palm fibres in hot-dry climate. *Cement and Concrete Composites*, 27(5): 554-564.

Kriker, A., Bali, A., Debicki, G., Bouziane, M., and Chabannet, M. (2008). Durability of date palm fibres and their use as reinforcement in hot dry climates. *Cement and Concrete Composites*, 30(7): 639-648.

- Li, G., Yu, Y., Li, J., Li, C., and Wang, Y. (2004a). Research on adaptability between crop-stalk fibers and cement. *Cement and Concrete Research*, 34(7): 1081-1085.
- Li, Z.J., Wang, L.J., and Wang, X.G. (2004b). Compressive and flexural properties of hemp fiber reinforced concrete. *Fibers and Polymers*, 5(3): 187-197.
- Li, Z.J., Wang, X.G., and Wang, L.J. (2006). Properties of hemp fibre reinforced concrete composites. *Composites Part A-Applied Science and Manufacturing*, 37(3): 497-505.
- Li, Z., Wang, L., and Wang, X. (2007). Cement composites reinforced with surface modified coir fibers. *Journal of Composite Materials*, 41(12): 1445-1457.
- Maekawa, K., Chaube, R., and Kishi, T. (1999). *Modelling of concrete performance: hydration, microstructure formation and mass transport*. London and New York: E & FN Spon.
- MacVicar, R., Matuana, L.M. and Balatinecz, J.J. (1999). Aging mechanisms in cellulose fiber reinforced cement composites. *Cement and Concrete Composites*, 21(3): 189-196.
- Mai, Y.W., Hakeem, M.I., and Cotterell, B. (1983). Effects of water and bleaching on the mechanical properties of cellulose fibre cements. *Journal of Materials Science*, 18(7): 2156-2162.
- Mohr, B.J., Nanko, H., and Kurtis, K.E. (2005). Durability of kraft pulp fiber-cement composites to wet/dry cycling. *Cement and Concrete Composites*, 27(4): 435-448.
- Morrissey, F. E., Coutts, R. S. P., and Grossman, P. U. A. (1985). Bond Between Cellulose Fibres and Cement. *International Journal of Cement Composites and Lightweight Concrete*, 7(2): 73-80.
- Neithalath, N. (2006). Damage assessment in cellulose-cement composites using dynamic mechanical characteristics. *Cement and Concrete Composites*, 28(7): 658-667.
- Olubayo, K. (2010). Durability of Chemically Treated Flax Fibre in Concrete Pore Water Solution. Technical Report, Department of Civil and Geological Engineering, University of Saskatchewan. March 2010.
- Pejic, B.M., Kostic, M.M., Skundric, P.D., and Praskalo, J.Z. (2007). The effects of hemicellulose and lignin removal on water uptake behaviour on hemp fibres. *Bioresource Technology*, 99: 7152-7159.
- Pichor, W., Petri, M., and Deja, J. (2000). Properties of FRC with modified cellulose fibres. *Fifth Rilem Symposium on Fibre-Reinforced Concretes (FRC)*, 15: 643-652.

- Portland Cement Association (PCA) (1991). *Fiber Reinforced Concrete*, Skokie, Illinois.
- Ramakrishna, G. and Sundararajan, T. (2005a). Studies on the durability of natural fibres and the effect of corroded fibres on the strength of mortar. *Natural Fibre Reinforced Cement Composites*, 27(5): 575-582.
- Ramakrishna, G. and Sundararajan, T. (2005b). Impact strength of a few natural fibre reinforced cement mortar slabs: A comparative study. *Cement and Concrete Composites*, 27(5): 547-553
- Rodrigues, C. d. S., Ghavami, K., and Stroeven, P. (2006). Porosity and water permeability of rice husk ash-blended cement composites reinforced with bamboo pulp. *Journal of Materials Science*, 41(21): 6925-6937.
- Roma Jr., L.C., Martello, L.S., and Savastano Jr., H. (2008). Evaluation of mechanical, physical and thermal performance of cement-based tiles reinforced with vegetable fibers. *Construction and Building Materials*, 22(4): 668-674.
- Romualdi, J.P. and Batson, G.B. (1963). Behavior of reinforced concrete beams with closely spaced reinforcement. *American Concrete Institute -- Journal*, 60(6): 775-790.
- Roy, D.M., Brown, P.W., Shi, D., Scheetz, B.E, and May, W. (1993). *Concrete microstructure porosity and permeability*. Strategic Highway Research Program, Washington, DC, 1993.
- Sargaphuti, M., Shah, S.P., and Vinson, K.D. (1993). Shrinkage cracking and durability characteristics of cellulose fiber reinforced concrete. *ACI Materials Journal*, 90(4): 309-318.
- Savastano Jr., H., and Agopyan, V. (1999). Transition zone studies of vegetable fibre-cement paste composites. *Cement and Concrete Composites*, 21(1): 49-57.
- Savastano Jr., H., Warden, P.G., and Coutts, R.S.P. (2000). Brazilian waste fibres as reinforcement for cement-based composites. *Cement and Concrete Composites*, 22(5): 379-384.
- Savastano Jr., H., John, V.M., Agopyan, V. and Pellegrino Ferreira, O. (2002). Weathering of vegetable fibre-clinker free cement composites. *Materials and Structures/Materiaux et Constructions*, 34(245): 64-68.
- Savastano Jr., H., Warden, P. G., and Coutts, R. S. P. (2005). Microstructure and mechanical properties of waste fibre-cement composites. *Natural Fibre Reinforced Cement Composites*, 27(5): 583-592.

Savastano Jr., H., Santos, S. F., Soboyejo, W. O., and Radonjic, M. (2009). Fracture and fatigue of natural fiber-reinforced cementitious composites. *Cement and Concrete Composites*, 31(4): 232-43.

Sedan, D., Pagnoux, C., Smith, A., and Chotard, T. (2008). Mechanical properties of hemp fibre reinforced cement: Influence of the fibre/matrix interaction. *Journal of the European Ceramic Society*, 28(1): 183-192.

Shao, Y., Moras, S., Ulkem, N. and Kubes, G. (2000). Wood fibre - Cement composites by extrusion. *Canadian Journal of Civil Engineering*, 27(3): 543-552.

Siddique, R. (2005). Fracture toughness and impact strength of high-volume class-f fly ASH concrete reinforced with san fibres. 2005 International Congress - Global Construction: Ultimate Concrete Opportunities, July 5, 2005 - July 7, 487-494.

Soroushian, P. and Marikunte, S. (1991). Moisture sensitivity of cellulose fiber reinforced cement. *Durability of concrete*, 1&2: 821-835.

Soroushian, P., Marikunte, S., and Won, J.P. (1994). Wood fibre-reinforced cement composites under wetting-drying and freezing-thawing cycles. *Journal of materials in civil engineering*, 6(4): 595-611.

Soroushian, P. and Marikunte, S. (1995). Statistical evaluation of long-term durability characteristics of cellulose fiber reinforced cement composites. *ACI Materials Journal*, 91(6): 607-616.

Soroushian, P., Marikunte, S., and Won, J.P. (1995). Statistical evaluation of mechanical and physical properties of cellulose fibre reinforced cement composites. *ACI Materials Journal*, 92(2): 172-180.

Soroushian, P., Shah, Z., and Won, J.P. (1996). Aging effects on the structure and properties of recycled wastepaper fiber cement composites. *Materials and structures*, 29(189): 312-317.

Soroushian, P. and Ravanbakhsh, S. (1998). Control of plastic shrinkage cracking with specialty cellulose fibers. *ACI Materials Journal*, 95(4): 429-435.

Soroushian, P. and Ravanbakhsh, S. (1999). High-early-strength concrete: Mixture proportioning with processed cellulose fibers for durability. *ACI Materials Journal*, 96(5): 593-599.

Soroushian, P., Simsek, O., Elzafraney, M., and Ghebrab, T. (2009). Compatibility of cereal straw with hydration of cement. *Journal of Solid Waste Technology and Management*, 35(1): 1-6.

- Stamboulis, A., Baillie C.A., and Peijs T. (2001). Effects of environmental conditions on mechanical and physical properties of flax fibre. *Composites: Part A* (32): 1105-1115.
- Stancato, A.C., Burke, A.K., and Beraldo, A.L. (2005). Mechanism of a vegetable waste composite with polymer-modified cement (VWCPMC). *Cement and Concrete Composites*, 27(5): 599-603.
- Toledo Filho, R.D., and Sanjuan, M.A. (1999) Effect of low modulus sisal and polypropylene fibre on the free and restrained shrinkage of mortars at early age. *Cement and Concrete Research*, 29: 1597-1604.
- Toledo Filho, R.D., Scrivener, K., England, G.L., and Ghavami, K. (2000). Durability of alkali-sensitive sisal and coconut fibres in cement mortar composites. *Cement and Concrete Composites*, 22(2): 127-143.
- Toledo Filho, R.D., Scrivener, K., England, G.L., and Ghavami, K. (2003). Development of vegetable fibre-mortar composites of improved durability. *Cement and Concrete Composites*, 25(2): 185-196.
- Toledo Filho, R.D., Scrivener, K., England, G.L., and Ghavami, K. (2005). Free, restrained and drying shrinkage of cement mortar composites reinforced with vegetable fibres. *Cement and Concrete Composites*, 27(5): 537-546.
- Tonoli, G.H.D., Joaquim, A.P., Arsene, M.-A., Bilba, K., and Savastano Jr., H. (2007). Performance and durability of cement based composites reinforced with refined sisal pulp. *Materials and Manufacturing Processes*, 22(1-2): 149-156.
- Tonoli, G.H.D., Rodrigues Filho, U.P., Savastano Jr., H., Bras, J., Belgacem, M.N., and Rocco Lahr, F.A. (2009). Cellulose modified fibres in cement based composites. *Composites Part A: Applied Science and Manufacturing*, 40(12): 2046-2053.
- Tonoli, G.H.D., Santos, S.F., Joaquim, A.P., and Savastano Jr., H. (2010a). Effect of accelerated carbonation on cementitious roofing tiles reinforced with lignocellulosic fibre. *Construction & Building Materials*, 24(2): 193-201.
- Tonoli, G.H.D., Savastano Jr., H., Fuente, E., Negro, C., Blanco, A., and Rocco Lahr, F.A. (2010b). Eucalyptus pulp fibres as alternative reinforcement to engineered cement-based composites. *Industrial Crops and Products*, 31(2): 225-232.
- Tonoli, G.H.D., Almeida, A.E.F., Pereira-da-Silva, M.A., Bassa, A., Oyakawa, D., and Savastano Jr., H. (2010c). Surface properties of eucalyptus pulp fibres as reinforcement of cement-based composites. *Holzforschung*, 64(5): 595-601.

Tonoli, G.H.D., Santos, S.F., Savastano Jr., H., Delvasto, S., Mejia de Gutierrez, R., and Lopez de Murphy, M. del M. (2011). Effects of natural weathering on microstructure and mineral composition of cementitious roofing tiles reinforced with fique fibre. *Cement and Concrete Composites*, 33(2): 225-232.

Ulrich, A. (2008). Canadian flax straw: present and future end use options. Proceedings of 2008 International Conference on Flax and Other Bast Fibres, Saskatoon, SK, July 21-23, 281-289.

Wang, T. (2003). Flexural Toughness of Flax Fibre Reinforced Concrete. Master of Science Thesis, Department of Civil and Geological Engineering, University of Saskatchewan. February 2003.

Zheng, X., Xu, J., and Li, X. (2010). Effect of alkaline treatment of straw fiber on mechanical properties of cement-bonded straw fiber board. 2010 International Conference on Mechanic Automation and Control Engineering, 3006-3008.

Appendix

Section A: Statistical Calculations

Table A.1. Statistical Data for Compressive strength (MPa) results of cylinders from all batches in Group One.

Sub-groups	First (28 days curing)			Second (50 cycles)			Third (25 cycles)			Fourth (50 ambient cycles)			Fifth (25 ambient cycles)							
	U	R	S	U	R	S	U	R	S	U	R	S	U	R	S					
Batches	23.71	25.29	26.73	27.19	24.47	24.71	24.93	24.83	24.32	23.90	27.61	28.59	30.36	33.28	34.42	38.10	33.65	32.93	33.52	36.02
Specimen Strength	25.50	23.09	24.54	26.47	25.29	27.69	25.52	28.49	23.58	26.22	26.25	28.86	32.79	34.51	31.72	33.05	32.36	30.42	34.06	33.63
	25.01	26.10	27.07	26.21	25.06	24.74	28.19	27.41	24.07	26.32	24.45	28.04	30.36	31.20	34.93	36.85	34.38	31.52	35.93	33.43
	24.60	26.32	24.48	27.26	24.29	23.23	25.30	27.18	23.86	25.89	27.22	28.45	31.06	35.90	36.54	36.65	31.68	32.98	35.20	36.95
Average Strength	24.70	25.20	25.70	26.78	24.78	25.09	25.98	26.98	23.96	25.58	26.38	28.49	31.14	33.72	34.41	36.16	33.02	31.96	34.68	35.01
Standard Deviation	0.76	1.48	1.39	0.52	0.47	1.87	1.49	1.54	0.31	1.14	1.41	0.34	1.14	1.99	2.00	2.17	1.22	1.23	1.09	1.75
Coefficient of Variation	3.06	5.85	5.40	1.96	1.91	7.45	5.74	5.72	1.30	4.45	5.34	1.19	3.67	5.91	5.82	6.01	3.69	3.85	3.14	5.01
Variance	0.57	2.18	1.93	0.27	0.22	3.49	2.22	2.38	0.10	1.29	1.98	0.12	1.31	3.98	4.02	4.72	1.49	1.52	1.18	3.07
Number of Specimens	4	4	4	4	4	4	4	4	4	4	4	4	4	4	4	4	4	4	4	4

Table A.2. Statistical Comparison of Compressive strength results of cylinders from all batches in Group One.

	Sub-groups											
	First (28 days curing)	Second (50 cycles)	Third (25 cycles)	Fourth (50 ambient cycles)	Fifth (25 ambient cycles)							
	Degrees of Freedom	t-value	Probability	Degrees of Freedom	t-value	Probability						
U and R	6	0.60	> 0.1	6	2.75	0.05	6	2.25	0.1	6	1.22	> 0.1
U and D	6	1.26	> 0.1	6	3.36	0.05	6	2.83	0.5	6	2.03	0.1
U and S	6	4.52	0.01	6	19.67	0.001	6	4.09	0.01	6	1.86	> 0.1
R and D	6	0.49	> 0.1	6	0.88	> 0.1	6	0.48	> 0.1	6	3.30	0.05
R and S	6	2.02	0.1	6	4.89	0.01	6	1.65	> 0.1	6	2.84	0.05
D and S	6	1.46	> 0.1	6	2.91	0.05	6	1.19	> 0.1	6	0.32	> 0.1

Table A.3. Statistical Comparison of Compressive strength results of cylinders from all batches in Group One.

	Batches											
	Unreinforced	Flax Fibre	Duralin	Silane								
	Degrees of Freedom	t-value	Probability	Degrees of Freedom	t-value	Probability						
First and Second	6	0.17	> 0.1	6	0.09	> 0.1	6	0.28	> 0.1	6	0.24	> 0.1
First and Third	6	1.83	> 0.1	6	0.41	> 0.1	6	0.69	> 0.1	6	5.46	0.01
First and Fourth	6	9.39	0.001	6	6.87	0.001	6	7.14	0.001	6	8.40	0.001
First and Fifth	6	11.58	0.001	6	7.04	0.001	6	10.18	0.001	6	9.00	0.001
Second and Fourth	6	10.28	0.001	6	6.32	0.001	6	6.74	0.001	6	6.89	0.001
Third and Fifth	6	14.40	0.001	6	7.61	0.001	6	9.32	0.001	6	7.31	0.001
Second and Third	6	2.90	0.05	6	0.45	> 0.1	6	0.39	> 0.1	6	1.91	> 0.1
Fourth and Fifth	6	2.24	0.1	6	1.50	> 0.1	6	0.24	> 0.1	6	0.83	> 0.1

Table A.4. Statistical Data for Compressive strength (MPa) results of blocks from all batches in Group One.

Sub-groups Batches	First (28 days curing)			Second (50 cycles)			Third (25 cycles)			Fourth (50 ambient cycles)			Fifth (25 ambient cycles)								
	U	R	S	U	R	S	U	R	S	U	R	S	U	R	S						
Specimen Strength	29.25	24.29	25.06	32.11	25.92	24.02	26.94	27.49	19.21	24.44	23.33	31.60	27.27	31.63	37.39	36.83	30.98	28.93	33.34	33.32	
	24.63	25.00	23.36	28.12	24.95	27.55	23.35	27.79	20.18	27.03	27.35	31.50	31.22	35.25	38.10	42.36	30.15	30.06	29.64	35.66	
	24.95	29.94	32.14	32.84	25.13	25.93	28.05	27.47	22.48	27.10	23.25	26.47	28.17	36.17	38.94	36.08	31.44	35.58	31.80	34.86	
	27.60	24.33	28.09	35.19	24.76	29.68	26.67	28.09	25.24	27.58	24.45	26.13	29.85	37.78	37.63	38.30	26.59	30.86	34.43	33.94	
	28.20	26.36	26.66	35.94	24.52	26.50	26.05	31.22	25.56	22.82	21.96		34.81	35.65	34.50	33.15	27.61	35.46	33.24	32.65	
	27.25	27.05	26.87		23.04	24.40	22.44	28.82	24.93	27.70	26.11		30.75	34.52	34.19	36.56	29.69	34.17	35.93	37.40	
	26.21	29.47	30.94		21.98	24.61	24.22	30.08	22.79	27.74	26.94		34.98	32.56	40.42		32.41	31.22	33.28	36.18	
	24.15	30.54	31.54			28.73	28.04	28.44	18.37	28.00	30.49							30.86			
	Average Strength	26.53	27.12	28.08	32.84	24.33	26.43	25.72	28.67	22.34	26.55	25.49	28.92	31.01	34.79	36.79	37.67	29.84	32.14	33.10	34.86
	Standard Deviation	1.84	2.56	3.20	2.74	1.35	2.09	2.14	1.34	2.82	1.88	2.78	3.03	2.99	2.11	1.97	3.02	2.09	2.56	1.98	1.68
Coefficient of Variation	6.94	9.45	11.38	8.33	5.55	7.92	8.30	4.66	12.64	7.10	10.92	10.49	9.65	6.08	5.36	8.03	6.99	7.95	5.98	4.82	
Variance	3.39	6.56	10.21	7.48	1.83	4.38	4.56	1.78	7.98	3.55	7.75	9.20	8.94	4.47	3.89	9.14	4.35	6.53	3.92	2.82	
Number of Specimens	8	8	8	5	7	8	8	8	8	8	8	4	7	7	6	7	7	8	8	7	

Table A.5. Statistical Comparison of Compressive strength results of blocks from all batches in Group One.

	Sub-groups														
	First (28 days curing)			Second (50 cycles)			Third (25 cycles)			Fourth (50 ambient cycles)			Fifth (25 ambient cycles)		
	Degrees of Freedom	t-value	Probability	Degrees of Freedom	t-value	Probability	Degrees of Freedom	t-value	Probability	Degrees of Freedom	t-value	Probability	Degrees of Freedom	t-value	Probability
U and R	14	0.53	> 0.1	13	2.33	0.05	14	3.51	0.01	12	2.74	0.05	13	1.92	0.1
U and D	14	1.19	> 0.1	13	1.52	> 0.1	14	2.24	0.05	11	4.17	0.01	12	3.00	0.05
U and S	12	4.88	0.001	13	6.25	0.001	10	3.62	0.01	12	4.15	0.01	12	4.96	0.001
R and D	14	0.66	> 0.1	14	0.67	> 0.1	14	0.90	> 0.1	11	1.76	> 0.1	13	0.81	> 0.1
R and S	12	3.98	0.01	14	2.56	0.05	10	1.43	> 0.1	12	2.06	0.1	13	2.46	0.05
D and S	12	2.99	0.05	14	3.32	0.01	10	1.90	0.1	11	0.63	> 0.1	12	1.80	0.1

Table A.6. Statistical Comparison of Compressive strength results of blocks from all batches in Group One.

	Batches											
	Unreinforced			Flax Fibre			Duralin			Silane		
	Degrees of Freedom	t-value	Probability									
First and Second	13	2.66	0.05	14	0.60	> 0.1	14	1.74	> 0.1	11	3.18	0.01
First and Third	14	3.51	0.01	14	0.51	> 0.1	14	1.73	> 0.1	7	2.01	0.1
First and Fourth	13	3.43	0.01	13	6.35	0.001	12	6.28	0.001	10	2.89	0.05
First and Fifth	13	3.24	0.01	14	3.92	0.01	13	3.70	0.01	10	1.47	> 0.1
Second and Fourth	12	5.38	0.001	13	7.68	0.001	12	10.03	0.001	13	7.28	0.001
Third and Fifth	13	5.89	0.001	14	4.98	0.001	13	6.16	0.001	9	3.61	0.01
Second and Third	13	1.77	0.1	14	0.13	> 0.1	14	0.19	> 0.1	10	0.16	> 0.1
Fourth and Fifth	12	0.85	> 0.1	13	2.20	0.05	11	3.36	0.01	12	2.15	0.1

Table A.7. Statistical Comparison of Compressive strength results of cylinders and blocks from all batches in Group One.

	Batches											
	Unreinforced			Flax Fibre			Duralin			Silane		
	Degrees of Freedom	t-value	Probability									
First (28 days curing)	10	2.43	0.01	10	1.64	> 0.1	10	1.79	> 0.1	8	7.60	0.001
Second (50 cycles)	9	-0.80	> 0.1	10	1.12	> 0.1	10	-0.25	> 0.1	10	1.88	0.1
Third (25 cycles)	10	-1.60	> 0.1	10	1.11	> 0.1	10	-0.74	> 0.1	6	0.29	> 0.1
Fourth (50 ambient cycles)	9	-0.11	> 0.1	9	0.84	> 0.1	8	1.86	> 0.1	9	0.96	> 0.1
Fifth (25 ambient cycles)	9	-3.19	0.01	10	0.16	> 0.1	9	-1.71	> 0.1	9	-0.14	> 0.1

Table A.8. Statistical Data for Flexural strength (MPa) results of beams from all batches in Group One.

Sub-groups Batches	First (28 days curing)			Second (50 cycles)			Third (25 cycles)			Fourth (50 ambient cycles)			Fifth (25 ambient cycles)							
	U	R	S	U	R	S	U	R	S	U	R	S	U	R	S					
Specimen Strength	3.98	3.91	3.50	4.20	3.28	3.65	2.70	3.32	2.87	3.35	2.82	3.56	4.61	5.79	4.34	5.24	4.96	4.71	4.79	4.14
	3.78	3.86	3.45	4.13	3.28	3.35	2.74	2.55	3.51	3.84	3.89	4.21	4.67	5.29	4.87	4.80	5.29	4.99	4.59	4.50
	3.72	3.47	3.42	4.44	3.08	2.83	4.21	3.24	3.15	3.43	3.15	3.37	4.12	4.55	4.00	4.91	5.11	4.65	4.56	4.08
	4.01	3.90	4.12	4.02		3.85	3.12	3.85	3.54	3.75	4.23		4.89	4.70	4.91		4.33	4.28	4.11	4.69
Average Strength	3.87	3.79	3.62	4.20	3.21	3.42	3.20	3.24	3.27	3.59	3.52	3.71	4.57	5.08	4.53	4.98	4.92	4.66	4.51	4.35
Standard Deviation	0.14	0.21	0.33	0.17	0.12	0.44	0.70	0.53	0.32	0.24	0.65	0.44	0.32	0.57	0.44	0.23	0.42	0.29	0.28	0.29
Coefficient of Variation	3.75	5.50	9.24	4.14	3.67	12.99	22.01	16.50	9.75	6.74	18.41	11.82	7.10	11.20	9.66	4.58	8.44	6.24	6.28	6.66
Variance	0.02	0.04	0.11	0.03	0.01	0.20	0.49	0.29	0.10	0.06	0.42	0.19	0.11	0.32	0.19	0.05	0.17	0.08	0.08	0.08
Number of Specimens	4	4	4	4	3	4	4	4	4	4	4	3	4	4	4	3	4	4	4	4

Table A.9. Statistical Comparison of Flexural strength results of beams from all batches in Group One.

	Sub-groups											
	First (28 days curing)		Second (50 cycles)		Third (25 cycles)		Fourth (50 ambient cycles)		Fifth (25 ambient cycles)			
	Degrees of Freedom	t-value	Probability	Degrees of Freedom	t-value	Probability	Degrees of Freedom	t-value	Probability	Degrees of Freedom	t-value	Probability
U and R	6	0.67	> 0.1	5	0.89	> 0.1	6	1.61	> 0.1	6	1.56	> 0.1
U and D	6	1.35	> 0.1	5	0.04	> 0.1	6	0.70	> 0.1	6	0.14	> 0.1
U and S	6	2.90	0.05	5	0.11	> 0.1	5	1.47	> 0.1	5	1.96	> 0.1
R and D	6	0.82	> 0.1	6	0.53	> 0.1	6	0.20	> 0.1	6	1.53	> 0.1
R and S	6	3.04	0.05	6	0.51	> 0.1	5	0.42	> 0.1	5	0.32	> 0.1
D and S	6	3.05	0.05	6	0.10	> 0.1	5	0.46	> 0.1	5	1.76	> 0.1

Table A.10. Statistical Comparison of Flexural strength results of beams from all batches in Group One.

	Batches											
	Unreinforced			Flax Fibre			Duralin			Silane		
	Degrees of Freedom	t-value	Probability									
First and Second	5	6.62	0.01	6	1.50	> 0.1	6	1.10	> 0.1	6	3.41	0.05
First and Third	6	3.43	0.05	6	1.21	> 0.1	6	0.28	> 0.1	5	1.82	> 0.1
First and Fourth	6	3.95	0.01	6	4.28	0.01	6	3.30	0.05	5	4.96	0.01
First and Fifth	6	4.79	0.01	6	4.88	0.01	6	4.05	0.01	6	0.92	> 0.1
Second and Fourth	5	7.73	0.001	6	4.61	0.01	6	3.22	0.05	5	5.84	0.01
Third and Fifth	6	6.31	0.001	6	5.64	0.01	6	2.80	0.05	5	2.20	0.1
Second and Third	5	0.34	> 0.1	6	0.69	> 0.1	6	0.68	> 0.1	5	1.28	> 0.1
Fourth and Fifth	6	1.34	> 0.1	6	1.32	> 0.1	6	0.08	> 0.1	5	3.21	0.05

Table A.11. Statistical Data for Flexural Toughness results of beams from the Second Sub-group in Group One.

Batches	First (28 days curing)											
	Unreinforced			Flax Fibre			Duralin			Silane		
	Pre-cracking	Post-cracking	Total	Pre-cracking	Post-cracking	Total	Pre-cracking	Post-cracking	Total	Pre-cracking	Post-cracking	Total
Toughness (J)	0.22	0.00	0.22	0.24	0.07	0.30	0.09	0.01	0.10	0.24	0.05	0.30
	0.13	0.00	0.13	0.14	0.03	0.16	0.14	0.04	0.18	0.20	0.05	0.25
	0.16	0.00	0.16	0.14	0.04	0.18	0.18	0.05	0.23	0.28	0.04	0.32
	0.12	0.00	0.12	0.15	0.02	0.18	0.30	0.02	0.32	0.23	0.00	0.23
Average Toughness	0.16	0.00	0.16	0.17	0.04	0.21	0.18	0.03	0.21	0.24	0.03	0.27
Standard Deviation	0.05	0.00	0.05	0.05	0.02	0.07	0.09	0.02	0.09	0.03	0.02	0.04
Coefficient of Variation	29.00	0.00	29.00	28.29	54.59	32.33	49.67	67.73	44.86	13.21	69.44	14.77
Variance	0.00	0.00	0.00	0.00	0.00	0.00	0.01	0.00	0.01	0.00	0.00	0.00
Number of Specimens	4			4			4			4		

Table A.12. Statistical Data for Flexural Toughness results of beams from the First Sub-group in Group One.

Batches	Second (50 cycles)											
	Unreinforced			Flax Fibre			Duralin			Silane		
	Pre-cracking	Post-cracking	Total	Pre-cracking	Post-cracking	Total	Pre-cracking	Post-cracking	Total	Pre-cracking	Post-cracking	Total
Toughness (J)	0.07	0.00	0.07	0.17	0.01	0.19	0.09	0.02	0.11	0.10	0.02	0.12
	0.11	0.00	0.11	0.12	0.04	0.16	0.10	0.04	0.14	0.09	0.01	0.11
	0.08	0.00	0.08	0.06	0.03	0.09	0.26	0.01	0.26	0.10	0.01	0.11
				0.18	0.05	0.23	0.08	0.02	0.09	0.18	0.02	0.20
Average Toughness	0.09	0.00	0.09	0.13	0.03	0.17	0.13	0.02	0.15	0.12	0.02	0.14
Standard Deviation	0.02	0.00	0.02	0.05	0.02	0.06	0.08	0.01	0.08	0.04	0.00	0.05
Coefficient of Variation	20.90	0.00	20.90	40.89	48.93	35.63	64.48	62.82	50.57	36.86	29.79	33.31
Variance	0.00	0.00	0.00	0.00	0.00	0.00	0.01	0.00	0.01	0.00	0.00	0.00
Number of Specimens	3			4			4			4		

Table A.13. Statistical Data for Flexural Toughness results of beams from the Third Sub-group in Group One.

Batches	Third (25 cycles)											
	Unreinforced			Flax Fibre			Duralin			Silane		
	Pre-cracking	Post-cracking	Total	Pre-cracking	Post-cracking	Total	Pre-cracking	Post-cracking	Total	Pre-cracking	Post-cracking	Total
Toughness (J)	0.03	0.00	0.03	0.12	0.05	0.17	0.14	0.02	0.16	0.14	0.06	0.21
	0.12	0.00	0.12	0.18	0.04	0.22	0.02	0.00	0.02	0.19	0.04	0.23
	0.09	0.00	0.09	0.11	0.03	0.14	0.12	0.09	0.22	0.17	0.04	0.20
	0.16	0.00	0.16	0.21	0.07	0.28	0.25	0.07	0.32			
Average Toughness	0.10	0.00	0.10	0.16	0.05	0.20	0.13	0.05	0.18	0.17	0.05	0.21
Standard Deviation	0.06	0.00	0.06	0.05	0.01	0.06	0.09	0.04	0.12	0.02	0.02	0.01
Coefficient of Variation	59.02	0.00	59.02	30.53	31.02	29.09	70.54	90.37	68.92	13.42	33.75	5.53
Variance	0.00	0.00	0.00	0.00	0.00	0.00	0.01	0.00	0.02	0.00	0.00	0.00
Number of Specimens	4			4			4			4		

Table A.14. Statistical Data for Flexural Toughness results of beams from the Fourth Sub-group in Group One.

Batches	Fourth (50 ambient cycles)											
	Unreinforced			Flax Fibre			Duralin			Silane		
	Pre-cracking	Post-cracking	Total	Pre-cracking	Post-cracking	Total	Pre-cracking	Post-cracking	Total	Pre-cracking	Post-cracking	Total
Toughness (J)	0.13	0.00	0.13	0.32	0.02	0.34	0.24	0.03	0.27	0.22	0.07	0.29
	0.20	0.00	0.20	0.22	0.04	0.26	0.24	0.00	0.24	0.15	0.04	0.19
	0.12	0.00	0.12	0.21	0.02	0.23	0.16	0.00	0.16	0.32	0.00	0.32
	0.19	0.00	0.19	0.28	0.03	0.30	0.29	0.07	0.36			
Average Toughness	0.16	0.00	0.16	0.26	0.03	0.28	0.23	0.02	0.26	0.23	0.04	0.27
Standard Deviation	0.04	0.00	0.04	0.05	0.01	0.05	0.05	0.03	0.08	0.08	0.04	0.07
Coefficient of Variation	25.49	0.00	25.49	19.85	31.04	17.03	23.67	128.46	32.26	36.68	99.05	25.63
Variance	0.00	0.00	0.00	0.00	0.00	0.00	0.00	0.00	0.01	0.01	0.00	0.00
Number of Specimens	4			4			4			3		

Table A.15. Statistical Data for Flexural Toughness results of beams from the Fifth Sub-group in Group One.

Batches	Fifth (25 ambient cycles)											
	Unreinforced			Flax Fibre			Duralin			Silane		
Toughness (J)	Pre-cracking	Post-cracking	Total	Pre-cracking	Post-cracking	Total	Pre-cracking	Post-cracking	Total	Pre-cracking	Post-cracking	Total
	0.14	0.00	0.14	0.25	0.00	0.26	0.17	0.05	0.23	0.19	0.14	0.33
	0.16	0.00	0.16	0.15	0.03	0.18	0.23	0.10	0.33	0.17	0.03	0.20
	0.13	0.00	0.13	0.12	0.02	0.14	0.11	0.00	0.11	0.11	0.00	0.11
	0.15	0.00	0.15	0.11	0.02	0.14	0.14	0.03	0.17	0.19	0.10	0.29
Average Toughness	0.14	0.00	0.14	0.16	0.02	0.18	0.16	0.05	0.21	0.17	0.07	0.24
Standard Deviation	0.01	0.00	0.01	0.06	0.01	0.06	0.05	0.04	0.09	0.04	0.06	0.10
Coefficient of Variation	7.07	0.00	7.07	39.87	63.58	31.15	32.13	92.49	45.22	22.91	94.10	42.23
Variance	0.00	0.00	0.00	0.00	0.00	0.00	0.00	0.00	0.01	0.00	0.00	0.01
Number of Specimens	4			4			4			4		

Table A.16. Toughness results for the beams from all batches in Group One.

Sub-group	Batch Type	Number of specimens	Toughness				
			Pre-cracking		Post-cracking		Total (J)
			(J)	(%)	(J)	(%)	
First (28 days curing)	U+	4	0.16	100.00	-	0.00	0.16
	R+	4	0.17	81.39	0.04	-18.61	0.21
	D+	4	0.18	85.74	0.03	-14.26	0.21
	S+	4	0.24	87.51	0.03	-12.49	0.27
Second (50 cycles)	U	3	0.09	100.00	-	0.00	0.09
	R	4	0.13	79.91	0.03	-20.09	0.17
	D	4	0.13	86.45	0.02	-13.55	0.15
	S	4	0.12	87.59	0.02	-12.41	0.14
Third (25 cycles)	U	4	0.10	100.00	-	0.00	0.10
	R	4	0.16	77.21	0.05	-22.79	0.20
	D	4	0.13	74.65	0.05	-25.35	0.18
	S	3	0.17	77.97	0.05	-22.03	0.21
Forth (50 ambient cycles)	U	4	0.16	100.00	-	0.00	0.16
	R	4	0.26	90.81	0.03	-9.19	0.28
	D	4	0.23	90.40	0.02	-9.60	0.26
	S	3	0.23	85.87	0.04	-14.13	0.27
Fifth (25 ambient cycles)	U	4	0.14	100.00	-	0.00	0.14
	R	4	0.16	88.99	0.02	-11.01	0.18
	D	4	0.16	78.31	0.05	-21.69	0.21
	S	4	0.17	70.85	0.07	-29.15	0.24

+ U=unreinforced; R=flax fibre; D=Duralin; S=silane

Table A.17. Statistical Data for Compressive strength (MPa) results of cylinders from the First Sub-group in Group Two.

Sub-groups	First (28 days curing)			
Batches	U	R	D	S
Specimen Strength	38.65	60.81	46.18	25.24
	39.78	58.69	37.24	30.46
	39.93	60.81	46.69	29.52
		58.89		28.92
Average Strength	39.45	59.80	43.37	28.54
Standard Deviation	0.70	1.17	5.32	2.29
Coefficient of Variation	1.78	1.96	12.26	8.02
Variance	0.49	1.37	28.27	5.23
Number of Specimens	3	4	3	4

Table A.18. Statistical Comparison of Compressive strength results of cylinders from the First Sub-group in Group Two.

	Sub-groups		
	First (28 days curing)		
	Degrees of Freedom	t-value	Probability
U and R	5	28.56	0.001
U and D	4	1.27	> 0.1
U and S	5	9.00	0.001
R and D	5	5.26	0.01
R and S	6	24.32	0.001
D and S	5	4.53	0.01

Table A.19. Statistical Data for Compressive strength (MPa) results of blocks from all batches in Group Two.

Sub-groups	First (28 days curing)				Second (Freeze-thaw cycles)				Third (Ambient cycles)			
Batches	U	R	D	S	U	R	D	S	U	R	D	S
Specimen Strength	43.17	64.07	45.83	35.03	35.27	62.44	40.93	28.79	40.96	64.33	53.11	30.94
	40.42	64.08	45.98	30.27	34.88	62.45	41.97	28.38	44.98	64.33	43.29	32.93
	49.14	63.91	34.40	28.73	33.76	63.14	42.46	30.89	43.48	63.74	51.91	32.82
	35.00	63.89	42.59	34.83	34.29	63.16	47.52	27.70	50.74	63.71	56.07	32.48
	41.26	62.67	46.84	31.95	41.14	62.95	48.47	24.78	46.34	64.14	44.27	37.32
	39.78	62.66	53.05	33.68	41.08	62.97	45.09	31.59	55.43	64.13	52.49	33.87
	40.07	60.60	43.96	30.26	35.79	62.74	46.64	29.89	48.14	63.88	55.36	33.12
	43.01	63.43	48.99	35.80	38.71	62.75	46.71	26.19	48.42	63.90		27.99
Average Strength	41.48	63.16	45.20	32.57	36.86	62.82	44.97	28.53	47.31	64.02	50.93	32.68
Standard Deviation	4.00	1.19	5.41	2.63	3.01	0.28	2.83	2.30	4.49	0.25	5.11	2.63
Coefficient of Variation	9.64	1.88	11.96	8.09	8.16	0.44	6.30	8.07	9.49	0.39	10.04	8.04
Variance	15.99	1.41	29.23	6.94	9.05	0.08	8.03	5.30	20.14	0.06	26.15	6.90
Number of Specimens	8	8	8	8	8	8	8	8	8	8	7	8

Table A.20. Statistical Comparison of Compressive strength results of blocks from all batches in Group Two.

	Batches											
	Unreinforced			Flax Fibre			Duralin			Silane		
Degrees of Freedom	t-value	Probability	Degrees of Freedom	t-value	Probability	Degrees of Freedom	t-value	Probability	Degrees of Freedom	t-value	Probability	
First and Third	14	2.61	0.05	14	0.79	> 0.1	14	0.11	> 0.1	14	3.27	0.01
First and Second	14	2.74	0.05	14	1.99	0.1	13	2.11	0.1	14	0.09	> 0.1
Second and Third	14	5.47	0.001	14	9.06	0.001	13	2.73	0.05	14	3.37	0.01

Table A.21. Statistical Comparison of Compressive strength results of blocks from all batches in Group Two.

	Sub-groups											
	First (28 days curing)			Second (Freeze-thaw cycles)			Third (Ambient cycles)					
Degrees of Freedom	t-value	Probability	Degrees of Freedom	t-value	Probability	Degrees of Freedom	t-value	Probability				
U and R	14	14.70	0.001	14	24.31	0.001	14	10.51	0.001			
U and D	14	1.57	> 0.1	14	5.55	0.001	13	1.45	> 0.1			
U and S	14	5.26	0.001	14	6.23	0.001	14	7.96	0.001			
R and D	14	9.18	0.001	14	17.73	0.001	13	6.77	0.001			
R and S	14	29.94	0.001	14	41.84	0.001	14	33.59	0.001			
D and S	14	5.94	0.001	14	12.74	0.001	13	8.51	0.001			

Table A.22. Statistical Comparison of Compressive strength results of cylinders and blocks from the First Sub-group in Group Two.

	Batches											
	Unreinforced		Flax Fibre		Duralin		Silane					
	of Freedom	t-value	Probability	of Freedom	t-value	Probability	of Freedom	t-value	Probability			
First (28 days curing)	9	1.38	> 0.1	10	4.67	0.001	9	0.51	> 0.1	10	2.73	0.05

Table A.23. Statistical Data for Flexural strength (MPa) results of beams from all batches in Group Two.

Sub-groups	First (28 days curing)				Second (Freeze-thaw cycles)				Third (Ambient cycles)			
Batches	U	R	D	S	U	R	D	S	U	R	D	S
Specimen Strength	3.99	6.45	5.46	4.32	5.91	7.38	5.94	4.51	6.24	7.86	7.39	5.84
	4.14	6.15	5.03	4.40	6.17	7.39	6.21	4.47	6.91	8.54	7.83	5.51
	5.24	6.43	5.65	4.51	6.05	7.26	6.19	4.89	7.06	9.06	7.43	5.17
	4.63	6.67	5.87	4.67	5.49	7.06	6.13	4.58	6.74	8.44		5.55
Average Strength	4.50	6.43	5.50	4.48	5.90	7.27	6.12	4.61	6.74	8.47	7.55	5.52
Standard Deviation	0.57	0.21	0.36	0.15	0.30	0.15	0.12	0.19	0.36	0.49	0.24	0.27
Coefficient of Variation	12.57	3.30	6.47	3.34	5.01	2.11	2.04	4.16	5.32	5.77	3.23	4.91
Variance	0.32	0.05	0.13	0.02	0.09	0.02	0.02	0.04	0.13	0.24	0.06	0.07
Number of Specimens	4	4	4	4	4	4	4	4	4	4	3	4

Table A.24. Statistical Comparison of Flexural strength results of beams from all batches in Group Two.

	Batches								
	Unreinforced		Flax Fibre		Duralin		Silane		
	Degrees of Freedom	t-value	Probability	Degrees of Freedom	t-value	Probability	Degrees of Freedom	t-value	Probability
First and Third	6	6.67	0.001	6	7.68	0.001	5	9.04	0.001
First and Second	6	4.39	0.01	6	6.46	0.001	6	3.27	0.05
Second and Third	6	3.59	0.05	6	4.69	0.01	5	9.31	0.001
							6	6.73	0.001
							6	1.14	> 0.1
							6	5.43	0.01

Table A.25. Statistical Comparison of Flexural strength results of beams from all batches in Group Two.

	Sub-groups								
	First (28 days curing)			Second (Freeze-thaw cycles)			Third (Ambient cycles)		
	Degrees of Freedom	t-value	Probability	Degrees of Freedom	t-value	Probability	Degrees of Freedom	t-value	Probability
U and R	6	6.37	0.001	6	8.23	0.001	6	5.73	0.01
U and D	6	2.99	0.05	6	1.34	> 0.1	5	3.58	0.05
U and S	6	0.09	> 0.1	6	7.32	0.001	6	5.43	0.01
R and D	6	4.47	0.01	6	11.67	0.001	5	3.27	0.05
R and S	6	15.03	0.001	6	21.63	0.001	6	10.57	0.001
D and S	6	5.31	0.01	6	13.13	0.001	5	10.41	0.001

Table A.26. Statistical Data for Flexural Toughness results of beams from the First Sub-group in Group Two.

Batches	First (28 days curing)											
	Unreinforced			Flax Fibre			Duralin			Silane		
	Pre-cracking	Post-cracking	Total	Pre-cracking	Post-cracking	Total	Pre-cracking	Post-cracking	Total	Pre-cracking	Post-cracking	Total
Toughness (J)	0.16	0.00	0.16	0.34	0.04	0.38	0.33	0.01	0.35	0.22	0.02	0.24
	0.23	0.00	0.23	0.33	0.15	0.48	0.27	0.00	0.27	0.21	0.01	0.22
	0.17	0.00	0.17	0.41	0.04	0.45	0.40	0.05	0.45	0.24	0.04	0.28
	0.26	0.00	0.26	0.40	0.24	0.64	0.35	0.00	0.35	0.25	0.03	0.28
Average Toughness	0.21	0.00	0.21	0.37	0.12	0.49	0.34	0.02	0.35	0.23	0.03	0.26
Standard Deviation	0.05	0.00	0.05	0.04	0.09	0.11	0.06	0.02	0.08	0.02	0.01	0.03
Coefficient of Variation	23.53	0.00	23.53	10.67	81.41	22.48	16.66	149.13	21.60	8.92	45.93	12.54
Variance	0.00	0.00	0.00	0.00	0.01	0.01	0.00	0.00	0.01	0.00	0.00	0.00
Number of Specimens	4			4			4			4		

Table A.27. Statistical Data for Flexural Toughness results of beams from the Second Sub-group in Group Two.

Batches	Second (Freeze-thaw cycles)											
	Unreinforced			Flax Fibre			Duralin			Silane		
	Pre-cracking	Post-cracking	Total	Pre-cracking	Post-cracking	Total	Pre-cracking	Post-cracking	Total	Pre-cracking	Post-cracking	Total
Toughness (J)	0.24	0.00	0.24	0.33	0.03	0.37	0.35	0.00	0.35	0.14	0.00	0.14
	0.39	0.00	0.39	0.26	0.00	0.26	0.28	0.01	0.29	0.22	0.02	0.24
	0.29	0.00	0.29	0.30	0.00	0.30	0.35	0.00	0.35	0.32	0.02	0.34
	0.35	0.00	0.35	0.25	0.01	0.26	0.37	0.02	0.39	0.18	0.01	0.19
Average Toughness	0.32	0.00	0.32	0.29	0.01	0.30	0.34	0.01	0.35	0.22	0.01	0.23
Standard Deviation	0.07	0.00	0.07	0.04	0.02	0.05	0.04	0.01	0.04	0.07	0.01	0.08
Coefficient of Variation	20.56	0.00	20.56	13.90	116.50	16.66	11.64	140.45	12.38	34.41	82.55	36.11
Variance	0.00	0.00	0.00	0.00	0.00	0.00	0.00	0.00	0.00	0.01	0.00	0.01
Number of Specimens	4			4			4			4		

Table A.28. Statistical Data for Flexural Toughness results of beams from the Third Sub-group in Group Two.

Batches	Third (Ambient cycles)											
	Unreinforced			Flax Fibre			Duralin			Silane		
Toughness (J)	Pre-cracking	Post-cracking	Total	Pre-cracking	Post-cracking	Total	Pre-cracking	Post-cracking	Total	Pre-cracking	Post-cracking	Total
	0.39	0.00	0.39	0.30	0.00	0.30	0.37	0.00	0.37	0.20	0.00	0.20
	0.45	0.00	0.45	0.23	0.00	0.23	0.55	0.00	0.55	0.32	0.02	0.34
	0.54	0.00	0.54	0.61	0.07	0.68	0.26	0.01	0.27	0.28	0.00	0.28
	0.51	0.00	0.51	0.25	0.03	0.28				0.39	0.00	0.39
Average Toughness	0.47	0.00	0.47	0.35	0.03	0.37	0.40	0.00	0.40	0.30	0.00	0.30
Standard Deviation	0.07	0.00	0.07	0.18	0.03	0.21	0.15	0.01	0.14	0.08	0.01	0.08
Coefficient of Variation	13.74	0.00	13.74	50.96	129.26	55.26	37.24	173.21	35.56	27.67	200.00	27.94
Variance	0.00	0.00	0.00	0.03	0.00	0.04	0.02	0.00	0.02	0.01	0.00	0.01
Number of Specimens	4			4			3			4		

Table A.29. Toughness results for the beams from all batches in Group Two.

Sub-group	Batch Type	Number of specimens	Toughness				
			Pre-cracking (J)	Pre-cracking (%)	Post-cracking (J)	Post-cracking (%)	Total (J)
First (28 days curing)	U+	4	0.21	100.00	-	0.00	0.21
	R+	4	0.37	76.00	0.12	24.00	0.49
	D+	4	0.34	95.52	0.02	4.48	0.35
	S+	4	0.23	89.84	0.03	10.16	0.26
Second (Freeze-thaw cycles)	U	4	0.32	100.00	-	0.00	0.32
	R	4	0.29	95.66	0.01	4.34	0.30
	D	4	0.34	98.11	0.01	1.89	0.35
	S	4	0.22	95.25	0.01	4.75	0.23
Third (Ambient cycles)	U	4	0.47	100.00	-	0.00	0.47
	R	4	0.35	93.00	0.03	7.00	0.37
	D	3	0.40	99.03	0.00	0.97	0.40
	S	4	0.30	98.67	0.00	1.33	0.30

+ U=unreinforced; R=flax fibre; D=Duralin; S=silane

Table A.30. Freeze-thaw cycling times

Date tested (2010)	Number of days in between tests	Number of cycles	Number of cycles between tests	Average number of cycles per day	Average hours per cycle
01-Jun	0	0	0	0	0
09-Jun	8	35	35	4.4	5.5
16-Jun	7	74	39	5.6	4.3
21-Jun	5	107	33	6.6	3.6
25-Jun	4	131	24	6.0	4.0
02-Jul	7	172	41	5.9	4.1
09-Jul	7	199	27	3.9	6.2
14-Jul	5	228	29	5.8	4.1
20-Jul	6	267	39	6.5	3.7
26-Jul	6	303	36	6.0	4.0

Section B: SEM Analysis

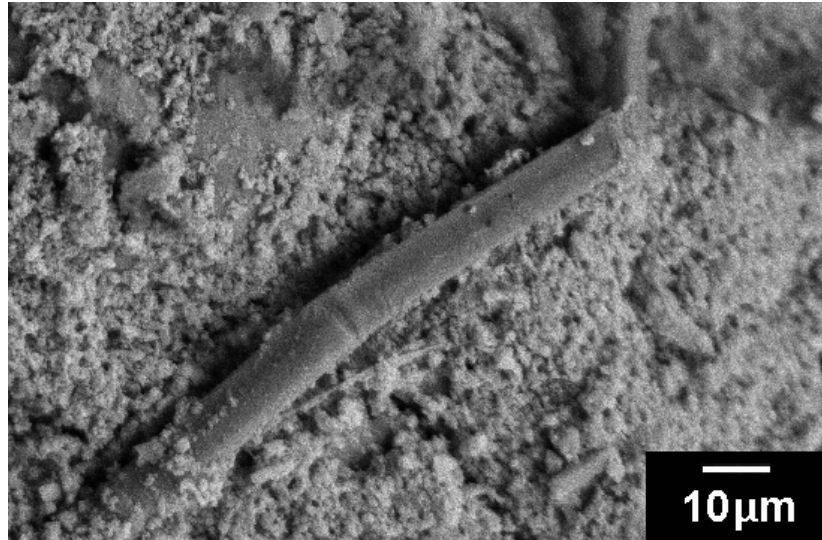


Figure B.1. Flax fibre on beam failure surface - Third sub-group of group one

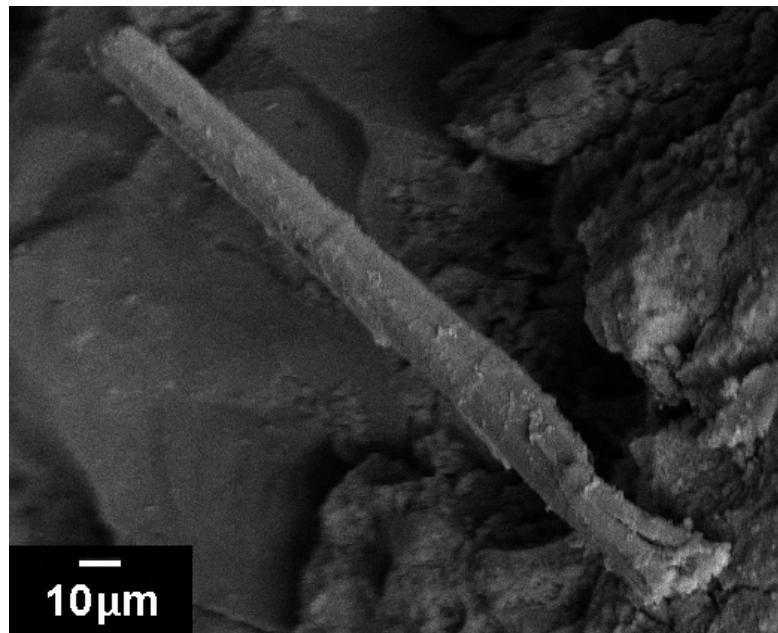


Figure B.2. Duralin fibre on beam failure surface - Third sub-group of group one

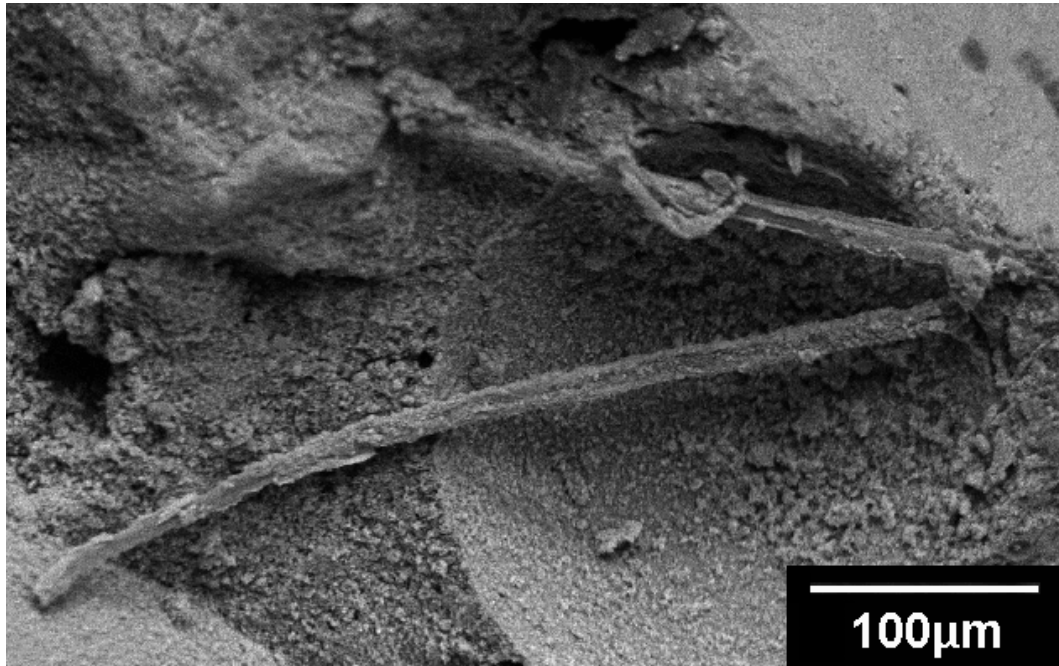


Figure B.3. Silane fibre on beam failure surface - Third sub-group of group one

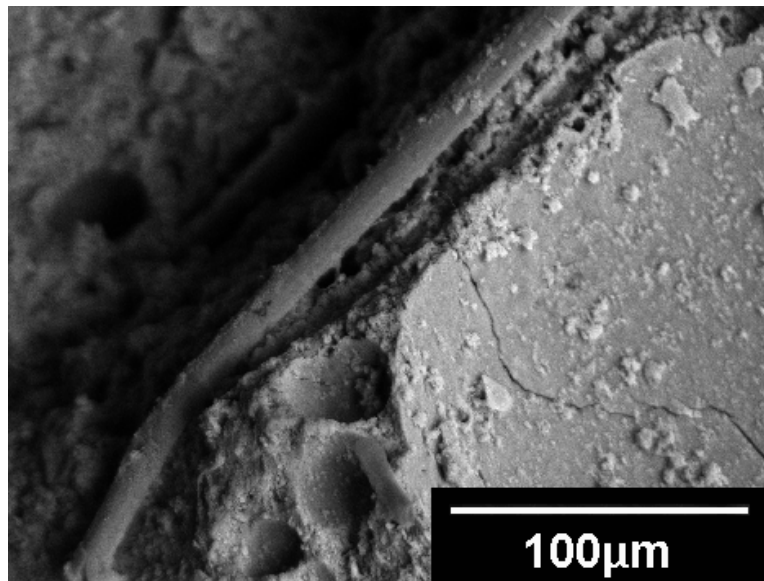


Figure B.4. Flax fibre on beam failure surface - Fourth sub-group of group one

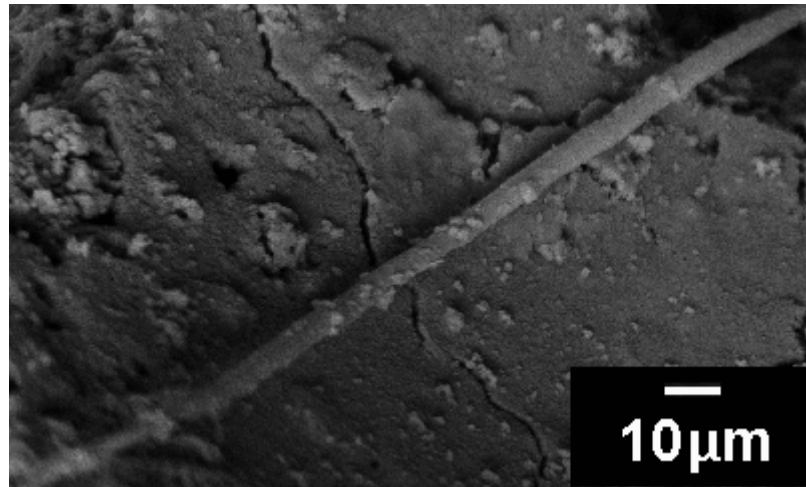


Figure B.5. Duralin fibre on beam failure surface - Fourth sub-group of group one

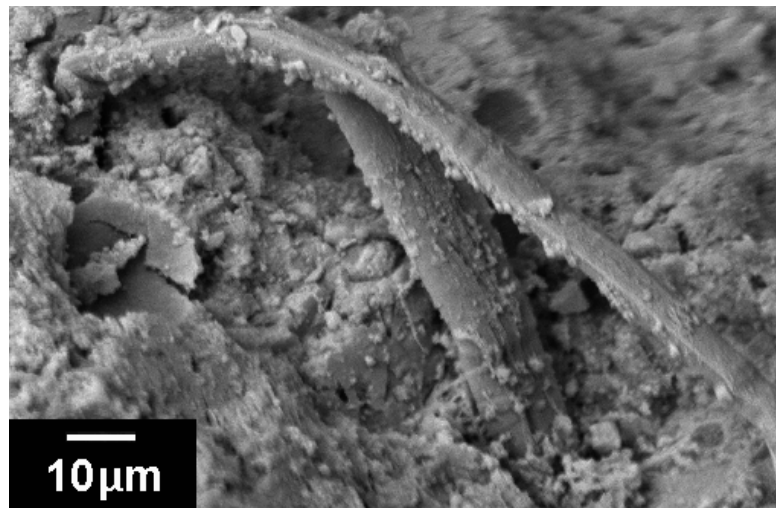


Figure B.6. Silane fibre on beam failure surface - Fourth sub-group of group one

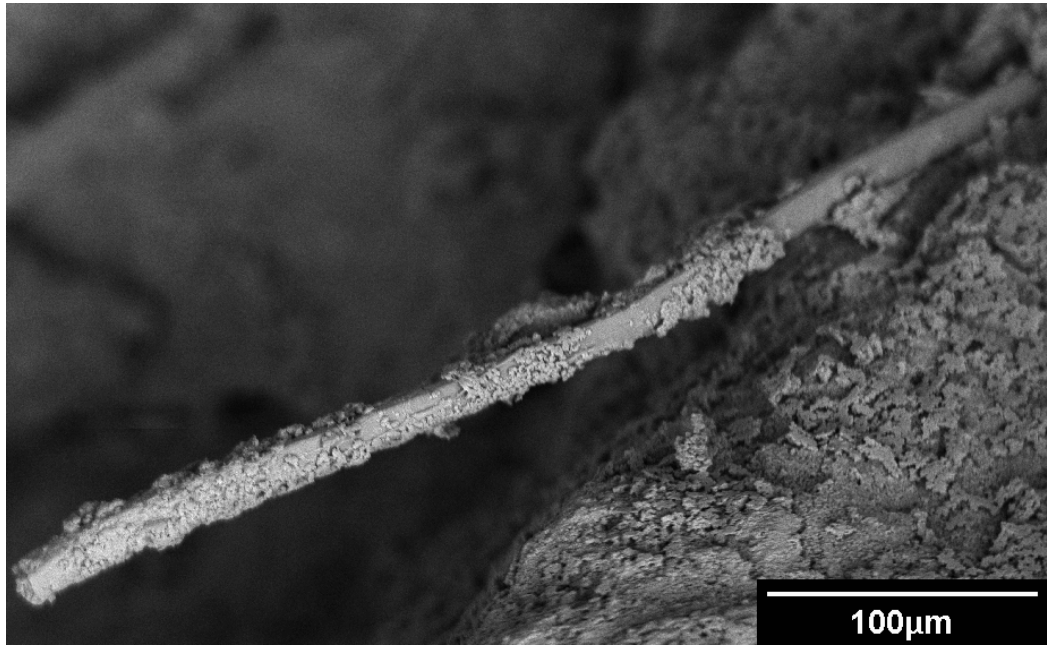


Figure B.7. Flax fibre on beam failure surface - Second sub-group of group one

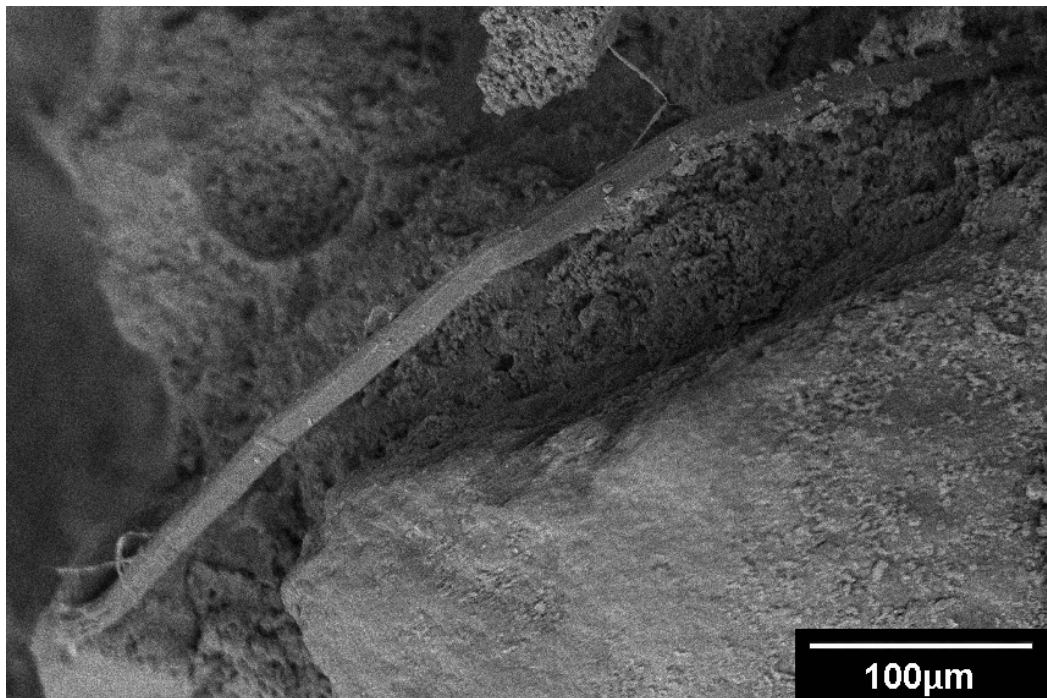


Figure B.8. Duralin fibre on beam failure surface - Second sub-group of group one

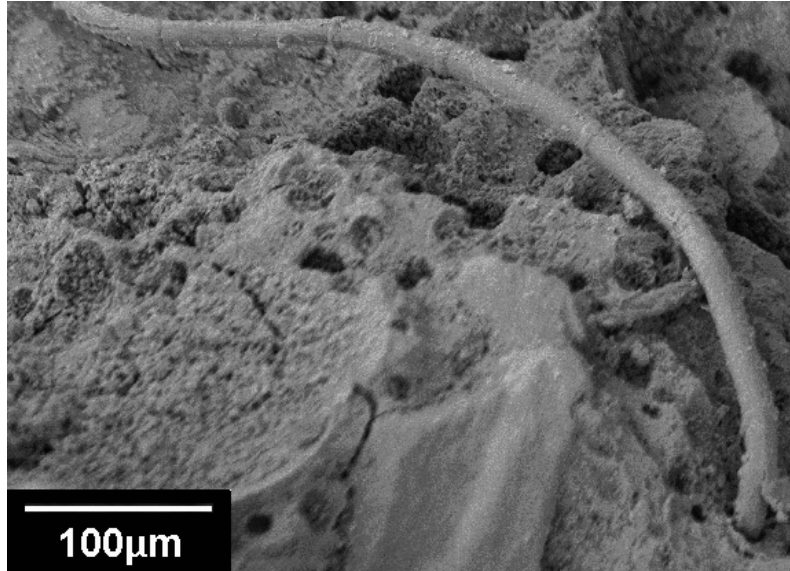


Figure B.9. Silane fibre on beam failure surface - Second sub-group of group one

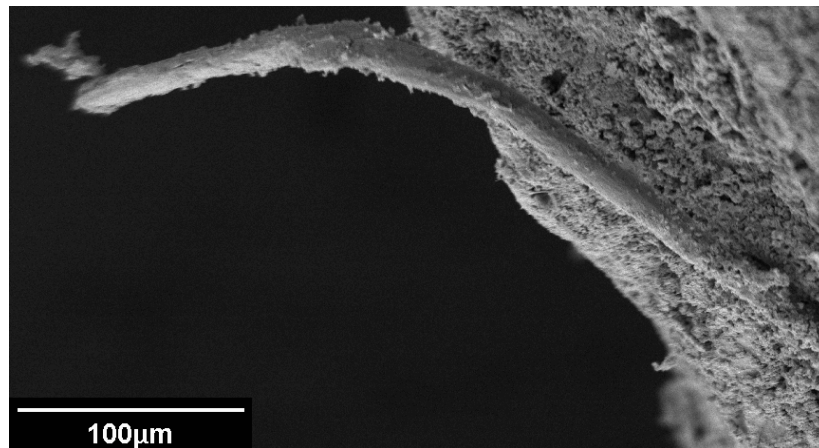


Figure B.10. Flax fibre on beam failure surface - Third sub-group of group one

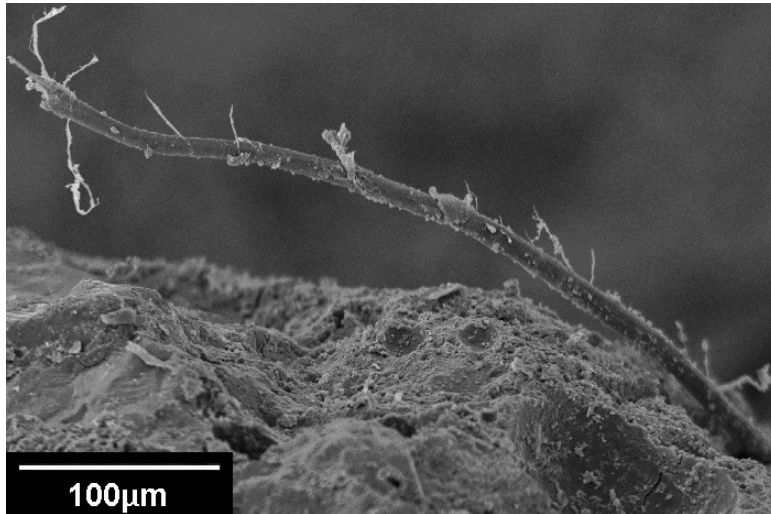


Figure B.11. Duralin fibre on beam failure surface - Third sub-group of group one

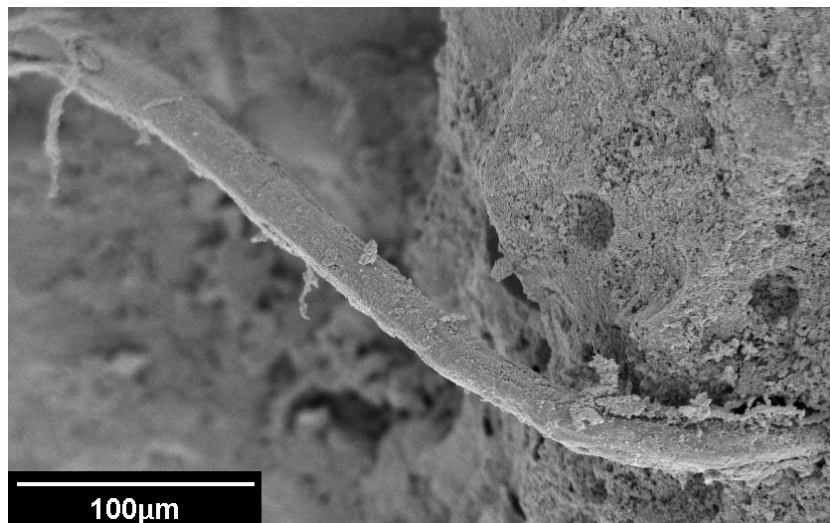


Figure B.12. Silane fibre on beam failure surface - Third sub-group of group one